Title
The role of the secretory pathway in dendrite and axon development

Permalink
https://escholarship.org/uc/item/70x58128

Author
Zhang, Ye

Publication Date
2009

Peer reviewed|Thesis/dissertation

The role of the secretory pathway in dendrite and axon development

by

Ye Zhang

DISSERTATION

Submitted in partial satisfaction of the requirements for the degree of

DOCTOR OF PHILOSOPHY

in

Neuroscience

in the

GRADUATE DIVISION

of the

UNIVERSITY OF CALIFORNIA, SAN FRANCISCO

Acknowledgements

First, I would like to thank my thesis advisor Yuh Nung Jan. Yuh Nung has set a powerful example of how to find the next key experiment in front of overwhelming and confusing data, how to see the big picture while attending to details, and how to be imaginative and remain practical. I would like to thank his dedication to my training. He always replies to my emails in a few hours and revises my manuscript in a day or two. His efficiency is admiring and is something I am always learning to achieve. I am also grateful for Yuh Nung's amazing ability to gather very talented people in his lab and guide them so that everyone is thriving to their full potential. Because of that, I am lucky enough to work with a wonderful group of colleagues whose help has shaped my project and my way of thinking. Every morning I step into Jan lab, I know the best resource and support is available, and all I have to do is to have some interesting work done and enjoy science. My experience in Yuh Nung's lab showed me that even though projects can go up and down, working in science is always fresh, fun, and rewarding.

I also thank Lily Jan, who proposed interesting hypotheses and suggested creative experiments every time I gave a group meeting. She also gave me great help during my practice talks and paper writing. Yuh Nung and Lily showed me the art of presenting science.

I thank my thesis committee members: Mark von Zastrow, John Rubenstein, Nirao

Shah, and Grae Davis. Their ideas, suggestions, and encouragements supported me through graduate school. They are sharp and passionate scientists that I deeply respect.

I would like to thank current and former members from both Yuh Nung Jan and Lily Jan's group that I overlapped with. They are such an excellent group of talented people that I feel lucky to interact with. I learned a tremendous amount from them and had great fun with them. I extend my special thanks to Bing Ye, former Jan lab postdoc with whom I closely collaborated. Bing taught me essentially all the lab techniques I used in this thesis. And more importantly, he showed me qualities of an excellent scientist who can always identify important questions and make solid discoveries. Bing's knowledge, creativity, optimism, kindness, and sense of humor have made our collaboration enjoyable and memorable.

I thank UCSF neuroscience community for the very helpful courses, seminars, retreats, etc. I thank Pat and Carrie for excellent administrative support.

Finally, and most of all, I thank my family for their tremendous support. I thank my parents Yuanzheng Ye and Qingmao Zhang for their love that I can feel every minute in my life. I thank my husband Xiaoyu Wu for his patience, care, and love, his amazing ability to cheer me up, and his selfless support for me to pursue what I enjoy. I also thank my son Alex Wu for the tremendous joy he is bringing to my life.

Project specific acknowledgements can be found at the end of Chapters 2, 3, and 4.

Contributions

Chapter 2 of this dissertation is a reprint of the material as it appears in an article in *Cell*. (Growing dendrites and axons differ in their reliance on the secretory pathway. Bing Ye*, Ye Zhang*, Wei Song, Susan H. Younger, Lily Yeh Jan, and Yuh Nung Jan. *Cell*, August 24, 2007; Vol. 130, p. 717-729. *equal contributions). The authors listed in the *Cell* paper contributed to the work as follows. Bing Ye and Susan Younger carried out the genetic screen. Bing Ye, Ye Zhang, and Susan Younger mapped the mutations. Wei Song generated the transgenic lines UAS-manII-GFP and UAS-GalT-YFP. All the other experiments are carried out by Bing Ye and Ye Zhang. Bing Ye, Ye Zhang, Lily Jan, and Yuh Nung Jan designed the experiments and wrote the paper.

Abstract

The secretory pathway supplies membrane proteins and lipids essential for cell growth. The development of neuronal dendrites and axons requires large amount of membrane molecules transported by the secretory pathway. However, little is known about the role of the secretory pathway in establishing the architectures of dendrites and axons. From a genetic screen, we isolated *dendritic arbor reduction (dar)* mutants with reduced dendritic arbors but normal axons of *Drosophila* neurons. We identified *dar2, dar3,* and *dar6* genes as the homologs of *Sec23, Sar1,* and *Rab1* of the secretory pathway. In both *Drosophila* and rodent neurons, defects in Sar1 expression preferentially affected dendritic growth, revealing evolutionarily conserved difference between dendritic and axonal development in the sensitivity to limiting membrane supply from the secretory pathway. Whereas limiting ER-to-Golgi transport resulted in decreased membrane supply from soma to dendrites, membrane supply to axons remained sustained. We also show that dendritic growth is contributed by Golgi outposts, which are found predominantly in dendrites. We found that dendritic Golgi outposts are at least in part generated in the soma, excluded from the axon by dynein based transport, and distributed in neuron type specific patterns. Furthermore, we found that a trans-Golgi network localized regulator of secretory trafficking, Rab6, has important roles in dendrite morphogenesis.

Table of Contents

List of Figures

List of Tables

CHAPTER 1: General introduction

Intracellular membrane transport, secretory pathway, and endocytic pathway

Eukaryotic cells contain various types of membrane delineated organelles. Compartmentalization of biochemical reactions and metabolites within these organelles is essential for the survival, growth, and proliferation of cells. Tightly regulated molecule trafficking between these organelles as well as in and out of cells are mainly carried out by the secretory pathway and the endocytic pathway.

The secretory pathway is responsible for the synthesis, modification, sorting, and trafficking of membrane lipids, membrane proteins, and secreted molecules (Figure 1-1) (van Vliet et al., 2003). Synthesis of membrane and secreted proteins and lipids happens in endoplasmic reticulum (ER). Two classes of ER: smooth ER (sER) and rough ER (rER) differ in their ultra-structural morphology and their function. Smooth ER is an important site of lipid biosynthesis and a reservoir of intracellular calcium in muscle and neuronal cells. Rough ER is characterized by ribosomes attached to ER membrane, which give them the "rough" appearance in electro-microscopic images. Membrane proteins are translated by ER-attached ribosomes. They are located on ER membrane after translation and remain on the membrane of the secretory pathway as they go through modifications and sorting, and eventually arrive at the plasma membrane. Secreted proteins enter ER lumen as they are translated by ER-attached ribosomes, and remain in the luminal side of organelles and vesicles of the secretory pathway. They enter extracellular space by vesicle exocytosis.

After synthesis at ER, cargos are sorted and packaged into COPII coated vesicles and bud from ER exit sites. Formation of COPII coated vesicles involves the coordinated action of a number of proteins (Figure 1-2): Sec12 converts a small GTPase, Sar1, to GTP bound form. GTP-Sar1 initiate the formation of COPII coated vesicle by (1) inserting its N-terminal into ER membrane and induce membrane curvature; and (2) recruiting COPII coat components Sec23 and Sec 24 (Huang et al., 2001). Sec23 is a multi-functional protein. It forms vesicle coat, binds cargo proteins, and promotes the hydrolysis of Sar1-GTP. Sar1-GDP then dissociates coat proteins from a mature vesicle and releases them to the cytosol for the next round of vesicle formation (Fromme et al., 2008).

COPII coated vesicles travel through ER Golgi intermediate compartment (ERGIC) and then dock at cis-Golgi cisternae. A small GTPase, Rab1, ensures proper vesicle fusion at cis-Golgi cisternae (Nuoffer et al., 1994).

Golgi apparatus is composed of stacks of cisternae. Membrane and secreted proteins undergo several steps of post translational modification (e.g. glycosylation, disulfide bond formation) as they are transported through cis-, medial-, and trans- Golgi cisternae (van Vliet et al., 2003). The size and orientation of Golgi apparatus usually reflect level and polarity of the secretory activity of a cell (Hanus and Ehlers, 2008). Cargos are sorted into various carriers at trans-Golgi network (TGN), and then targeted either to the plasma membrane or the endocytic pathway (see below) (De Matteis and Luini, 2008).

Endosome is the major organelle of the endocytic pathway. Endosomes are classified

into early endosome, recycling endosome, and late endosome based on their function and molecular markers. Endocytosis starts by the formation of clathrin coated vesicles. Endocytosed cargos first fuse with early and recycling endosome, where they are recognized by different types of adaptor proteins, and they are sorted back to the plasma membrane or late endosome and lysosome for degradation (Sann et al., 2009). The endocytic pathway is not only an important route of membrane flow in neurons, but also critical for signaling of membrane bound receptors (von Zastrow and Sorkin, 2007).

There is extensive crosstalk between the two intracellular membrane transport pathways: secretory pathway and endocytic pathway. Accumulating evidence suggests that membranous vesicles travel bidirectionally between trans-Golgi network and endosome (Johannes and Popoff, 2008).

The secretory pathway in neurons

Secretory pathway is not a passive supplier of building materials for plasma membrane. Instead, the activity of the secretory pathway and the organization of secretory organelles undergo dynamic changes critical for the growth and function of cells. Golgi apparatus reorient rapidly in a variety of cells undergoing polarized secretion or polarized membrane expansion. For example, during Drosophila early embryogenesis, new membrane forms and divides a syncytial embryo to multiple cells in a process called cellularization. Golgi apparatus moves along microtubule tracks and accumulates in

locations where active membrane addition happens (Papoulas et al., 2005). In muscle cells, Golgi apparatus are restricted underneath motor end plates, where local processing and routing of acetylcholine receptor is required. This focal distribution of Golgi apparatus depends on the presence of axon terminals. Denervation results in movement of Golgi to the perinuclear region (Jasmin et al., 1989). In cytotoxic T-lymphocyte, binding of a target cell induces rapid reorientation of the Golgi apparatus to the site of cell contact, presumably facilitating the secretion of cytotoxic enzymes that destruct the target cell (Kupfer and Singer, 1989). Similarly, Golgi apparatus reorient towards direction of cell migration or wound healing (Singer and Kupfer, 1986).

Studying the regulation of the secretory pathway is important for understanding the development and physiology of cells. This is particularly relevant for neurons for the following reasons:

First, neurons are among the most morphologically complex cells. With the branched long dendrites and axons, the surface area of a neuron can be up to 10^6 μm^2. This is 10,000 times the surface area of a typical cell with a roughly spherical shape. The typical speed of neurite growth in cultured rat neurons is 0.5 mm a day, requiring membrane expansion at the rate of approximately $1 \mu m^2$ per minute (Pfenninger, 2009). The sheer volume of membrane in neurons and the morphological complexity necessitates an extremely efficient and tightly regulated secretory pathway as the membrane supplier (Hanus and Ehlers, 2008; Pfenninger, 2009).

Second, the signal transmitting and computing function of the nervous system

depends on changes of electrical potential across the plasma membrane, which is established by ion channels and pumps on the plasma membrane. These membrane proteins need to be targeted to correct subcellular locations for their proper function (Horton and Ehlers, 2004; Lai and Jan, 2006). Moreover, they are dynamically transported on and off the plasma membrane, forming the basis for neuronal plasticity (Kennedy and Ehlers, 2006). Therefore, studying the targeting and transport of membrane proteins by the secretory pathway is critical for understanding the function of neurons.

Third, a number of neurological disorders involve pathological changes of the secretory pathway. For example, alpha-synuclein accumulation is associated with Parkinson's disease. The earliest defect in yeast expressing alpha-synuclein is blockage of ER-Golgi traffic. Elevated expression of Rab1, which is required for vesicle docking at Golgi, rescues neuron loss in Parkinson's models (Cooper et al., 2006). Mutation in presenilin is identified as a cause for early onset Alzheimers' disease. Presenilin is mostly located in ER and involve in proteolytic processing of amyloid precursor protein and ER stress (Aridor and Hannan, 2000). A large number of rare neurological diseases are disorders of intracellular membrane transport, such as Fabri disease, Tay-Sachs, I cell disease, and Batten disease (Aridor and Hannan, 2000).

The majority of a neuron's metabolic activities were once believed to happen in the soma, although discoveries made in recent years led to a model in which neurites are more autonomous than they were originally thought. For example, local protein synthesis

was found in neurites (Steward and Schuman, 2003). Conceivably, presence of secretory

pathway organelles in the far reaches of a neuron would enable fast response to local

signals. Indeed, a satellite secretory pathway is found in dendrites. However, axons

appear to lack major secretory organelles required for the processing and sorting of

membrane proteins. In the nineteen eighties, De Camilli and colleagues reported the

presence of Golgi in dendrites but not axons in rat brain sections (De Camilli et al., 1986).

In the nineteen nineties and early this century, there was increased interest in the search

for secretory organelles in neurites, partly resulted from important discoveries of local

translation of membrane proteins relevant to neuronal plasticity. Several groups carried

out detailed immunohistochemistry and immuno-electromicrosopy studies and found a

complete set of secretory organelles in dendrites: ER, ER exit sites, ERGIC, Golgi, and

TGN. Golgi apparatus located in dendrites are called dendritic Golgi outposts (Aridor et

al., 2004; Gardiol et al., 1999; Horton and Ehlers, 2003; Horton et al., 2005; Pierce et al.,

2001; Pierce et al., 2000). Ehlers and colleagues reported that dendritic Golgi outposts

are involved in the trafficking of both integral membrane proteins and secreted proteins,

revealing that dendritic satellite secretory pathway is functional (Horton and Ehlers,

2003). Different dendritic membrane proteins are sorted through different pathways. For

example NMDA receptor is sorted by the satellite secretory pathway in dendrites whereas

AMPA receptor is sorted by the conventional somatic secretory pathway (Jeyifous et al.,

2009). Despite of extensive search for immunoreactivity of secretory organelle markers

and morphological identification by electromicroscopes, axons appear to lack rough ER

and Golgi apparatus (De Camilli et al., 1986; Horton et al., 2005) (a few pieces of recent evidence that challenge this view are discussed in Chapter 5).

In cells with simple geometry, such as fibroblast and HELA cell, ER is distributed throughout the cytosol whereas Golgi is located in the perinuclear region. Vesicles leave ER and move centripetally towards Golgi in the perinuclear region, and then leave Golgi and move centrifugally to the plasma membrane. How would the presence of a satellite secretory pathway in dendrites but not axons affect the routes of membrane trafficking in neurons? In axons that lack ER and Golgi, membranous cargos have to be packaged and processed in the soma, exit somatic Golgi and travel over a long distance to axonal plasma membrane. In dendrites, in addition to this long distance transport of vesicles synthesized from somatic secretory pathway, local synthesis, processing and targeting of membranous vesicles by dendritic ER and Golgi likely happens. A third route for the trafficking of dendritic secretory vesicles is also proposed: Ehlers and colleagues followed vesicles exiting dendritic ER by live imaging of GFP tagged temperature-sensitive mutant of the vesicular stomatitis virus glycoprotein (VSVG). They found that the majority of post-ER carriers in dendrites move in the retrograde direction towards soma (Horton and Ehlers, 2003). They propose that these vesicles are synthesized in dendritic ER, transported to somatic Golgi, and then targeted back to dendritic plasma membrane. It remains to be determined whether this surprising indirect route of membrane trafficking is specific to this viral protein or reflect a major route of trafficking for other cargos.

Establishing different architectures of dendrites and axons

Neuronal dendrites receive and integrate synaptic or sensory signal (input) whereas axons are responsible for fast transmission of neuronal impulses (output). According to the geometry of dendrites, axons, and the cell body, neurons are classified to multipolar neurons and unipolar neurons. The majority of mammalian neurons (e.g. rodent hippocampal neurons) and some invertebrate neurons (e.g. dendritic arborization neurons (da) neurons in *Drosophila*) are multipolar neurons, *i.e.* multiple dendrites and one axon emanate from the cell body. The majority of insect neurons (e.g. *Drosophila* mushroom body neurons) and a minority of mammalian neurons (e.g. rodent dorsal root ganglion neurons) are unipolar neurons, *i.e.* only one single "cell body fiber" connects with the cell body and dendrites and axons branch out from this cell body fiber. The dendrites and axons of both multipolar neurons and unipolar neurons display morphological and molecular differences which are highly conserved in evolution. Dendrite diameter decreases from proximal to distal end (tapering) whereas axons have largely uniform diameters (Prochiantz, 1995). The orientations of dendritic microtubules are mixed whereas axonal microtubules are uniformly plus-end distal (Baas et al., 1988). Dendrites express molecules unique to dendrites such as MAP2, transferrin receptor, and glutamate receptors (Bradke and Dotti, 1998), whereas a different set of molecules, such as tau, L1/NgCAM, and Kv1, are located only to axons or enriched in axons (Gu et al., 2003;

Yap et al., 2008). As mentioned above, the major secretory organelle, Golgi apparatus, is located in cell bodies and dendrites but largely absent from the axons (De Camilli et al., 1986; Horton and Ehlers, 2003).

The polarization of neurons to distinct dendritic and axonal compartments is an early event in neuronal differentiation. *In vitro*, multiple immature neurites form before polarization. Breakage of symmetry happens when random fluctuation of intracellular and extracellular signals and positive feedback mechanisms lead to accumulation of signaling complexes (Par3/Par6/aPKC, LKB1/STRAD etc.) in one of the immature neurites, which grows faster than the other neurites and becomes the axon. The other neurites become dendrites. *In vivo*, asymmetrically localized extracellular cues and intracellular signals (e.g. intracellular asymmetry resulted from cell division) orchestrate above mentioned signaling complexes in specifying axons and dendrites (Arimura and Kaibuchi, 2005; Barnes and Polleux, 2009; Bradke and Dotti, 2000c; de Anda et al., 2005; Shelly et al., 2007; Shi et al., 2003). After the initial polarization, neuronal polarity is actively maintained by GSK3-beta signaling pathway (Jiang et al., 2005). Yet dendrite-axon polarity displays plasticity after injury: dendrites retain the capacity to become axons if the axon of a neuron is removed (Bradke and Dotti, 2000b; Gomis-Ruth et al., 2008).

The role of the secretory pathway in neuronal polarization is not well understood. Whether polarization of secretory organelles occurs before morphological polarization of neurons is controversial. One study reported that Golgi apparatus and centrosome cluster

together close to there area where the axon forms (de Anda et al., 2005). Two other studies did not find this correlation (Dotti and Banker, 1991; Horton et al., 2005). PKD, a kinase required for vesicle budding from trans-Golgi network, is required for neuronal polarization, although the mechanism by which PKD influences polarization is unclear (Yin et al., 2008).

Diverse types of neurons are characterized by the diversity of dendrite and axon morphology. Establishing stereotypical morphology of dendrites and axons in each type of neurons involves various cell autonomous and non-autonomous signals. Dendrite morphogenesis, for example, is a complex process only beginning to be understood (Parrish et al., 2007b). Transcription factors control dendrite growth and specify neuron type specific morphology patterns (Cobos et al., 2007; Grueber et al., 2003a; Jinushi-Nakao et al., 2007; Kim et al., 2006; Li et al., 2004; Parrish et al., 2007a; Sugimura et al., 2004). Extrinsic cue, for example neural trophic facters, influence dendritic arbor size (McAllister et al., 1997). Dendritic field is refined by cell-cell interactions (Emoto et al., 2004; Grueber et al., 2003b; Matthews et al., 2007; Soba et al., 2007). Dendritic arbors are further shaped by neuronal activities (Cline, 2001; Wong and Ghosh, 2002). The role of the secretory pathway in dendrite and axon morphogenesis is unclear.

In addition to neuronal morphological polarization, membrane molecules are segregated to dendritosomatic compartment and axonal compartments. The secretory pathway and endocytic pathway establish such polarity of membrane molecule

distribution either by compartment selective targeting or by non-discriminating targeting followed by selective retention in one compartment (e.g. targeting of L1/NgCAM) (Bradke and Dotti, 1998; Yap et al., 2008). Segregation of membrane molecules are further maintained by barriers at the axon initial segment. A diffusion barrier involving ankrin and actin cytoskeleton at axon initial segment plasma membrane prevents free diffusion within the membrane (Kobayashi et al., 1992; Winckler et al., 1999). There is also a selective filter for cytoplasmic transport at the axon initial segment (Song et al., 2009). Dynein motor prevents leakage of somato-dendritic cargos to axons, including the secretory pathway organelle Golgi (Zheng et al., 2008).

Does the secretory pathway contribute to the differential growth of dendrites and axons?

The growth of dendrites and axons, with their elongated morphology, requires enormous amount of membrane. The proportion of membrane distributed to dendrites vs. axons, however, is very different across neuronal types. Mouse cerebellar purkinje cells, for example, have highly branched dendrites and relatively simple axons. The total dendritic length of one purkinje cell is about 6 mm (Pysh and Weiss, 1979), whereas the length of purkinje axon is only about 2 mm (Rico et al., 2004). In contrast, *Drosophila* larval external sensory (es) neurons have one short unbranched dendrite less than 0.1 mm in length and an axon about 2 mm in length. There must be either cell intrinsic signals or

external cues that regulate dendrite and axon growth differently and determine the allocation of membrane resources between dendrites and axons. Indeed, numerous molecules are identified that affect dendrite and axon growth differently. For example, semaphorin inhibits axon growth but promotes dendrite growth (Goldberg et al., 2004; Polleux et al., 2000). In *Drosophila* mushroom body neurons, rhoA is required for dendrite growth but not axon growth (Lee et al., 2000).

Ehlers and colleagues found that asymmetric secretory trafficking contribute to the different morphology of apical dendrite and basolateral dendrite of hippocampal neurons (Horton et al., 2005). It is tempting to hypothesize that the secretory pathway, which supplies membrane molecules for dendrites and axons, contributes to the differential growth of dendrites and axons. Before axon specification, there is biased secretory trafficking towards future axon (Bradke and Dotti, 1997). The role of the secretory pathway in the differential growth of dendrites and axons after polarization is unclear. How is membrane resource divided between dendrites and axons when there is limited membrane supply also remains to be determined. These are interesting open questions that I attempted to address in my thesis work (Chapter 2).

What is the function of dendritic Golgi outposts?

Numerous proteins are found to be locally translated in neuronal dendrites (e.g. CAMKII, Arc) (Ashraf et al., 2006; Waung et al., 2008). These include membrane

proteins that require the secretory pathway for processing, sorting and targeting (e.g. AMPA receptor, Kv1.1) (Kacharmina et al., 2000; Raab-Graham et al., 2006). The local synthesis of membrane receptors and channels enables response to local signals and local changes of membrane permeability. Local protein synthesis is important for neuronal plasticity and potentially for learning and memory (Glanzer and Eberwine, 2003; Steward and Schuman, 2003; Sutton and Schuman, 2006). The presence of ER and Golgi outposts in dendrites fits a model in which locally translated membrane proteins go through local dendritic ER and Golgi for post translational modifications and targeting. Thus one proposed function of dendritic Golgi outposts is processing and targeting of locally synthesized membrane proteins (Hanus and Ehlers, 2008).

A second function proposed for dendritic Golgi outposts is the formation of apical dendrite in hippocampal pyramidal neurons. Hippocampal pyramidal neurons have a single apical dendrite that extends hundreds of microns towards the pia surface and several shorter basolateral dendrites that terminate not far from the soma. Both somatic Golgi and dendritic Golgi are polarized towards apical dendrite in pyramidal neurons. Disruption of this polarity by over expression of GRASP65 disrupts the morphological distinction of apical dendrites and basolateral dendrites (Horton et al., 2005). Since a manipulation that specifically disrupts dendritic Golgi outposts has not been reported, the role of dendritic Golgi outposts in dendrite morphogenesis remains to be determined.

In addition to the role of the secretory pathway in differential growth of dendrites and axons, I attempted to identify the role of dendritic Golgi outposts in dendrite

morphogenesis and study the biogenesis and transport of dendritic Golgi outposts during

my thesis work (Chapters 2 and 3).
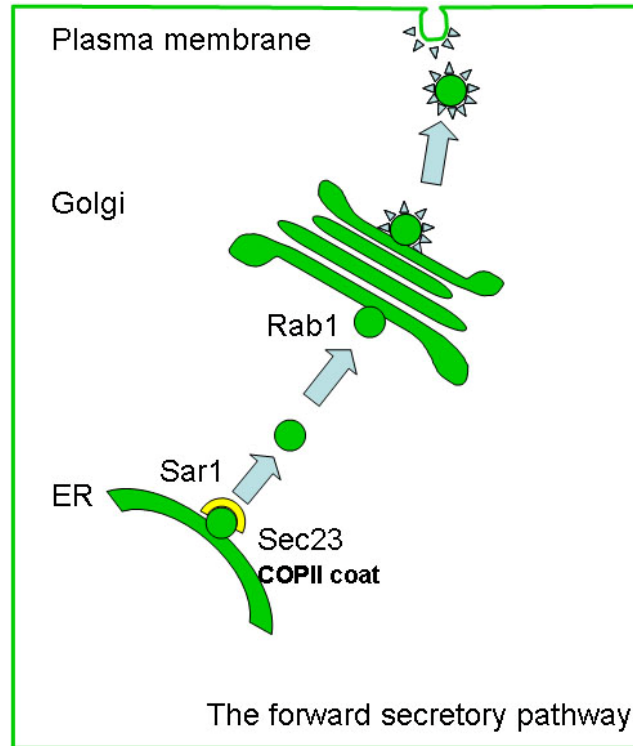
Figure 1-1. The forward secretory pathway.

Membrane protein and secreted protein are synthesized in ER, packaged into COPII coated vesicles, transported to Golgi, where they undergo post-translational modifications and sorting, and then sorted and targeted to different destinations on the plasma membrane. Sar1, Sec23, and Rab1 are required for ER to Golgi trafficking. This figure is modified from an illustration by Bing Ye.
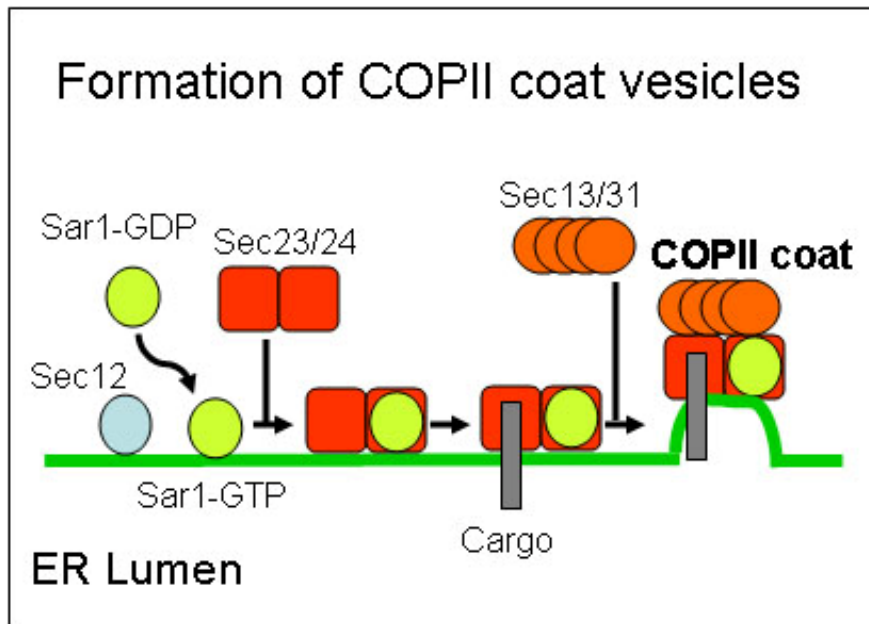
Figure 1-2. Formation of COPII coated vesicles.

Formation of COPII coated vesicles involves the coordinated action of a number of proteins: Sec12 converts a small GTPase, Sar1, to GTP bound form. GTP-Sar1 initiate the formation of COPII coated vesicle by (1) inserting its N-terminal into ER membrane and induce membrane curvature; and (2) recruiting COPII coat components Sec23 and Sec 24. Sec23 is a multi-functional protein. It forms vesicle coat, binds cargo proteins, and promotes the hydrolysis of Sar1-GTP. Sar1-GDP then dissociates coat proteins from a mature vesicle and releases them to the cytosol for the next round of vesicle formation. This figure is modified from an illustration by Bing Ye.

CHAPTER 2: Growing dendrites and axons differ in their reliance on the secretory pathway

Growing dendrites and axons differ in their reliance on the secretory pathway

Bing Ye[1], Ye Zhang[1], Wei Song, Susan H. Younger, Lily Yeh Jan, and Yuh Nung Jan*

Howard Hughes Medical Institute, Departments of Physiology, Biochemistry, and Biophysics, University of California, San Francisco, CA 94143, USA

*Correspondence: yuhnung.jan@ucsf.edu; 415-476-8747 (phone), 415-476-5774 (fax)

[1] These authors contributed equally to this work.

Summary

Little is known about how the distinct architectures of dendrites and axons are established. From a genetic screen, we isolated *dendritic arbor reduction* (*dar*) mutants with reduced dendritic arbors but normal axons of *Drosophila* neurons. We identified *dar2*, *dar3*, and *dar6* genes as the homologs of *Sec23*, *Sar1*, and *Rab1* of the secretory pathway. In both *Drosophila* and rodent neurons, defects in *Sar1* expression preferentially affected dendritic growth, revealing evolutionarily conserved difference between dendritic and axonal development in the sensitivity to limiting membrane supply from the secretory pathway. Whereas limiting ER to Golgi transport resulted in decreased membrane supply from soma to dendrites, membrane supply to axons remained sustained. We also show that dendritic growth is contributed by Golgi outposts, which are found predominantly in dendrites. The distinct dependence between dendritic and axonal growth on the secretory pathway helps to establish different morphology of dendrites and axons.

Introduction

Dendrites and axons, two major compartments of neurons, exhibit a number of morphological distinctions. Little is known about how the structural differences between dendrites and axons are established. The growth of dendrites and axons likely involves coordinated cytoskeletal reorganization and membrane trafficking (Bradke and Dotti, 2000a; Lecuit and Pilot, 2003). The cytoskeleton is organized differently in dendrites and axons (Baas et al., 1988). Furthermore, the cytoskeleton regulators RhoA (Lee et al., 2000) and MAP2 (Harada et al., 2002) preferentially control dendritic growth. It may also be important to regulate the membrane supply for dendrites and axons differently to establish their different morphology.

The secretory pathway, which includes the endoplasmic reticulum (ER), Golgi complex, and post-Golgi intermediates (van Vliet et al., 2003), is the major source of plasma membrane. Unique to neurons is the presence of an additional satellite secretory pathway, including ER and Golgi outposts, in dendrites (Aridor et al., 2004; Gardiol et al., 1999; Horton and Ehlers, 2003). Golgi outpost has so far not been found in axons (Horton and Ehlers, 2003), raising the question whether the polarized distribution of Golgi in neurons plays a role in the differential development of dendrites and axons. Recent findings suggest an active role of the polarized secretory trafficking in the formation of specific

compartments of the dendritic arbors (Horton et al., 2005). Whether the secretory pathway also plays a role in distinguishing the growth of dendrites and axons is an important open question. Furthermore, whether dendritic Golgi outposts are required for dendritic growth and thus contribute to the generation of distinct dendrite and axon morphology is still unknown.

From a large scale genetic screen by taking advantage of a highly specific marker for the class IV dendritic arborization (da) neurons in *Drosophila*, we isolated 8 complementation groups of *dendritic arbor reduction* (*dar*) mutants, which share a common phenotype of reduced dendritic arbors but normal axonal growth. Strikingly, 3 of the 5 *dar* genes that we have so far identified molecularly encode critical regulators of the forward secretory pathway. Mosaic analysis revealed that these genes function cell-autonomously to regulate both dendritic growth and the secretory pathway. Similar functions of *Sar1* were observed in cultured mammalian neurons, corroborating the notion that dendritic and axonal growth exhibit distinct sensitivity to changes in ER-to-Golgi transport. We further show that such distinct sensitivity involves preferential reduction of membrane transport from soma to dendrites upon global reduction in ER-to-Golgi transport, and requirement of Golgi outposts for dendritic growth.

Results

Dendritic and axonal growth exhibit distinct sensitivity to the reduction of ER-to-Golgi transport in da neurons *in vivo*

We recently carried out a genetic screen to identify mutants with defects in dendritic and/or axonal development (Grueber et al., 2007) by taking advantage of the highly specific marker for the class IV da neurons in *Drosophila* peripheral nervous system (PNS), *pickpocket*-EGFP (*ppk*-EGFP) (Grueber et al., 2003b). These neurons resemble mammalian neurons in morphological and cell biological features, such as multipolar morphology and the tapering of dendrites but not axons, making them a suitable model to study the differential development of dendrite and axon.

From 3299 3rd chromosomes carrying lethal mutations, we isolated 12 mutants that showed defects in dendritic but not axonal growth (Figure 2-1A). These 12 mutants fell into 8 complementation groups, which we named *dendritic arbor reduction* (*dar*) *1-8* (Table 2-1). Through genetic mapping and molecular characterization, we identified 3 *dar* genes, namely *dar2*, *dar3*, and *dar6*, as the *Drosophila* homologs of *Sec23*, *Sar1*, and *Rab1*, respectively (Supplemental data and Figure 2-7 & 2-8), all of which are critical regulators of ER-to-Golgi transport mediated by the COPII vesicles (Lee et al., 2004). Defects in the functions of Sar1 (Zaal et al., 1999), Rab1 (Wilson et al., 1994), or Sec23

(Morin-Ganet et al., 2000) result in dispersion of Golgi complexes. We focused on Sar1/Dar3 in subsequent studies, because Sar1 is the primary component that initiates the formation of COPII coated vesicles for forward trafficking from ER to Golgi.

We examined *dar3* functions in da neurons by mosaic analysis with a repressible cell marker (MARCM) (Lee and Luo, 1999). We incorporated a Golgi marker, α-mannosidase II-EGFP (ManII-EGFP) (Velasco et al., 1993) into this analysis in addition to the membrane marker mouse CD8-dsRed (mCD8-dsRed) for marking neuron morphology. We refer to this assay as Golgi-MARCM.

The Golgi-MARCM analysis revealed that class IV da neurons with defective *dar3* exhibited reduced dendritic arbors (Figure 2-1B), demonstrating that *dar3* gene is cell-autonomously required for dendritic growth. The class IV neuron ddaC normally had a total dendrite length of 10,016 ± 633 μm (n=3; data represent mean ± standard error of means in this paper). The total dendritic length of *dar3* mutant neurons was reduced to 1,488 ± 171 μm (n=3), only 14.9% of control (Figure 2-1E).

In contrast to the dramatic reduction in dendritic growth, the axonal growth appeared normal except for subtle changes in the terminals. As the animal increases from ~ 0.5 to ~ 4 mm in length from embryonic to 3rd instar larval stages, the axons of da neurons extend in proportion between the body wall and the ventral nerve cord (VNC), where

short terminal projections form a simple arbor (Grueber et al., 2007). From early 1st instar stage (24 hr after egg laying, AEL) to late 3rd instar stage (112 hr AEL) the axons of the ddaC neurons in abdominal segment 5 (A5) grew from 384 ± 41 to 2,151 ± 64 µm (Figure 2-1D). During this period of extensive axonal growth, the axons of *dar3*-deficient ddaC neurons not only grew into the VNC but also formed projections that were comparable to those of wild-type neurons except that the short fibers which resemble filopodia were often missing (Figure 2-1C-b). In VNC, the ddaC (segments A3-A5) terminal projection contains one anterior, one contra-lateral, and, in some cases, one posterior branch (Figure 2-1C-a). Several (7.5 ± 0.7, n=4) short and fine fibers, resembling filopodia, originate from these terminal branches. The average total length of axonal terminals of *dar3* mutant ddaC neurons (44.3 ± 5.5 µm, n=7), excluding the filopodium-like fibers, was comparable to that of wild-type ddaC neurons (45.8 ± 7.0 µm, n=4, p>0.05) (Figure 2-1F). The filopodium-like fibers, with a total length of 24.8 ± 3.5 µm (n=4), comprise only a small fraction of total axonal length (1.2%). In contrast to this minor reduction in filopodium-like structures at the axonal endings, the reduction of dendritic arbors in *dar3* mutant neurons by 8,528 µm, which is 85.1% of the total dendritic length (Figure 2-1E), was much greater in extent.

Our Golgi-MARCM experiment also showed that discrete Golgi structures in the soma were replaced by diffuse distribution of the marker ManII-EGFP in *dar3* mutant neurons (Figure 2-1B). Similarly, discrete, bright, and round/oval-shaped Golgi outposts in

dendrites, labeled by ManII-EGFP, were replaced by weak and diffuse signal in neurons with defective *dar3* (Figure 2-1G). The diffuse signal covered a greater area than Golgi outposts (3.09 ± 0.62 μm^2 *versus* 0.84 ± 0.06 μm^2 in wild-type neurons, P<0.001) (Figure 2-1H), and took on irregular shape with an average circularity of 0.45 ± 0.04, unlike Golgi outposts which normally have an average circularity of 0.71 ± 0.03 (P<0.001) (Figure 2-1I). Therefore, Sar1 is required for normal morphology of both somatic Golgi and dendritic Golgi outposts.

Dendritic and axonal growth exhibit distinct sensitivity to the reduction of ER-to-Golgi transport in cultured hippocampal neurons

In most neurons, the initiation of axonal growth precedes that of dendrites. One potential cause of the observed "dar" phenotype is that the maternally contributed Dar proteins in the embryos rescued defects in axonal growth but was insufficient to rescue dendritic growth. We eliminated maternal contribution by generating mosaic clones defective of *dar3* or *dar6* in germline cells but found that females with such mutant germline cells were sterile, thus precluding us from examining the dendrite phenotype of germline clones.

To test whether temporal differences between dendritic and axonal growth account for the "dar" phenotype, we need to alter *dar* gene function when both dendrites and axons actively grow. In the MARCM experiments described above, the da neurons were born

during early embryogenesis and imaged several days later in 3rd instar larvae. During this period, both dendrites and axons grow extensively (Figure 2-1D). Despite the dramatic reduction in the dendrite length, these *dar3*-defective class IV da neurons had normal total axon length. These results suggest that dendritic and axonal growth indeed exhibit different dependence on the *dar3* gene.

Another system in which the function of *dar* genes could be altered when both dendrites and axons actively grow is the hippocampal neuronal culture. Although the initiation of axonal growth is also earlier than dendrites, there is an extensive period in which both axons and dendrites actively grow after 2 days in vitro (DIV) (Dotti et al., 1988). In our system, dendritic length increased by 194.4 μm, and axonal length increased by 2939.9 μm from 2 (n=19) to 7 DIV (n=47) (Figure 2-2A). To interfere with ER-to-Golgi transport, we generated small interfering RNAs that specifically and effectively knocked down the expression of Sar1 (Sar1-siRNA) (Figure 2-9). After introduction into cultured neurons at 2 DIV, Sar1-siRNA reduced endogenous Sar1 protein level to 42% at 5 DIV compared to control neurons. Knockdown of Sar1 also caused dispersion of Golgi complex in cultured neurons (Figure 2-2B), consistent with findings from non-neuronal cells (Ward et al., 2001).

Reducing Sar1 protein level in hippocampal neurons dramatically decreased the total length of dendrites but not axons as revealed by double-blind analysis (Figure 2-2C and

D). At 5 DIV, total dendritic length of control and Sar1-siRNA-transfected neurons were 185.6 ± 15.0 μm and 109.7 ± 11.7 μm, respectively (P<0.01, ANOVA), while total axonal length were 861.3 ± 60.1 μm (n=37) and 964.7 ± 86.0 μm (n=15) (p>0.05, ANOVA), respectively. A siRNA-resistant Sar1a construct (Sar1a^R) rescued the dendrite and Golgi defects (Figure 2-2B-D & 2-9) (dendrite length=203.1 ± 16.8 μm, p>0.05; axon length=880.8 ± 67.9 μm, P>0.05, ANOVA), suggesting the siRNA knockdown was specific. Comparison of dendrite and axon length between control and Sar1-siRNA-expressing neurons at 3, 4, 5, and 6 DIV revealed that dendrites ceased to extend following knockdown of Sar1 (Figure 2-2E) while axons continued to grow normally (Figure 2-2F). Thus, reducing Sar1 expression in hippocampal neurons significantly reduced dendrite length but not axon length, revealing different dependence of dendritic and axonal growth on the secretory pathway in mammalian neurons as in *Drosophila* neurons.

Supply of membrane labeled by mCD8-GFP was adjusted unequally between dendrites and axons in response to perturbation of secretory pathway function

To test how the membrane supply to dendrites and axons may be adjusted upon reducing the activity of secretory pathway, we employed fluorescence recovery after photo-bleaching (FRAP) analysis in rat hippocampal neurons and examined the effects of Sar1-siRNA. FRAP monitors the traffic of molecules into a selected area that has previously been photo-bleached (Lippincott-Schwartz et al., 2001). To examine

membrane supply from soma to dendrites and axons, including both intracellular vesicle transport and lateral diffusion of plasma membrane, we marked membrane with the fluorescent transmembrane protein mCD8-EGFP. Photo-bleaching of the EGFP signal was carried out for the entire dendritic and axonal arbors but not the soma. The fluorescence recovery in dendrites and axons, due to supply from the soma, was monitored immediately following photo-bleaching over a 15-min period. We sampled fluorescence recovery at proximal dendrites and axons (5 μm away from the soma) as an indicator of the amount of membrane passing through this segment as well as the limited amount of membrane being added to this segment (Figure 2-3A). Control neurons exhibited comparable rate and extent of fluorescence recovery in dendrites and axons (Figure 2-3B). However, Sar1-siRNA significantly reduced the delivery of fluorescent membrane proteins from soma to dendrites, without affecting the supply to axons (Figure 2-3B), as evident from quantitation of the maximal percentage of recovery (control dendrites: 27.0 ± 1.7; Sar1-siRNA dendrites: 18.6 ± 2.0; $P<0.01$, t-test; control axons: 26.5 ± 2.7; Sar1-siRNA axons: 25.7 ± 4.6; $P>0.05$) and the time constant (control dendrites: 129.7 ± 13.4 sec; Sar1-siRNA dendrites: 185.6 ± 25.5 sec; $P<0.05$, t-test; control axons: 118.6 ± 22.1 sec; Sar1-siRNA axons: 113.1 ± 26.6 sec; $P>0.05$) (Figure 2-3C). These results suggest that the membrane supply from soma to dendrites and axons, at least that labeled by mCD8-GFP, is regulated in an unequal way upon reduction in secretory pathway activity.

Directional movements of dendritic Golgi outposts correlate with the extension and retraction of dendritic branches

The secretory pathway in neurons contains not only ER and Golgi in the soma, but also a satellite secretory pathway in dendrites (Gardiol et al., 1999; Horton and Ehlers, 2003; Pierce et al., 2001). Given the enrichment of Golgi outposts in dendrites over axons in mammalian neurons (Horton and Ehlers, 2003), we explored the possibility that Golgi outposts contribute to dendritic growth. In class IV da neurons, Golgi outposts appeared as punctate structures in both major and fine terminal dendritic branches but rarely in the axons (Figure 2-4A & C). They were often enriched at dendritic branching points, While the primary dendrites contained 10.34 ± 1.34 (n=13) Golgi outposts per 100 μm, the proximal 100 μm of the axon contained only 1.00 ± 0.32 (n=5) (Figure 2-4B).

To characterize the involvement of Golgi outposts in dendritic growth, we monitored the behavior of Golgi outposts during branch extension and retraction by time-lapse imaging in live *Drosophila* larvae. We found a strong correlation between Golgi outpost dynamics and dendritic branch dynamics. Specifically, a branch either extended or remained stable after the Golgi outposts moved distally or appeared *de novo* within the branch (Figure 2-4C & D) (extension: 32.4%; stable: 67.6%; retraction: 0%; n = 34), while the majority of the branches retracted after the Golgi outpost moved proximally or disappeared (Figure 2-4C & D) (extension: 5.9%; stable: 23.5%; retraction: 70.6%; n=17). An interesting implication of this finding is that dendritic Golgi outposts could contribute to

the supply of the membrane needed for branch growth in their vicinity. Outposts move distally or proximally prior to the extension or retraction of the dendritic branches, serving as a mobile station for membrane traffic.

Dendritic Golgi outposts are important for the dynamics of dendritic branches

To test whether the function of Golgi outposts is required for dendritic growth, we attempted to damage Golgi outposts with laser. Terminal branches of class IV da neurons are highly dynamic. In 3rd instar larvae, $20.8 \pm 5.9\%$ branches showed extension (>0.5 μm) and $41.7 \pm 7.1\%$ branches showed retraction (>0.5 μm) over a period of just 5 minutes (n=48) (Figure 2-5B & C). After Golgi outposts labeled by β-1,4-galactosyltransferase:EYFP (GalT-EYFP) were focally illuminated by intense laser, most of the branches did not extend or retract (percentage of branches that extended = $5.0 \pm 4.9\%$, percentage of branches that retracted = $5.0 \pm 4.9\%$, n=20). To confirm that the reduction of branch dynamics resulted from damage to Golgi outposts, we illuminated dendritic regions lacking a Golgi outpost (extension: $22.6 \pm 7.5\%$; retraction: $38.7 \pm 8.8\%$; n=31), regions labeled by actin-GFP (extension: $30.0 \pm 10.3\%$; retraction: $25.0 \pm 9.7\%$; n=20), or mito-GFP (a mitochondria marker) (Cox and Spradling, 2003) (extension: $23.8 \pm 9.3\%$; retraction: $23.8 \pm 9.3\%$; n=21),with the same laser energy used in damaging Golgi outposts (Figure 2-5A). Neither the extension nor the retraction of dendritic branches showed significant change after any of these control illuminations

compared to dendrites without laser illumination (p>0.05) (Figure 2-5B & C). Despite

that the nature and extent of laser damages to Golgi outposts remain unclear, Golgi

outposts appeared to be the most sensitive locations for affecting dendritic branch

dynamics among all the targets tested. We thus conclude that dendritic Golgi outposts are

important for the extension and retraction of dendritic branches.

**Redistribution of dendritic Golgi outposts correlates with morphological changes of
dendritic arbors**

To further test whether Golgi outposts are critical for dendritic growth, we examined the

effect of redistributing Golgi outposts. The positioning of Golgi complex involves

several molecular motors, among which dynein has the major role (Allan et al., 2002).

The cargo specificity of dynein relies on the dynactin complex (Schroer, 2004). In

Drosophila, Lava lamp (Lva) mediates the interactions between Golgi and the

dynein/dynactin complex (Papoulas et al., 2005).

We found that Lva protein was expressed in da neurons and was located juxtaposed to

ManII-EGFP, which labels the medial/trans-Golgi (Figure 2-10). We reasoned that

blocking the function of Lva could impair the transport and thus change the distribution

of Golgi outposts in da neurons. We took two different approaches to test this. First, we

expressed a dominant negative form of Lva (Lva^{DN}) in class IV da neurons to disrupt

Lva-dynactin interaction. Lva^{DN} is a coiled-coil portion of Lva that binds the dynactin

complex and has been shown to interfere with dynein-based movement of Golgi during cellularization (Papoulas et al., 2005). Second, we knocked down Lva expression using inducible RNAi. To achieve RNAi-mediated knockdown, we generated two transgenic lines that expressed inverted repeats, each targeting a distinct part of the *lva* mRNA (UAS-Lva-RNAi[1] and UAS-Lva-RNAi[2], see Supplemental Experimental Procedures), and tested an additional line from the Vienna *Drosophila* RNAi center (VDRC). All three lines showed similar phenotypes.

When expressed in class IV da neurons, both Lva[DN] and Lva-RNAi[1] altered the distribution of Golgi outposts. In the distal part of dendritic arbors, both Lva[DN] and Lva-RNAi[1] reduced the size of Golgi outposts (control: 1.66 ± 0.24 μm^2 per 100 μm of dendrites, n=6; Lva[DN]: 0.49 ± 0.21 μm^2, n=5; Lva-RNAi[1]: 0.59 ± 0.18 μm^2, n=8; p<0.01) (Figure 2-6A & B). In proximal dendrites, Lva[DN] caused an increase of the size of Golgi outposts whereas Lva-RNAi[1] caused a reduction (control: 5.46 ± 1.27 μm^2 per 100 μm of dendrites, n=11; Lva[DN]: 10.83 ± 1.36 μm^2, n=20; Lva-RNAi[1]: 2.47 ± 0.67 μm^2, n=13; p<0.05) (Figure 2-6A & C). No change in the number and size of somatic Golgi was observed in either Lva[DN]- or Lva-RNAi[1]-expressing neurons (Figure 2-6D & 2-11).

Parallel to the redistribution of Golgi outposts, there were changes in dendritic branches in the Lva[DN]- and Lva-RNAi[1]-expressing neurons (Figure 2-6E). In both Lva[DN]- and Lva-RNAi[1]-expressing neurons, the number of dendritic branches in distal dendrites was

dramatically reduced, while that in proximal dendrites was increased in Lva[DN]-expressing neurons and decreased in Lva-RNAi[1]-expressing neurons. Alterations in dendritic growth were quantified by the Sholl analysis (Sholl, 1953) (Figure 2-6F), which determines the number of intersections between dendritic branches and circles centered at the soma. The number of intersections between distal dendrites and a 180 μm-radius circle was 48.5 ± 3.7 in control (n=4), 17.0 ± 4.3 in Lva[DN] (n=4) ($p < 0.05$), and 25.5 ± 1.4 in Lva-RNAi[1] (n=4) ($p < 0.01$) (Figure 2-6G). The number of intersections between proximal dendrites and an 80 μm-radius circle was 28.5 ± 3.3 in control (n=4), 39.0 ± 1.4 in Lva[DN] (n=4) ($p < 0.01$), and 9.0 ± 1.2 in Lva-RNAi[1] (n=4) ($p < 0.01$) (Figure 2-6H). As a result, total dendritic length was reduced in both Lva[DN]- and Lva-RNAi-expressing neurons (control: $12,600 \pm 810$ μm; Lva[DN]: $7,964 \pm 452$ μm, $p<0.01$; Lva-RNAi: $5,828 \pm 351$ μm, $p<0.001$) (Figure 2-6I). Similar results were obtained with UAS-Lva-RNAi[2], which targets a distinct region of *lva* mRNA, and the VDRC line, confirming the specificity of the RNAi effects (data not shown). Thus, the effects of Lva[DN] and Lva-RNAi on dendritic branching (Figure 2-6G & H) correlated very well with the effects on Golgi outpost redistribution (Figure 2-6B & C).

Interestingly, numerous Golgi outposts were also found in proximal axons of neurons expressing Lva[DN] (Figure 2-6J). Parallel to this, exuberant branching was observed in the proximal segment of the axons but not in the middle and distal segments. These branches are likely axons rather than ectopic dendrites because the dendritic marker,

Nod:βGalactosidase (Nod:βGal) (Clark et al., 1997), was absent from these branches (Figure 2-12). We also examined the distal axonal projection pattern and found that the axons in Lva^{DN} expressing neurons reached the VNC and formed normal projection patterns (data not shown).

Taken together with the correlation between dendritic growth dynamics and Golgi outpost movement and the impaired dendritic branch dynamics caused by laser-damaging of Golgi outposts, these results underscore the importance of these components of dendritic satellite secretory pathway in dendritic growth.

Discussion

In the present study, we demonstrated that growing dendrites and axons display different sensitivity to changes in the activity of the secretory pathway. Our findings add to the accumulating evidence that the secretory pathway is involved in cell polarity and provide one of the first evidence of the importance of the satellite secretory pathway in dendrite development.

Roles of the secretory pathway in cell polarity

The secretory pathway is important for cell polarity. For example, during the cellularization of *Drosophila* embryos, membrane growth is tightly controlled in a polarized fashion (Lecuit and Wieschaus, 2000). New membrane produced through the secretory pathway is predominantly added to the apical side early in polarization and to the lateral side at later stages. Other examples of targeted membrane transport during cell polarization include the apical-basolateral polarization of Madin-Darby canine kidney epithelial cells (Simons and Fuller, 1985), cell cycle of the budding yeast (Finger et al., 1998), and cell migration (Kupfer et al., 1982). Thus, membrane trafficking is tightly controlled in order to supply membrane to specific subcellular compartments of polarized cells.

The establishment of dendritic and axonal arbors is a major compartmentalization process of neurons. Before dendrites and axons are formed, selective delivery of post-Golgi vesicles to one neurite precedes the specification of that neurite as the axon (Bradke and Dotti, 1997). After axon specification, large amount of plasma membrane is added to these two compartments with distinct architecture. Whether the secretory pathway is involved in the differential growth of dendrites and axons is an important but poorly understood question. Horton et al. (2005) found that blockade of post-Golgi trafficking by expressing a dominant-negative protein kinase D1 (PKD-KD) causes a preferential reduction in dendritic growth. Although this result may appear similar to our results from manipulation of Sar1 function, there is in fact an important difference. PKD is required for cargo trafficking to the basolateral but not the apical membrane in epithelial cells (Yeaman et al., 2004). Since the targeting of dendritic proteins shares some of the mechanisms of the basolateral protein transport in epithelial cells (Dotti and Simons, 1990), PKD-KD may only affect dendrite-specific cargo transport. In this study, we assessed how membrane resource is allocated between growing dendrites and axons when global membrane production is limited. It is possible that the efficiency of dendrite- and axon-specific transport, including those mediated by PKD, changes differently in response to global restriction of membrane resource.

Distinct membrane dynamics in growing dendrites and axons

The plasma membrane of cells can be inserted via exocytosis and internalized through endocytosis. The expansion of plasma membrane in growing dendrites and axons is achieved through the interplay between these two antagonistic processes. Before dendrites are formed in cultured hippocampal neurons, membrane is selectively added to the growth cone of growing axons as well as minor neurites that will later become dendrites (Craig et al., 1995). In more mature neurons, there is insertion of new membrane to the axonal growth cone but not to the dendritic growth cone (Craig et al., 1995). This raises the possibility that plasma membrane is added to either multiple sites along the dendritic surface or throughout the dendritic surface. It is conceivable that dendritic Golgi outposts play a role in such membrane addition given their requirement for dendritic growth as shown in this study.

It has been reported that plasma membrane of cultured hippocampal neurons is internalized throughout the dendrites but only in the presynaptic terminals in axons (Parton et al., 1992). Parton et al. also found that essentially all internalized structures, from both dendritic and axonal surface, move in the retrograde direction to the soma. We compared the rate of membrane removal from dendritic and axonal surfaces and found that, consistent with Parton et al. (1992), endocytosis is more prominent in dendrites than in axons (Figure 2-14). The plasma membrane of dendrites was endocytosed 8.27 ± 1.79 (n=3) times faster than that of axons at 3 DIV. Thus, the demand for membrane supply to

dendrites is likely greater than what appears based on the length of dendrites.

The difference in the ways that membrane is supplied to growing dendrites and axons is poorly understood. Notwithstanding much progress made on dendritic traffic of the temperature sensitive mutant of the vesicular stomatitis virus glycoprotein (VSVG) fused to GFP (Horton and Ehlers, 2003; Horton et al., 2005), the preferential targeting of VSVG to dendrites (Dotti and Simons, 1990) precludes its application for comparing dendritic and axonal membrane dynamics. In this work, we compared the membrane supply from soma to dendrites and axons using the FRAP analysis. We sampled fluorescence recovery in the dendritic and axonal segment 5 µm away from the soma as an indicator of the amount of the membrane passing though this segment. The sampling approach was taken because even with moderate magnification (20X) only a fraction of the arbors can be included in the imaging field, precluding the monitoring of fluorescence recovery along the entire dendritic and axonal arbor. This FRAP analysis revealed that, when the secretory pathway function is limiting, membrane supply from soma to growing dendrites is preferentially affected.

Notably, the secretory pathway with reduced activity could still provide sufficient membrane to support axonal growth at least during the period described in this study. It is possible that there are mechanisms involving post-Golgi carriers to allocate different amount of membrane to dendrites and axons. Alternatively, endocytosed dendritic

membrane can also support axonal growth via the transcytosis pathway (Bartheld, 2004). Lastly, trafficking that bypasses COPII-based ER to Golgi transport (Hasdemir et al., 2005), although not widely observed, might also contribute to axonal growth.

Function of dendritic Golgi outposts in dendritic growth

The finding that Golgi outposts are present in dendrites has generated great interests in the function of these structures. Two main functions have been proposed for Golgi outposts. One hypothesis is that they are involved in local protein translation (Steward and Schuman, 2003). This is supported by the presence of protein synthesis machinery in the dendrites (Steward and Levy, 1982; Steward and Reeves, 1988) and findings of local translation of membrane proteins in dendrites (Eberwine et al., 2001; Raab-Graham et al., 2006). Recently, Horton et al. (2005) suggest that Golgi outposts, together with somatic Golgi complex, participate in forming the apical dendrites of pyramidal neurons.

In this study, we monitored the dynamics of Golgi outposts in intact neurons of live *Drosophila* larvae and observed that the direction of outpost movement correlates with dendrite branch dynamics. This suggests that Golgi outposts are probably involved in both the extension and retraction of a dendritic branch. Indeed, laser damaging of the outposts in a branch reduced branch dynamics, making the dendrite excessively stable, which will lead to retarded growth during the expansion of dendritic arbors. It should be

noted that, in our laser damaging experiments, the nature and extent of damages to Golgi outposts are unclear. It is indeed technically challenging to manipulate organelle function in a small, localized subcellular region. We consider the laser damaging experiment one of the first attempts of such manipulations. Although we can conclude that Golgi outposts are the most sensitive locations for affecting dendritic branch dynamics among the various target locations, alternative approaches are needed to test the function of Golgi outposts. In the present study, we complemented the laser damaging experiment with genetic manipulations to redistribute Golgi outposts. We found that dendritic branching patterns changed with the redistribution of Golgi outposts by Lva^{DN} and Lva-RNAi. High level of Lva^{DN} expression led to the strongest defect in Golgi outpost distribution and dendritic branching pattern (Figure 2-13). Although it is difficult to rule out the contribution of non-specific effects of Lva^{DN}, there is very good correlation between the distribution of Golgi outposts and that of dendritic branches in neurons with varying extent of disruption of Lva function. These findings underscore the importance of Golgi outposts in dendritic growth.

It remains unclear how Golgi outposts are produced, transported to dendrites, and largely excluded from axons. Our results on Lva suggest that they are probably produced in the soma and transported to dendrites. The presence of Golgi outposts in axons of Lva^{DN}-expressing neurons suggest that they might be actively transported out of axons

under normal condition. The absence of Golgi outposts and exuberant branches in the proximal axons of neurons expressing Lva-RNAi is likely due to partial interference of Lva function as similar phenotype was seen in neurons expressing low level of Lva^{DN} (Figure 2-13). The increase in the size of Golgi outposts and dendritic branches in neurons expressing high level of Lva^{DN} possibly reflect the requirement of Lva-dynactin interaction for the budding of Golgi outposts, a phenomenon that we have observed (data not shown).

Although it is difficult to rule out the presence of outposts that are below the detection sensitivity in this study, axonal Golgi outposts, if any, must be dramatically smaller and/or fewer than dendritic outposts. Therefore, the requirement of Golgi outposts for dendritic growth provides a mechanism to differentially control dendrite and axon growth.

The secretory pathway is possibly under regulation to control dendritic growth

The distinct dependence of dendrites and axons on the secretory pathway, as well as the involvement of Golgi outposts for local dendritic dynamics, raise the possibility that the secretory pathway may be regulated to influence the elaboration of dendrites. Such regulation might involve both genetic programs for specifying intrinsic differences in dendritic patterning of different neurons and activity-dependent modifications of

dendritic arbors.

Several molecules are known to be specifically involved in dendritic but not axonal growth. Some of these molecules function in a neural activity-dependent fashion, such as the calcium/calmodulin-dependent protein kinase IIα (CaMKIIα), the transcription factor NeuroD (Gaudilliere et al., 2004), and the Ca^{2+}-induced transcriptional activator CREST (Aizawa et al., 2004), while others are neural activity-independent such as bone morphogenetic protein 7 (BMP-7) (Lein et al., 1995) and Dasm1 (Shi et al., 2004). It will be important to find out whether the secretory pathway contributes to their regulation of dendritic growth.

In summary, we have demonstrated that dendritic and axonal growth exhibit different sensitivity to changes in membrane supply from the secretory pathway. Our findings raise a number of questions regarding membrane trafficking in dendrite and axon development. Answers to these questions will provide cell biological basis for understanding how the tremendous diversity of neuron morphology is achieved during development and how the changes in morphology happen in pathological conditions.

Experimental Procedures

Genetic screen for *dar* mutants

The procedure for establishing mutagenized *Drosophila* lines and imaging of fly embryos

for da neuron dendrites and axons are described in Grueber et al., 2007 in detail.

Golgi-MARCM

To image neuron morphology and Golgi structure in the same neuron using MARCM

analysis, we crossed *hs-flippase*; UAS-mCD8-dsRed; FRT[82B] tubulin-Gal80 flies with

either GAL4[109-2-80], UAS-ManII-EGFP; FRT[82B] flies to generate control clones or

GAL4[109-2-80], UAS-ManII-EGFP; FRT[82B] *dar3*[11-3-63]/TM6B, Tb to generate mutant clones.

Mosaic clones were generated as described previously (Ye et al., 2004) and examined

either by live imaging or staining with rat anti-mCD8 (for neuron morphology), chicken

anti-GFP (for Golgi complex), and goat anti-HRP crosslinked to Cy5 (for the

morphology of the entire PNS).

Fluorescence recovery after photo-bleaching (FRAP)

Cultured neurons were transfected with pCDNA3 or Sar1-siRNAs together with

mCD8-EGFP and mCherry (Shaner et al., 2004) at 2 DIV and used for FRAP

experiments at 5 or 6 DIV. The neurons were maintained in HEPES-based artificial

cerebrospinal fluid (ACSF) at 35 °C during experiment. FRAP was carried out with a Zeiss LSM510 confocal system with a 20X lens. EGFP signal in dendrites and axons, but not the soma, was photo-bleached by applying a 488 nm laser (66% of full power; 30 mW) for 6.4 μsec per pixel with 150-180 iterations. Immediately after photo-bleaching, images of EGFP-fluorescence were acquired every 30 sec. Intensity of EGFP signal in dendrites and axons was measured at a point 5 μm away from the soma with ImageJ software and the background was subtracted. Only neurites with more than 80% bleaching were used for quantitation. Percent recovery at time point t (R_t) was calculated as (I_t-I_0) x100/(I_i-I_0) where I_t, I_0, and I_i are the fluorescence intensity at time point t, immediately after photobleaching, and before bleaching, respectively. The recovery time course was fit with the following equation by the OriginPro software (OriginLab Co., Northampton, MA): R_t=R∞ x (1-$e^{-t/\tau}$), where R_t is the percentage recovery, R∞ is the maximal recovery, t is time in seconds, and τ is the time constant.

Live imaging of dendritic Golgi outposts

To study the correlation between Golgi outpost movement and dendritic branch dynamics, 3rd instar larvae were mounted in halocarbon oil and imaged with a Zeiss LSM510 confocal system. Images were taken every 30 minutes for 2-6 hours. The larvae were released to a grape juice agar plate between imaging sessions. We followed the movement of Golgi outposts labeled by GalT-EYFP between the tip of a terminal branch and the branch point. When no outpost is present in the branch, we followed the outpost

closest to the branch point. The movement of Golgi outposts was counted if one of the outposts moved in or away from a branch, regardless of the presence of remaining stable outposts in the branch. A dendritic branch was considered stable if its length did not change for more than 0.5 μm since our measurement error was within 0.5 μm.

Laser damaging of dendritic Golgi outposts

Early 3rd instar larvae were used for laser damaging of dendritic Golgi outposts. For efficient damaging of Golgi outposts, terminal branches that contained one or two Golgi outposts were selected. The power of 488 nm-laser was set at 15mW. After laser illumination, the larvae were transferred to a grape-juice agar plate before mounted again for imaging 5 minutes later. Images of the same dendritic region were taken before, immediately after, and 5 minutes after illumination. Laser damaging substantially reduced or eliminated GalT-EYFP, actin-GFP, or mito-GFP signal in every experiment. The length of dendritic branch immediately after illumination and 5 min after illumination was measured.

The statistical analysis of laser damaging data was carried out according to standard methods for analyzing nominal variables (Glantz, 2005). Briefly, standard error σ was calculated as $[r(1-r) /n]^{1/2}$, where r is the percentage of extended or retracted branches, and n is the total number of branches. To test for the difference between two nominal data sets, a value of z was calculated by the equation $z = (r_1-r_2)/ [r_1(1-r_1)/n_1+r_2(1-r_2)/n_2]^{1/2}$,

where r_1 and r_2 are the percentage of extended or retracted branches of the two experimental groups to be compared, and n_1, n_2 are the total number of branches of the two groups. The probability (p) corresponding to the z value was then obtained from the standard normal distribution table.

Acknowledgements

Supplemental Experimental Procedures

1. Mapping *dar2*, *dar3*, and *dar6* mutations

To map the *dar* mutations, we first carried out recombination-based mapping to localize the mutations to genomic regions between the markers of the *ru h th st cu sr e ca* (rucuca) chromosome. We then conducted complementation tests for both lethality and dendrite defects between the mutants and the deficiencies (Df) in these genomic regions.

dar2

We found that Df(3R)BSC47 and Df(3R)Exel7283 failed to complement *dar2*$^{8-2-55}$, which suggested that the *dar2*$^{8-2-55}$ mutation was in the 83B7-83C1 cytological region. A semi-lethal P-element inserted into the *Sec23* gene, P{EPgy2}Sec23^{EY06757}(Figure 2-7B), and a micro-deletion of the *Sec23* gene generated by imprecise excision of this P-element, ΔP{EPgy2}Sec23^{EY06757}-1, each failed to complement the *dar2* mutation in lethality and dendrite defects (Figure 2-7B & 2-8B). We verified by PCR of genomic DNA that the genes flanking *Sec23* were intact in ΔP{EPgy2}Sec23^{EY06757}-1. Furthermore, a precise excision line of P{EPgy2}Sec23^{EY06757} (ΔP{EPgy2}Sec23^{EY06757}) complemented the dendrite defects of *dar2* mutation (Figure 2-8B), confirming that the dendrite defects were not due to other mutations. We sequenced the *Sec23* genomic DNA in *dar2*$^{8-2-55}$ mutant and found a missense mutation (C to T) that results in a serine (S721) being

changed to phenylalanine (F) (Figure 2-7B). S721 is strictly conserved in different species from yeast to human (Figure 2-7B) and at least 6 other *Drosophila* species. The side chain hydroxyl group of S721 physically interacts with aspartate[32] of Sar1, and is critical for the positioning of arginine[724] of Sec23, which facilitates the hydrolysis of GTP that is bound to Sar1 (Bi et al., 2002). Therefore, the S721F mutation is very likely to affect the function of Sec23 as a GTPase activating protein for Sar1.

dar3

The *dar3^{11-3-63}* mutation was first localized to the cytological regions 94A2-A9 or 94D1-D4 by recombination-based mapping and complementation tests with deficiencies (Figure 2-7A). One lethal P-element insertion in the *Drosophila Sar1*(*dSar1*) gene, P{PZ}*Sar1^{05712}*, failed to complement both the lethality and dendrite defects of *dar3^{11-3-63}* mutation, suggesting that the *dar3^{11-3-63}* mutation is in the *dSar1* gene. To verify this assignment, we generated a deletion, ΔP{PZ}*Sar1^{05712}*-1, by imprecise excision of P{PZ}*Sar1^{05712}*. We verified by PCR of genomic DNA that this deletion removed part of the 5'-end exon of *dSar1* but left the genes flanking *dSar1* intact. The trans-heterozygous embryos of ΔP{PZ}*Sar1^{05712}*-1 and *dar3^{11-3-63}* exhibited the same dendrite defects and normal axons as *dar3^{11-3-63}* homozygous mutant did (Figure 2-8A), confirming that ΔP{PZ}*Sar1^{05712}*-1 is an allele of *dar3*.

To confirm that defects in *dar3* gene were responsible for the dendrite phenotype, we

attempted to rescue of *dar3* dendrite defects with a Sar1 transgene. We first generated the

transgenic line UAS-*dSar1*. Overexpression of *dSar1* did not lead to any discernable

defects in dendritic growth (data not shown). To express this transgene in *dar3* mutant

animals, virgin females of *heatshock*-Gal4/Cyo, *Kruppel*-GFP; ΔP{PZ}*Sar1*^{05712}-1/TM3,

Sb, *Kruppel*-GFP were crossed to UAS-*dSar1*/CyO, *Kruppel*-GFP; *dar3*$^{11\text{-}3\text{-}63}$,

ppk-EGFP/TM3, Sb, *Kruppel*-GFP males. Embryos were collected in a grape-juice agar

vial for 2 hrs, aged for 3 hrs at 25°C, heat shocked at 37°C for 1 hr, and then imaged at

late embryonic to early larval stage. As shown in Figure S2A, expression of *dSar1* in

dar3/ΔP{PZ}*Sar1*^{05712}-1 mutants dramatically enhanced dendritic growth.

We then sequenced the coding region of the *dar3*$^{11\text{-}3\text{-}63}$ allele and found a cytidine (C) to

thymidine (T) mutation, which results in a premature stop codon after amino acid

threonine[75] (Figure 2-7A). Given that this truncation leaves out the bulk (118 residues) of

Sar1, including residues forming the nucleotide binding site, which is essential for Sar1

function (Huang et al., 2001), *dar3*$^{11\text{-}3\text{-}63}$ is likely a null allele of *dSar1*.

dar6

Two alleles of *dar6* (*11-4-72* and *12-3-73*) were isolated from the genetic screen. The

trans-heterozygotes of *dar6*$^{11\text{-}4\text{-}72}$ and *dar6*$^{12\text{-}3\text{-}73}$ died in late embryonic stage and

exhibited the same dendrite defects as the embryos homozygous of each allele alone.

Df(3R)e-H4, Df(3R)e-F1, and Df(3R)e-R1 failed to complement *dar6*$^{11\text{-}4\text{-}72}$ and

dar6^{12-3-73} and thus localized the *dar6* mutations to the cytological region between 93D2 and 93D6-7. A lethal piggyBac transposable element inserted in Rab1, PBac{RB}Rab1^{e01287} (Figure 2-7C), failed to complement both lethality and the mutant phenotype (Figure 2-8C). In contrast, a precise excision line of PBac{RB}Rab1^{e01287} complemented the dendrite defects of *dar6* (Figure 2-8C). We sequenced the Rab1 genomic DNA in *dar6^{11-4-72}* and *dar6^{12-3-73}* and found one point mutation in each as compared to the isogenic wild-type allele. A missense mutation (C to T) in *dar6^{11-4-72}* changes a serine (S25) to phenylalanine (F) (Figure 2-7C). The S25 interacts with the phosphate moiety of GTP and is involved in Mg^{2+} coordination required for GTPase activity. A change of S25 into asparagine (S25N) restricted Rab1 to the GDP-bound state and functions as a dominant-negative mutation (Wilson et al., 1994). Thus the mutation in allele *dar6^{11-4-72}* is likely to interfere with the function of Rab1. The allele *dar6^{12-3-73}* has a point mutation (G to A) resulting in the replacement of a glycine (G86) with aspartate (D) (Figure 2-7C). Gly86 is located at the start of a β-strand that is next to the switch 2 domain, which is essential for the interaction with the Rab escort proteins (Chen et al., 2003; Overmeyer et al., 1998). The amino acids mutated in the two *dar6* alleles, S25 and G86, are strictly conserved in different species ranging from yeast, plant, mouse, to human (Figure 2-7C), as expected given their critical roles for Rab1 function.

2. Generation of transgenic fly lines

The UAS-ManII-EGFP and UAS-GalT-EYFP constructs were generated by subcloning

cDNA encoding ManII-EGFP (Bard et al., 2006) and the N-terminal 81 amino acids of human β-1,4-galactosyltransferase (GalT) fused to EYFP into pUAST. To generate UAS-*dSar1* transgenic lines, the coding region of dSar1 was amplified from EST clone RE74312 by PCR and inserted into pUAST.

To generate UAS-Lva^{DN} transgenic lines, the cDNA encoding amino acids from glutamate^{1122} to alanine^{1800} (similar to the Lva3 construct described in (Papoulas et al., 2005)) of *lva* was amplified from the EST clone SD02391 by PCR. Two UAS-Lva-RNAi constructs (UAS-Lva-RNAi^1 and UAS-Lva-RNAi^2) targeting distinct regions of *lva* mRNA were made to generate transgenic lines. The target regions were chosen to avoid any 19 nucleotide that is homologous to the transcript of another gene (Perrimon and Mathey-Prevot, 2007). For UAS-Lva-RNAi^1, genomic DNA encoding amino acids leucine^{1301} to threonine^{1520} (gDNA fragment) was amplified from the genomic DNA of *white*^{1118} flies by PCR and then inserted into pUAST vector at EcoRI and BglII sites. cDNA encoding the same region was amplified from EST clone SD02391 and inserted inversely into the pUAST-gDNA fragment at BglII and KpnI sites. The same approach was applied to make UAS-Lva-RNAi^2 except that the gDNA and cDNA containing alanine^{2481} to aspartate^{2699} were used.

These transformation constructs were then injected into *w*^{1118} embryos, together with a DNA construct encoding the transposase Δ2-3 to generate transgenic flies.

3. Generation of Sar1-siRNAs and siRNA-resistant Sar1 cDNA for studying Sar1 function in rat hippocampal neurons

There are two Sar1 genes, Sar1a and Sar1b, in rodents. To generate siRNAs for knocking down Sar1 gene expression, we first selected 5 and 6 target sequences, each of 19-21 nucleotides in length, in Sar1a and b respectively. Based on these sequences, we synthesized a sense and an antisense oligonucleotides (oligos) for each siRNA. The sense oligo contain the target sequence and its reverse and complementary sequence separated by a loop sequence (TTCAAGAGA). Two nucleotides, T and G, were added to the 5' end so the G can serve as the transcriptional start at +1 position for U6 promoter. The antisense oligo is complementary to the sense oligo and contains a sticky end TCGA at the 5'-end. The sense and antisense oligos were annealed and inserted in vector pLentiLox3.7 at the HpaI and XhoI sites (Rubinson et al., 2003). The oligos used to generate the effective siRNAs used in this study are listed below.

Sar1a-siRNA-1

Sense:TGAACCACTCTTCTTCACATGTTCAAGAGACATGTGAAGAAGAGTGGTT CTTTTTTGGAAC

Antisense:TCGAGTTCCAAAAAAGAACCACTCTTCTTCACATGTCTCTTGAACAT GTGAAGAAGAGTGGTTCA

Sar1b-siRNA-1

Sense:TGAACTACCTTCCTGCTATCATTCAAGAGATGATAGCAGGAAGGTAGTTC

TTTTTTGGAAC

Antisense:TCGAGTTCCAAAAAAGAACTACCTTCCTGCTATCATCTCTTGAATGAT
AGCAGGAAGGTAGTTCA

To screen for the siRNAs that are effective in knocking down Sar1a and Sar1b expression, we first tested their effectiveness on knocking down overexpressed Sar1a and Sar1b tagged with HA-epitope in Cos-7 cells. Rat Sar1a and mouse Sar1b cDNAs were generated by PCR with expressed sequence tag (EST) clones BC079228 and BC082550 (Invitrogen, Carlsbad, CA) as templates, respectively, and inserted at the SalI and NotI sites into the mammalian expression vector pRK5 that contains a HA-tag.

To generate the siRNA-resistant Sar1a construct, a part of Sar1a cDNA which is the target sequence of Sar1a-siRNA-1 "ACTCTTCTT" was site-mutated into "ACCTTGTTG". This change of 5 nucleotides does not change the coding sequence of Sar1a.

4. Hippocampal neuronal culture

Hippocampi from embryonic day 18 Sprague-Dawley rats were digested with 3 mg/ml protease XXIII (Sigma, St. Louis, MO) at 37 °C for 15 minutes and then dissociated in the plating medium (10% fetal bovine serum/0.45% sucrose/5 mM sodium pyruvate/25 μM L-glutamine/Penicillin-Streptomycin/MEM Earle medium). Cells were plated at a density of $10^5/cm^2$ on coverslips coated with poly-D-lysine (Sigma, St. Louis, MO) and

rat tail collagen (Roche, Indianapolis, IN). The medium was changed to the serum-free medium 3 hrs after plating. The serum-free medium contained Neurobasal media supplemented with B27 (Invitrogen, Carlsbad, CA) and 0.5 mM L-glutamine. Ten micromoles of Fluorodeoxyuridine and 10 μM of uridine were added to the culture about 48 hrs after plating to inhibit glia proliferation and were included in media thereafter (Devon, 2001).

5. Endocytosis assay

Cultured hippocampal neurons were transfected with a construct that encodes mCherry driven by CMV promoter at 2 DIV. At 3 DIV, the neurons were incubated with 2.5 mg/ml lysine-fixable Dextran conjugated to Rhodamine Green (10,000 MW) (Invitrogen, Eugene, OR) (Jurney et al., 2002) and 1mg/ml Cy5-conjugated transferrin (Invitrogen) for 10 minutes. Immediately after the incubation, the cells were washed with ice-cold 1X PBS once, ice-cold 500mM NaCl/0.2N acetic acid in PBS for three times, and ice-cold 1X PBS twice before being fixed with 4% PFA/4% sucrose in PBS (Cowan et al., 2005).
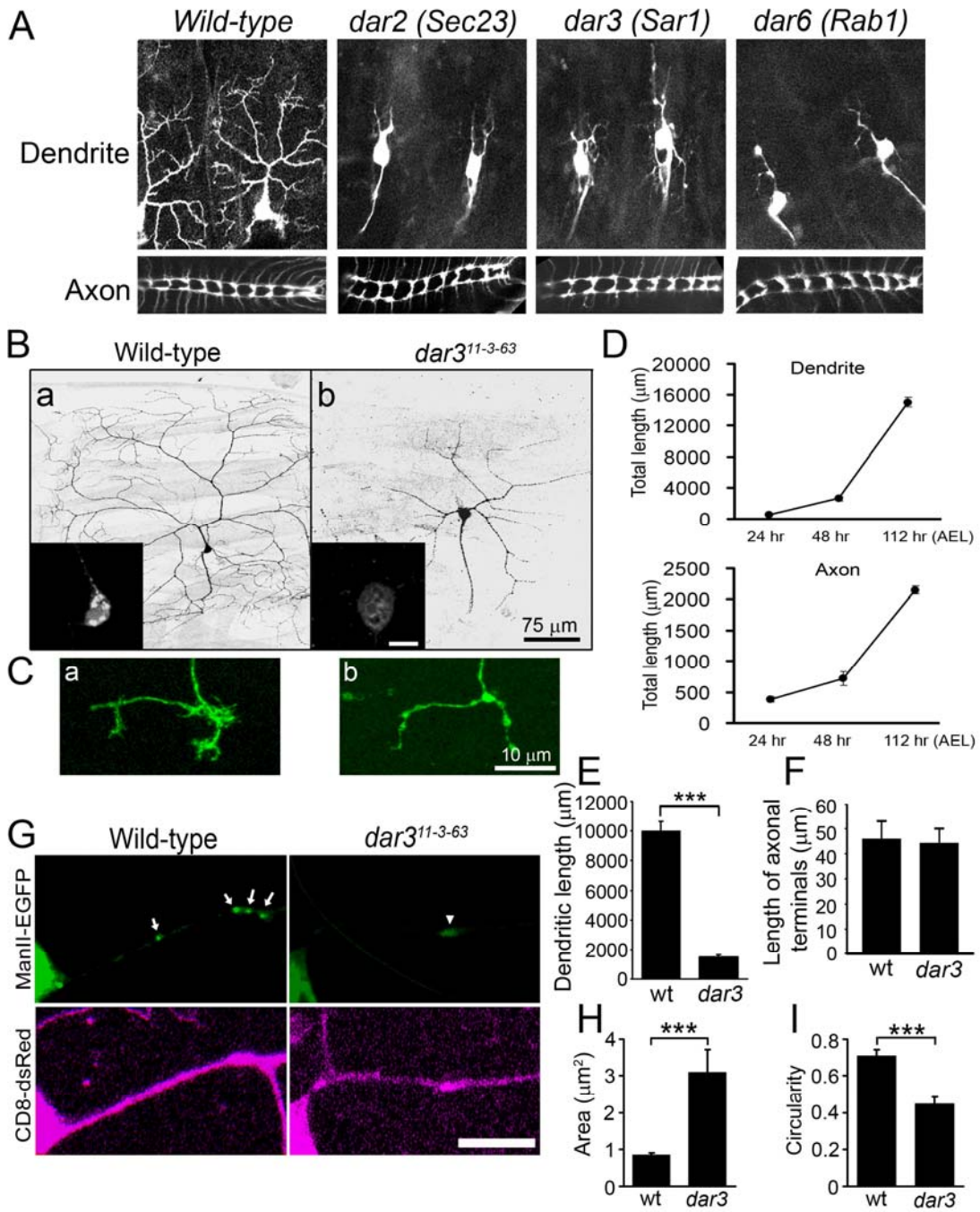
Figure 2-1. Dendritic and axonal growth exhibit distinct sensitivity to the reduction of ER-to-Golgi transport in da neurons *in vivo*. (A) Dendritic arbors (top panels) and axon terminal projections (bottom panels) of class IV da neurons in wild-type, *dar2*, *3*, and *6* mutant embryos (stage 17). (B) Dendrite morphology of wild-type (a) and *dar3*[11-3-63] mutant (b) mosaic clones generated by Golgi-MARCM. Scale bar: 75 μm. The insets show the somatic Golgi structure labeled by ManII-EGFP. Scale bar: 10 μm. (C) Axonal terminals of wild-type (a) and *dar3*[11-3-63] mutant (b) ddaC neurons. Scale bar: 10 μm. (D) Time course of dendritic and axonal growth of class IV ddaC neurons (segment A5) during larval development. For larvae cultured at 25°C, 24 hr, 48 hr, and 112 hr after egg laying (AEL) correspond to early 1st, 2nd, and late 3rd instar, respectively. Error bars represent S.E.M. in this paper. N=3. (E) Quantitation of total dendritic length of wild-type (wt) and *dar3* mutant ddaC neurons. The dendritic arbors of wild-type neurons that were quantified here did not include the fine braches close to the segment borders for the convenience of image collection. "*", "**", and "***" indicate $p<0.05$, 0.01, and 0.001, respectively, in this paper. t-test was used in this paper unless otherwise specified. (F) Quantitation of the length of axonal terminals excluding filopodium-like structures ($p>0.05$). (G) Discrete Golgi outpost structures are replaced by diffuse ManII-EGFP signal in the dendrites of *dar3*[11-3-63] mutant neurons. Arrows point to Golgi outposts in a wild-type neuron and the arrowhead points to diffuse ManII-EGFP signal in a *dar3* mutant neuron. Scale bar: 10 μm. (H-I) Quantitation of the size (H) and circularity (4π X area/perimeter^2) (I) of Golgi outposts in wild-type neurons and diffuse ManII-EGFP

signal in *dar3* mutant neurons.
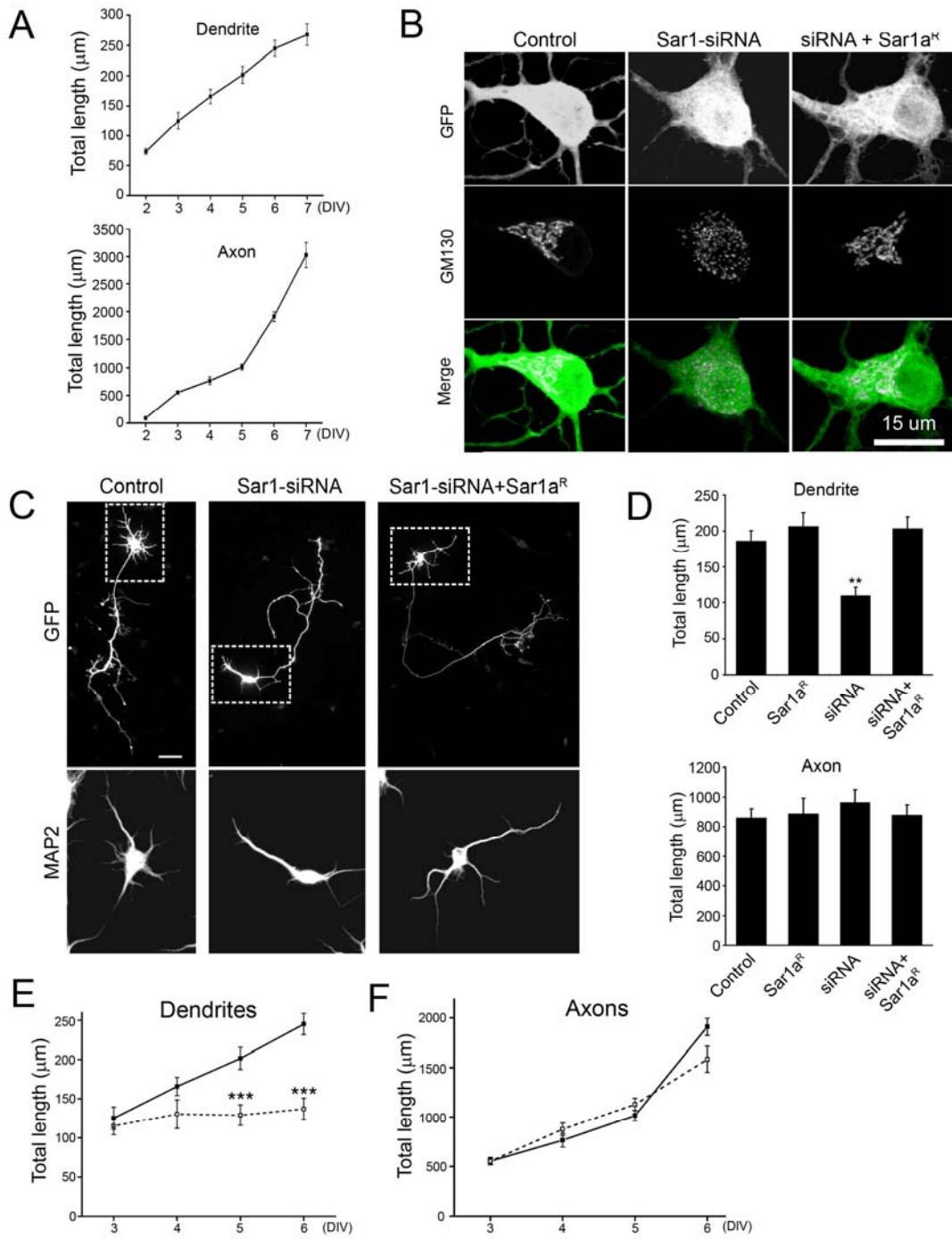
Figure 2-2. Dendritic growth is preferentially reduced in cultured hippocampal neurons with defective ER-to-Golgi transport. (A) Time course of dendritic and axonal growth in cultured hippocampal neurons. Neurons transfected with a plasmid encoding EGFP were stained with anti-MAP2 and anti-GFP antibodies, together with the nuclear dye DAPI. The neurites positive for MAP2 were identified as dendrites. The neurites negative for MAP2 were identified as axons. Only neurons with normal nuclear morphology as revealed by DAPI-stain were included for quantitation to eliminate dying neurons. (B) Sar1-siRNAs dispersed Golgi complex in cultured hippocampal neurons and a siRNA-resistant construct of Sar1a (Sar1a^R) rescued Golgi defects. The Golgi complex was labeled with anti-GM130 antibody. (C) Neurons transfected with Sar1-siRNA exhibit dramatically reduced dendritic growth and a siRNA-resistant Sar1a (Sar1a^R) construct restored dendritic growth. Scale bar: 50 μm. The somatodendritic regions are boxed with dashed lines. The images of MAP2 staining for the boxed regions are shown in the bottom panel. (D) Quantification of dendritic and axonal growth in cultured hippocampal neurons. N= 37, 9, 15, and 24 for control, Sar1a^R, siRNA, and siRNA+ Sar1a^R, respectively. ANOVA test. The experiments were carried out in a double-blind fashion. (E-F) Time course of the effect of Sar1-siRNA on dendritic and axonal growth. The mean total dendritic (E) and axonal (F) length of control (solid line) and Sar1-siRNA-transfected (dashed line) neurons was shown.
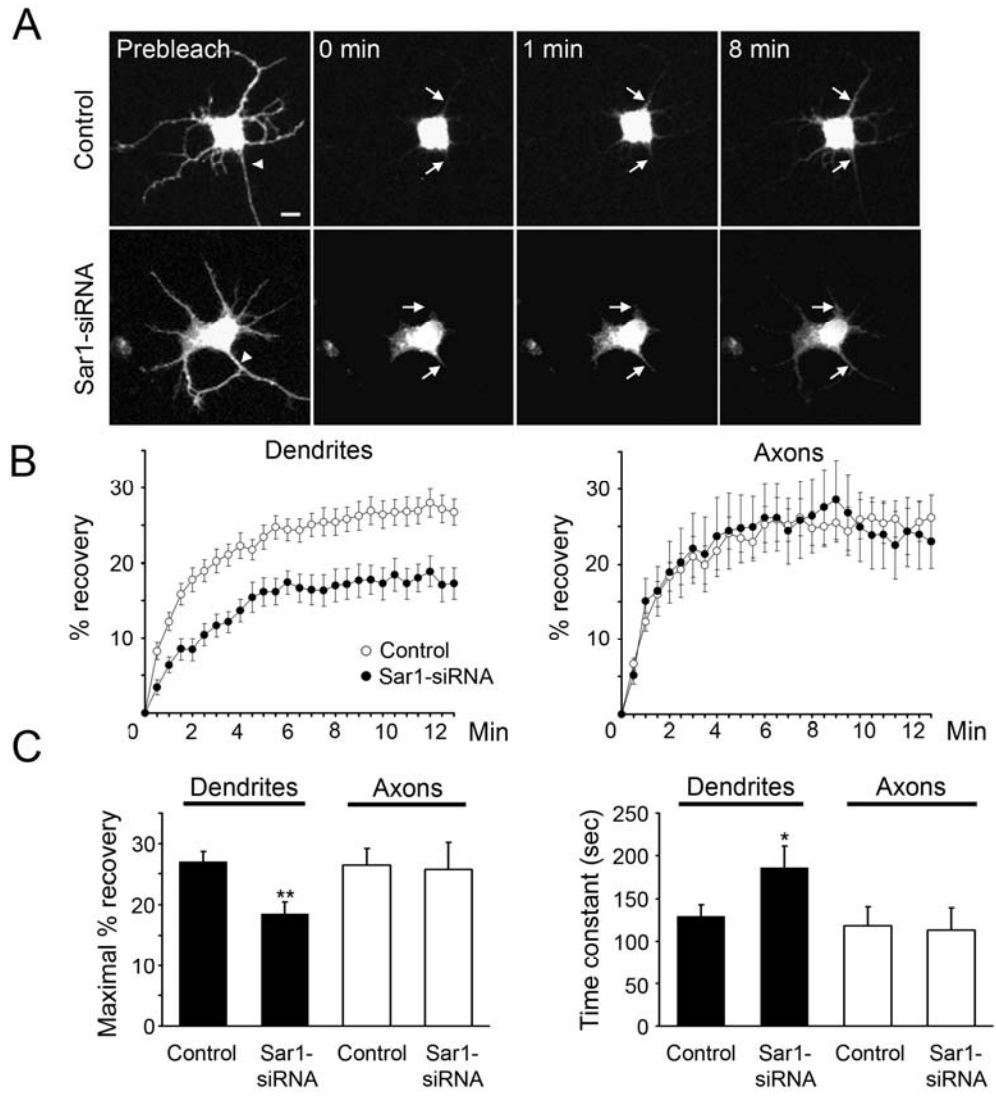
Figure 2-3. Limiting ER-to-Golgi transport leads to preferential reduction of dendritic membrane supply. (A) Representative pictures of membrane-bound EGFP (mCD8-EGFP) moving from soma to dendrites and axons during the FRAP experiments. Zero min is defined as immediately after bleaching. Arrowheads point to the axon. Arrows point to areas that are 5 μm away from soma in representative dendrites and axons. Scale bar: 10 μm. (B) Time course of recovery of mCD8-EGFP signals in photo-bleached dendrites and axons. Open circles: control neurons (n=26); filled circles: Sar1-siRNA-transfected neurons (n=12). (C) Maximal fluorescence recovery is reduced, while time constant is increased, in the dendrites but not axons of the siRNA-transfected neurons.

A

mCD8-dsRed   ManII-EGFP   Overlay

B

C

	a	b
0 min		
30 min		
60 min		

D

- Extend
- Stable
- Retract
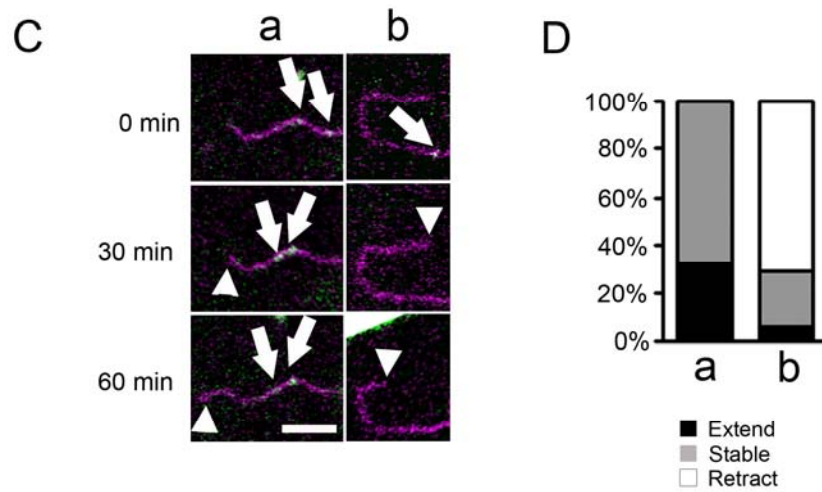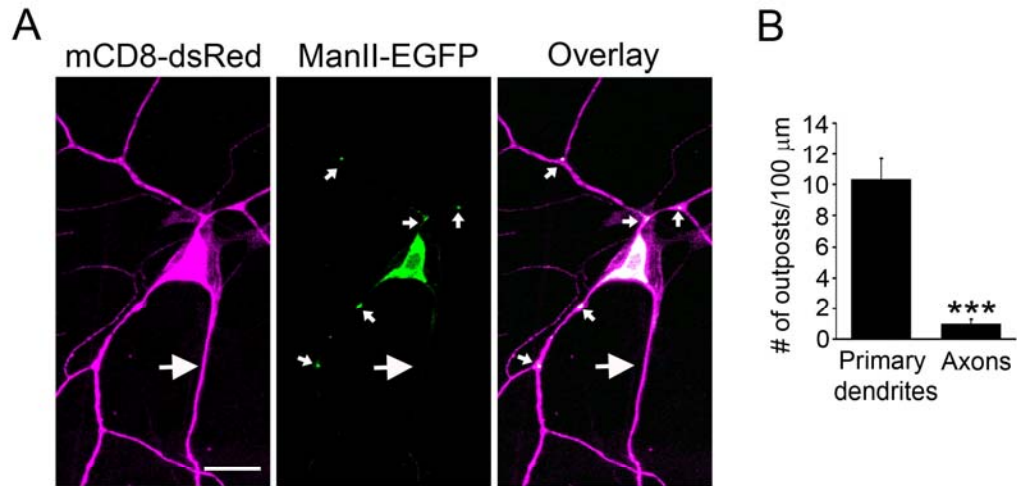
Figure 2-4. Golgi outpost dynamics correlates with dendritic branch dynamics. (A) A class IV da neuron expressing mCD8-dsRed (magenta) and ManII-EGFP (green). Golgi complex are present in the soma and dendrites, but rarely seen in the axon. Small arrows point to dendritic Golgi outposts and large arrows point to the axon. Scale bar: 15 μm. (B) Quantitation of the number of outposts in primary dendrites and the proximal 100 μm of axon. Primary dendrites were defined as those that originated from the soma and ended at the first branch point. (C) Time-lapse imaging of the movement of Golgi outposts and dendritic dynamics. The panels show that Golgi outposts moved distally prior to branch extension (a) and disappeared prior to branch retraction (b). Arrows point to the Golgi outposts that appeared, disappeared or moved. Arrow heads point to the tip of the branch. Scale bar: 5 μm. (D) Quantitation of the correlation between Golgi outpost dynamics and branch dynamics. a, Golgi outposts move distally or appear *de novo* in a branch; b, Golgi outposts move proximally or disappear in a branch.
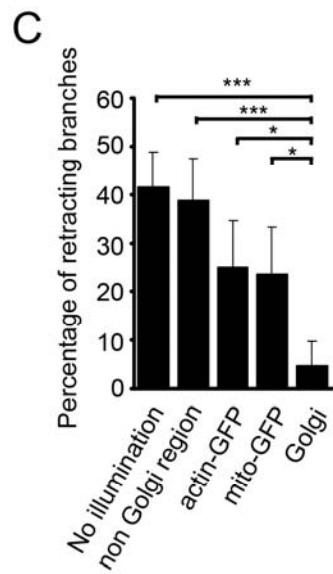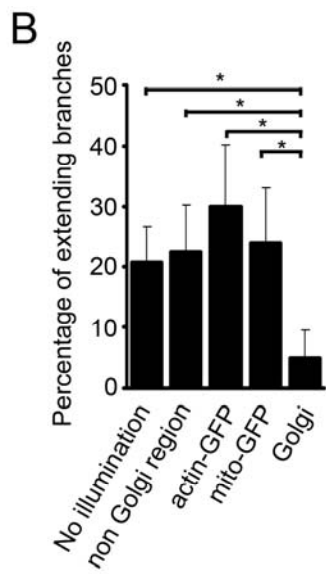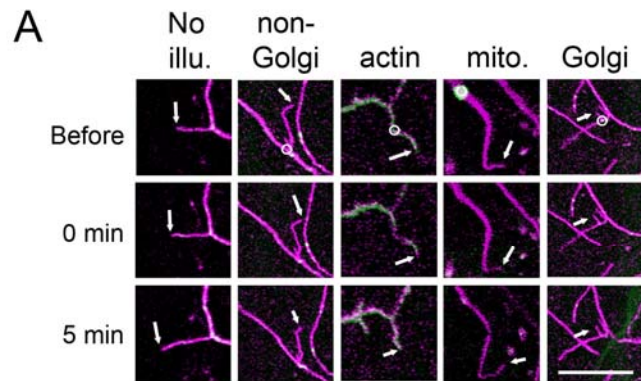
Figure 2-5. Laser damaging of dendritic Golgi outposts reduces the extension and retraction of dendritic branches. (A) Examples of dendritic branches without laser illumination (No illu.), after focal intense laser illumination on regions lacking Golgi outposts (non-Golgi), on regions with actin-GFP (actin), on mitochondria (mito.), and on Golgi outposts (Golgi). Magenta: mCD8-dsRed. Green: actin-GFP in "actin", mito-GFP in "mito.", GalT-EYFP in the other 3 panels. Upper, middle, and lower panels represent images before, immediately after, and 5 minutes after laser damaging, respectively. Circles indicate the regions of laser illumination. Arrows point to the tips of the branches being tested. Scale bar: 10 μm. (B-C) Percentage of branches that extended (B) or retracted (C) after each manipulation.
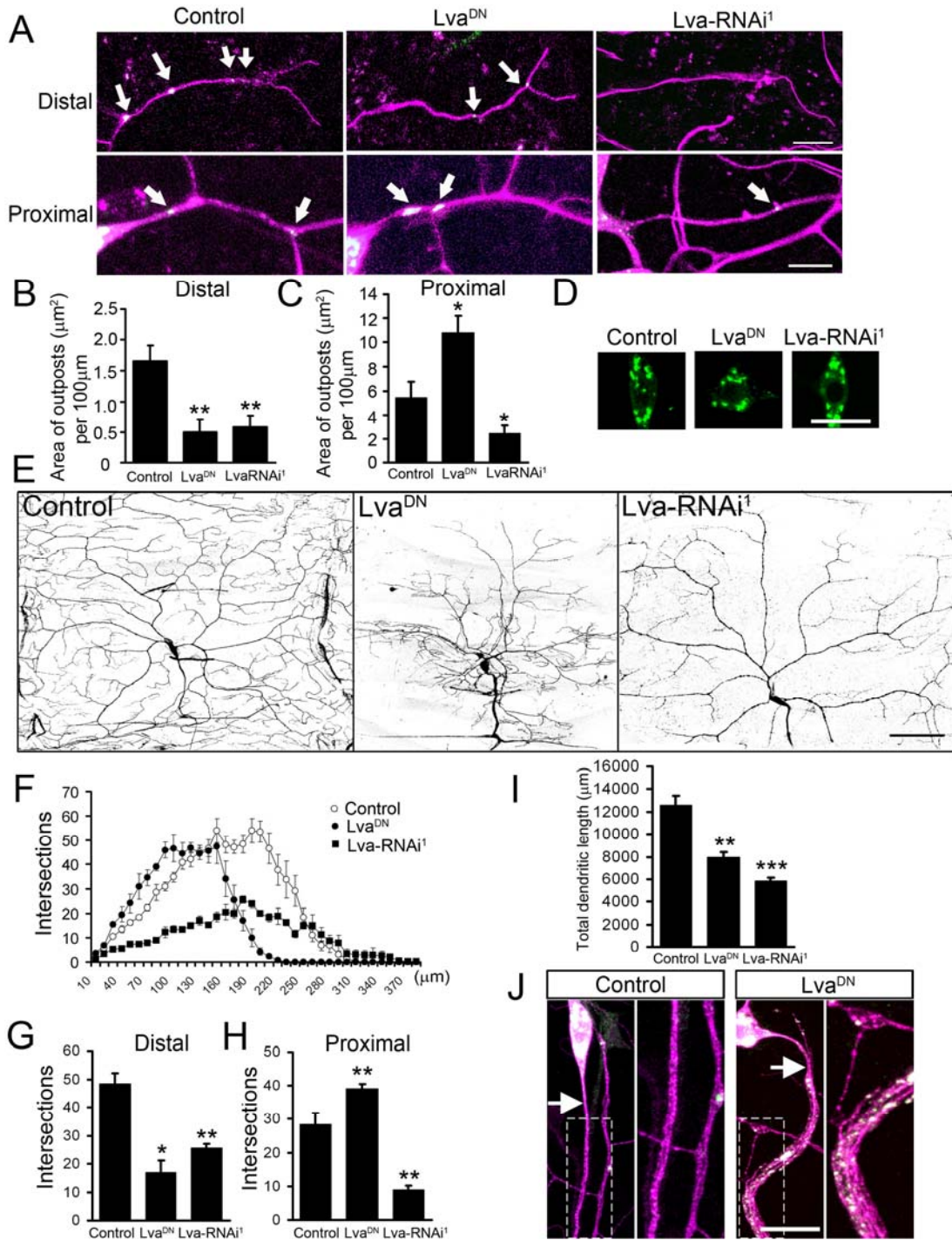
Figure 2-6. Redistribution of Golgi outposts by Lva^{DN} and Lva-RNAi correlates with morphological changes of dendritic arbors. Magenta: mCD8-dsRed. Green: GalT-EYFP. (A) Representative pictures of Golgi outposts in distal and proximal dendrites in control, Lva^{DN}-, and Lva-RNAi[1]-expressing ddaC neurons. Expression of Lva^{DN} was driven by Gal4$^{4-77}$. Expression of Lva-RNAi was driven by Gal4$^{109-2-80}$ to achieve earlier and stronger knockdown effect. Arrows point to Golgi outposts. Scale bars: 10 μm. (B-C) Quantification of the total size of Golgi outposts in distal dendrites (100μm in length from the tip of the dorsal-most branch toward the soma) and proximal dendrites (30μm from the soma). (D) Golgi structure in the soma. Scale bar: 15 μm. (E) Dendrite morphology of control, Lva^{DN}-, and Lva-RNAi[1]-expressing ddaC neurons. Dendrites of Lva-RNAi[1]-expressing neurons were labeled by *ppk*-EGFP. Scale bar: 75 μm. (F) Sholl analysis histogram. (G) Number of intersections between distal dendritic branches and circles with 180 μm radius. (H) Number of intersections between proximal dendritic branches and circles with 80 μm radius. (I) Quantitation of total dendritic length. (J) Golgi outposts and exuberant branches appear in the proximal axons of Lva^{DN}-expressing neurons. Magnified view of the boxed areas is shown in the right panels. The arrows point to the axons. Scale bar: 15 μm.

A

P{PZ}Sar1[05712]

CG7077 | Sar1 | PSR | CG7071

ΔP{PZ}Sar1[05712]-1

Start   C→T stop codon   Stop

Sar1-RA

Wildtype

ACTACATTCGACTTGGGTGGCCACACT**C**AGGCACGACGCGTC

T T F D L G G H T Q A R R V

dar3[11-3-63]

ACTACATTCGACTTGGGTGGCCACACT**T**AGGCACGACGCGTC

T T F D L G G H T Stop

B

P{EPgy2}Sec23[EY06757]

mTa1-like | Sec23 | CG2185

ΔP{EPgy2}Sec23[EY06757]-1

	D	T	E	H	G	G	S	Q	A	R	F	L	L	S
Homo sapiens Sec23	D	T	E	H	G	G	S	Q	A	R	F	L	L	S
Mus musculus Sec23	D	T	E	H	G	G	S	Q	A	R	F	L	L	S
Saccharomyces cerevisiae Sec23	D	T	E	A	G	G	S	Q	A	R	F	L	L	S
Arabidopsis thalinana Sec23	C	D	Q	H		G	S	Q	A	R	F	L	L	A

Drosophila melanogaster Sec23

GATACGGAGCACGGCGGAT**C**CCAGGCCCGCTTCCTGCTGTCC

D T E H G G S Q A R F L L S

dar2[8-2-55]

GATACGGAGCACGGCGGA**T**TCCAGGCCCGCTTCCTGCTGTCC

D T E H G G F Q A R F L L S

C

PBac{RB}Rab1[e01287]

ETHR | Rab1 | AP-2 | CG5919

	S	Y	Y	R	G	A	H	G	I	I	V	V	Y	D	V	T
Homo sapiens Rab1	S	Y	Y	R	G	A	H	G	I	I	V	V	Y	D	V	T
Mus musculus Rab1	S	Y	Y	R	G	A	H	G	I	I	V	V	Y	D	V	T
Saccharomyces cerevisiae Ypt1	S	Y	Y	R	G	S	H	G	I	I	I	V	Y	D	V	T
Arabidopsis thalinana Rab1	S	Y	Y	R	G	A	H	G	I	I	V	T	Y	D	V	T

Drosophila melanogaster Rab1

TCATATTATAGGGGCGCCCATG**G**CATCATTGTCGTATACGATTGCACG

S Y Y R G A H G I I V V Y D C T

dar6[12-3-73]

TCATATTATAGGGGCGCCCATG**A**CATCATTGTCGTATACGATTGCACG

S Y Y R G A H D I I V V Y D C T

	D	S	G	V	G	K	S	C	L	L	L	R	F	A
Homo sapiens Rab1	D	S	G	V	G	K	S	C	L	L	L	R	F	A
Mus musculus Rab1	D	S	G	V	G	K	S	C	L	L	L	R	F	A
Saccharomyces cerevisiae Ypt1	N	S	G	V	G	K	S	C	L	L	L	R	F	S
Arabidopsis thalinana Rab1	D	S	G	V	G	K	S	C	L	L	L	R	F	A

Drosophila melanogaster Rab1

GACTCGGGCGTTGGAAAGTC**C**TGTCTTCTGTTGCGATTTGCC

D S G V G K S C L L L R F A

dar6[11-4-72]

GACTCGGGCGTTGGAAAGT**T**CTGTCTTCTGTTGCGATTTGCC

D S G V G K F C L L L R F A

Figure 2-7. *dar2, dar3,* and *dar6* encode critical regulators of the secretory pathway.

(A) *dar3* encodes the *Drosophila* Sar1 (dSar1). Top panel: schematic of the genomic

region of the *dSar1* locus. The RA splicing form of *Sar1* gene contains 6 exons that span

a 4 kb genomic region. (B) *dar2* encodes the *Drosophila* Sec23. The dashed lines

indicate that the exact excision site of the deletion ΔP{EPgy2}Sec23^{EY06757}-1 has not

been identified. (C) *dar6* encodes the *Drosophila* Rab1.

A

+/*dar3*[11-3-63]   ΔP{PZ}Sar1[05712]-1/*dar3*[11-3-63]   *hs*-GAL4/UAS-*dSar1*;
ΔP{PZ}Sar1[05712]-1/*dar3*[11-3-63]

Dendrites

Axons

50 μm

50 μm

B   ΔP{EPgy2}Sec23[EY06757]-1/*dar2*[8-2-55]   ΔP{EPgy2}Sec23[EY06757]/*dar2*[8-2-55]

C   PBac{RB}Rab1[e01287]/*dar6*[12-2-73]   ΔPBac{RB}Rab1[e01287]/*dar6*[12-2-73]
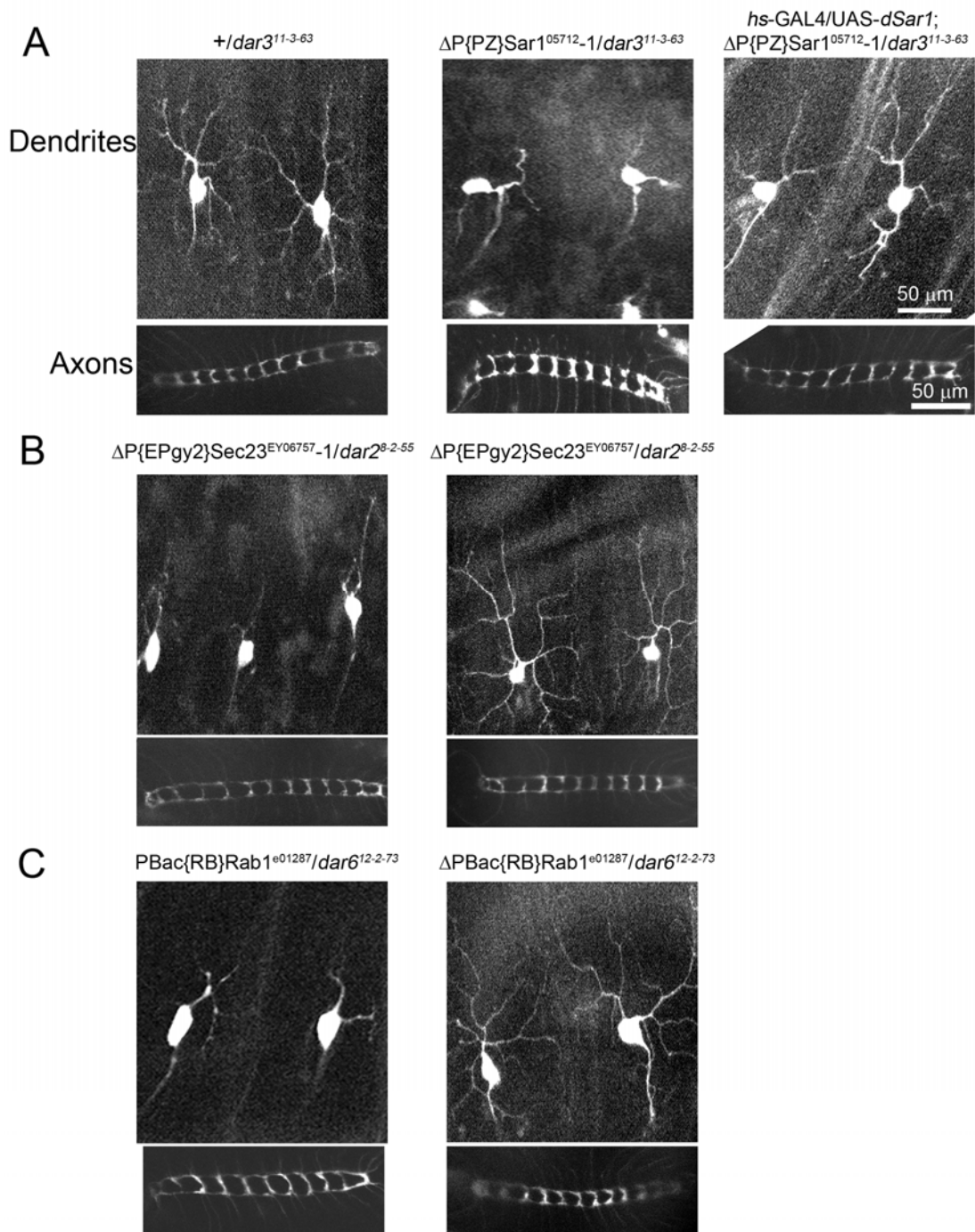
Figure 2-8. Identification of *dar2, dar3,* and *dar6* as the *Drosophila* homologs of *Sec23*, *Sar1*, and *Rab1*, respectively. (A) *dar3* encodes the dSar1. Left panel: the dendrite morphology and axon terminal projections of class IV da neurons in embryos heterozygous for *dar3* mutation. The *ppk*-EGFP signal in this figure is weaker than those in Figure 1A because a single copy of *ppk*-EGFP was used for these complementation tests. Middle panel: ΔP{PZ}Sar1^{05712}-1, which carries a deletion in *dSar1* gene, fails to complement the dendrite defect of *dar3$^{11-3-63}$*. Right panel: *dSar1* transgene rescues the dendrite defect in ΔP{PZ}Sar1^{05712}-1/*dar3$^{11-3-63}$* mutants. (B) *dar2* encodes dSec23. Left panel: ΔP{EPgy2}Sec23^{EY06757}-1, which carries a deletion in dSec23 gene, fails to complement the dendrite defects of *dar2*. Right panel: a precise excision line of P{EPgy2}Sec23^{EY06757} (ΔP{EPgy2}Sec23^{EY06757}) complements the dendrite defects of *dar2*. (C) *dar6* encodes dRab1. Left panel: the PiggyBac transposable element PBac{RB}Rab1^{e01287}, which is inserted into the *Rab1* locus, fails to complement the dendrite phenotype of *dar6$^{12-3-73}$*. Right panel: a precise excision line of PBac{RB}Rab1^{e01287} (ΔPBac{RB}Rab1^{e01287}) complements the dendrite defects of *dar6*.

A

| | Sar1a-siRNA-1 | Sar1a-siRNA-2 | Sar1a-siRNA-3 | unrelated siRNA | Sar1b-siRNA-1 | Sar1b-siRNA-2 | Sar1b-siRNA-3 | unrelated siRNA |

25 kD —

HA-Sar1a   HA-Sar1b

55 kD —

Tubulin   Tubulin

B

Control   Sar1-siRNAs   siRNA+Sar1a^R

GFP

Sar1

20 μm

C

Fluorescence Intensity (arbitrary unit)

*** ***

3 DIV   4 DIV   5 DIV

D

Fluorescence Intensity (arbitrary unit)

*

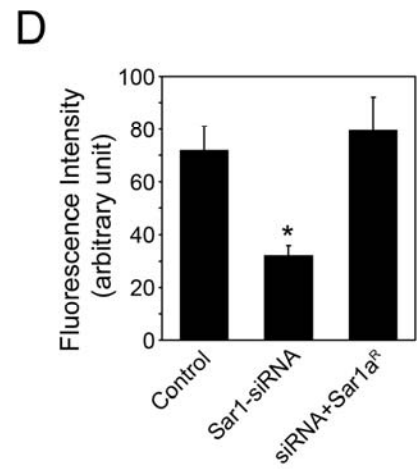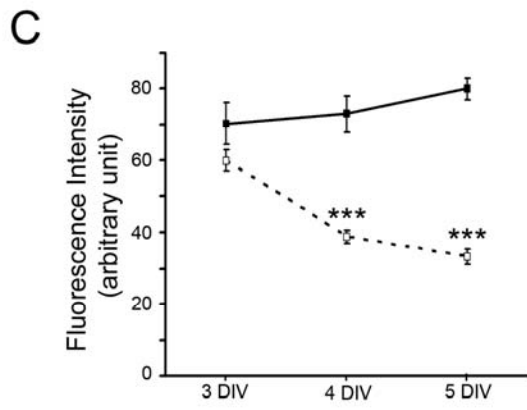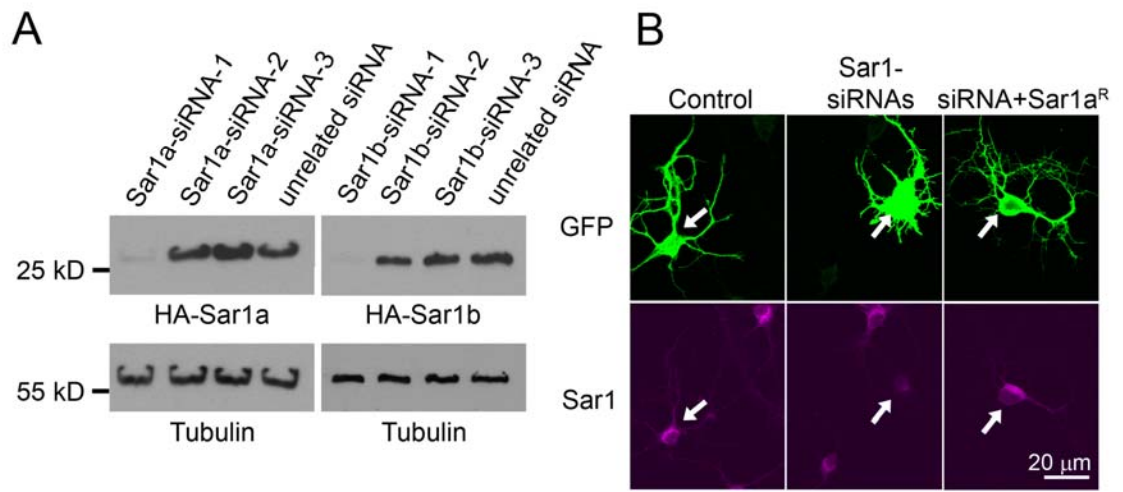Control   Sar1-siRNA   siRNA+Sar1a^R

Figure 2-9. Sar1-siRNAs specifically knock down Sar1 expression level. (A) Western blot of the effectiveness of siRNAs in reducing the expression of HA-tagged Sar1a or Sar1b in Cos-7 cells. Individual siRNAs were cotransfected with the HA-tagged target gene cDNA. Sar1a siRNA-1 effectively reduced the expression of HA-Sar1a, while two other siRNAs against Sar1a and an unrelated siRNA had no effect. Similarly, Sar1b siRNA-1 efficiently knocked down the expression of HA-Sar1b. The same Western blot was probed with anti-tubulin antibody to reveal comparable amount of proteins in each sample. (B) Sar1 protein level, as revealed by immunostaining with anti-Sar1 antibody (Upstate Co., Charlottesville, VA), was reduced in Sar1-siRNA-transfected neurons and normal in neurons co-transfected with Sar1-siRNAs and a siRNA-resistant construct Sar1a^R. Arrows point to the somata of the transfected neurons. (C) Time course of Sar1 knockdown. Immunostaining with anti-Sar1 antibody was carried out on control (solid line) and Sar1-siRNA-transfected neurons (dashed line) at 3, 4, and 5 DIV. The mean intensity of fluorescence of each neuron, shown in arbitrary units (between 0 and 255), was quantified with the ImageJ software. (D) Quantification of Sar1 protein level in the somata of control, siRNA-transfected, and siRNA/Sar1a^R-transfected neurons at 5 DIV. * indicates $p < 0.05$, ANOVA.
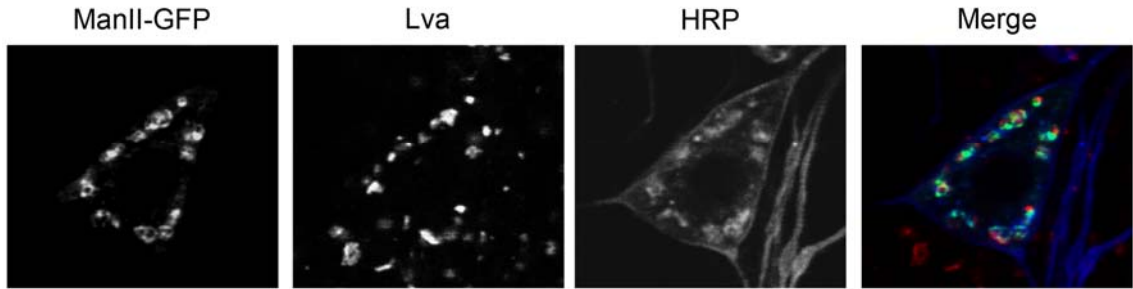
Figure 2-10. Lva is located in Golgi complex in *Drosophila* da neurons. Triple staining of class IV ddaC neurons with antibodies against GFP, Lva, and HRP in 3rd instar larvae expressing ManII-EGFP driven by Gal4[4-77]. In the merged image, green: ManII-EGFP; red: Lva; blue: HRP.
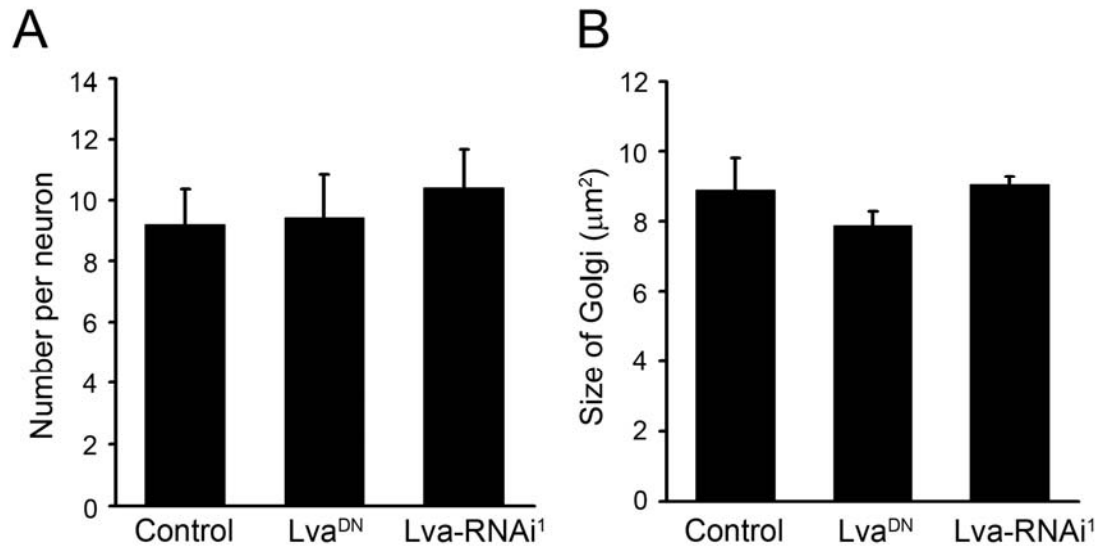
Figure 2-11. Somatic Golgi structure is not affected in Lva[DN]- or Lva-RNAi-expressing neurons, as indicated by the quantitation of average number (A) and total area (B) of discrete Golgi granules in the soma of each neuron (P>0.05, t-test).

mCD8   Nod:βGal   Merge

Control

Lva^{DN}

Figure 2-12. The dendritic marker Nod:βGal is absent in the axons of both control and Lva^{DN}-expressing neurons. Arrows point to the axons. Expression of mCD8-dsRed, Nod:βGal, and Lva^{DN} in the class IV da neuron ddaC was driven by Gal4$^{4-77}$. Third instar larval fillet preparations were doubly stained with anti-mCD8 and anti-βGal antibodies. Scale bar: 40μm.
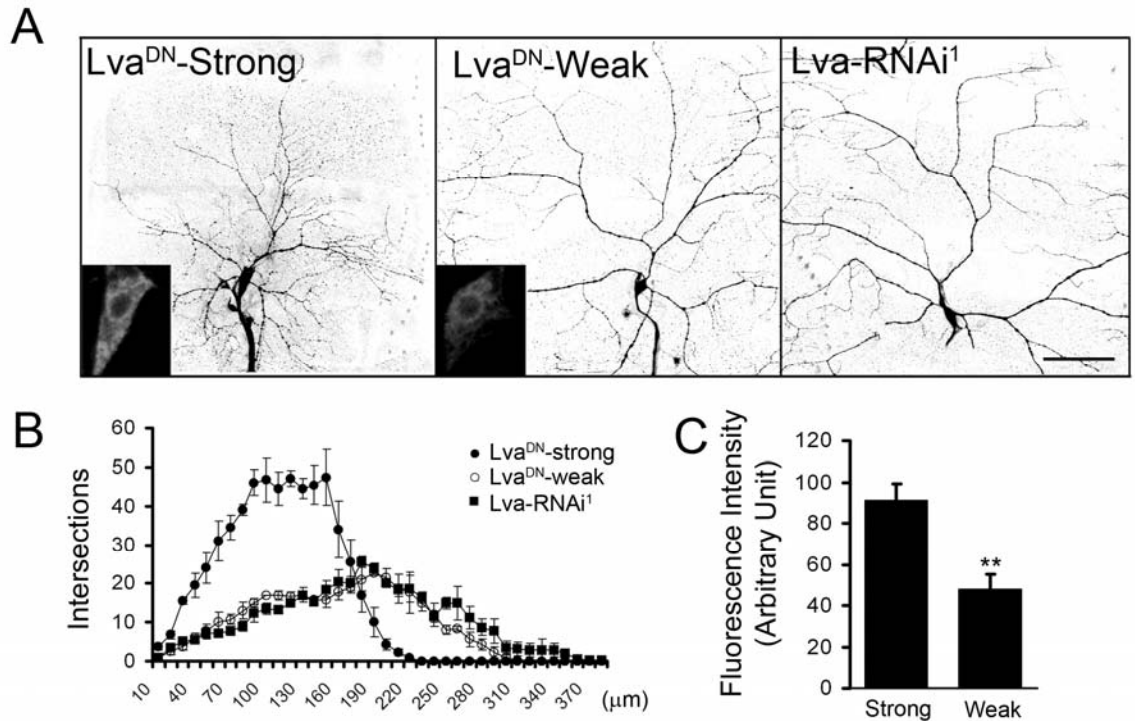
Figure 2-13. Neurons expressing low level of Lva^{DN} show similar dendrite defects to those expressing Lva-RNAi. The defects caused by Lva^{DN} varied 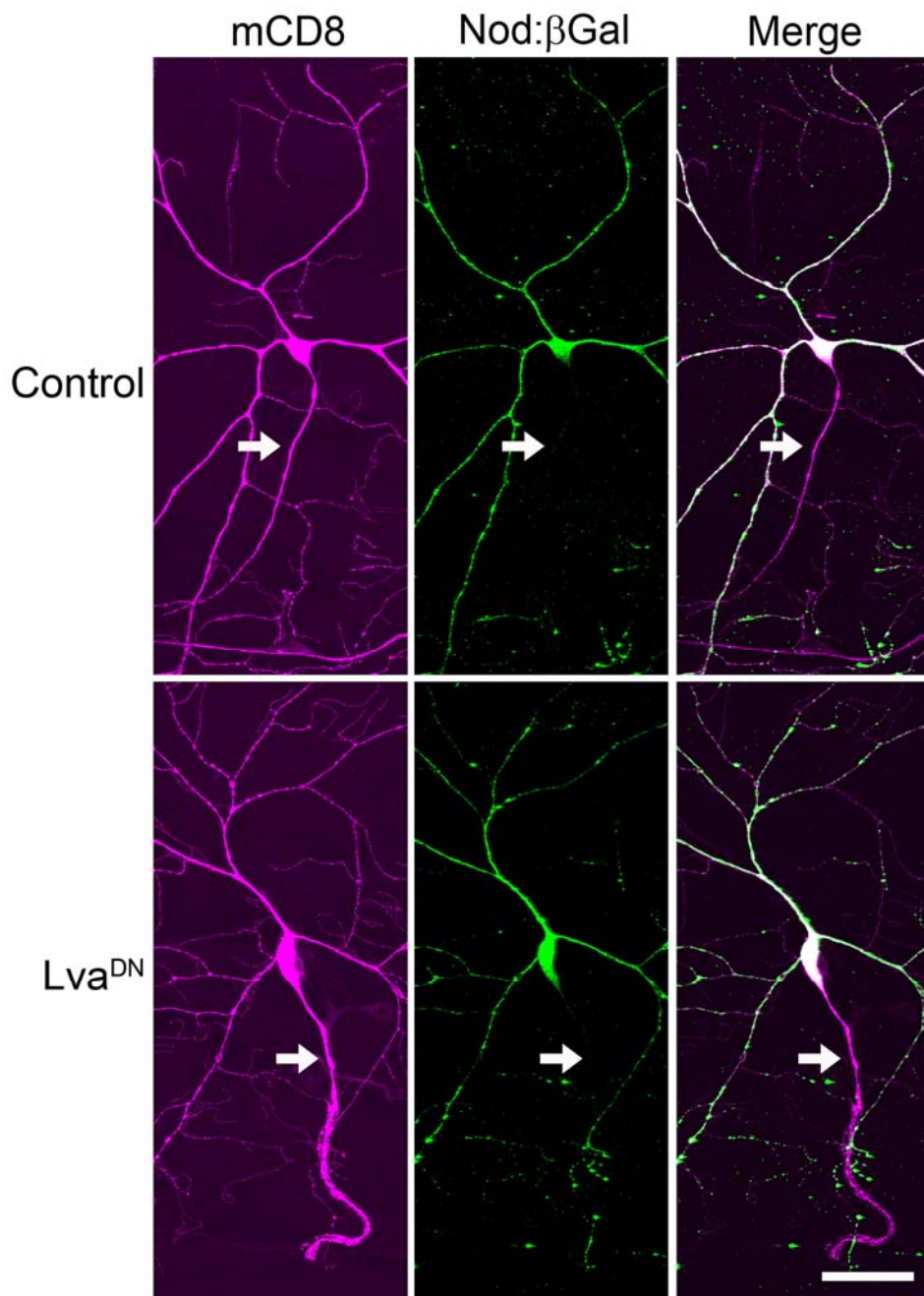with the extent of Lva^{DN} expression. Among different Lva^{DN} transgenic fly lines that we generated, low level of Lva^{DN} expression led to dendrite defects similar to those caused by RNAi, which may only reduce Lva function after the turnover of existing Lva protein. (A) Dendrite morphology of neurons expressing high level of Lva^{DN} by a strong transgene (Lva^{DN}-Strong), low level of Lva^{DN} by a weak transgene (Lva^{DN}-Weak), and Lva-RNAi[1]. Scale bar: 75μm. The expression level of Lva^{DN} was determined by immunostaining with an antibody against the Flag-tag fused to the 5'-end of Lva^{DN} cDNA. Inset: anti-Flag staining in the soma. (B) Sholl analysis. Note that the histograms of Lva^{DN}-Weak and Lva-RNAi[1] expressing neurons are similar. (C) Quantitation of anti-Flag immunofluorescence in neurons expressing Lva^{DN}-Strong (n=5) and Lva^{DN}-Weak (n=3).

**, p<0.01.

A a

b

Dendrite

Axon

Growth cone

B

Dextran

Transferrin

Merge

5 μm

82
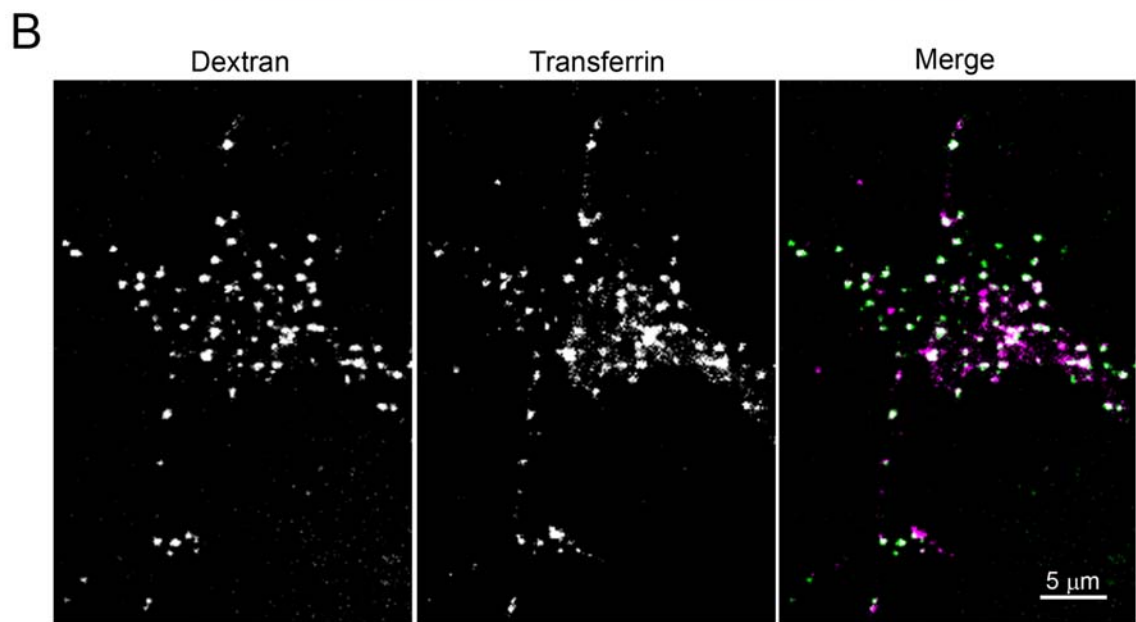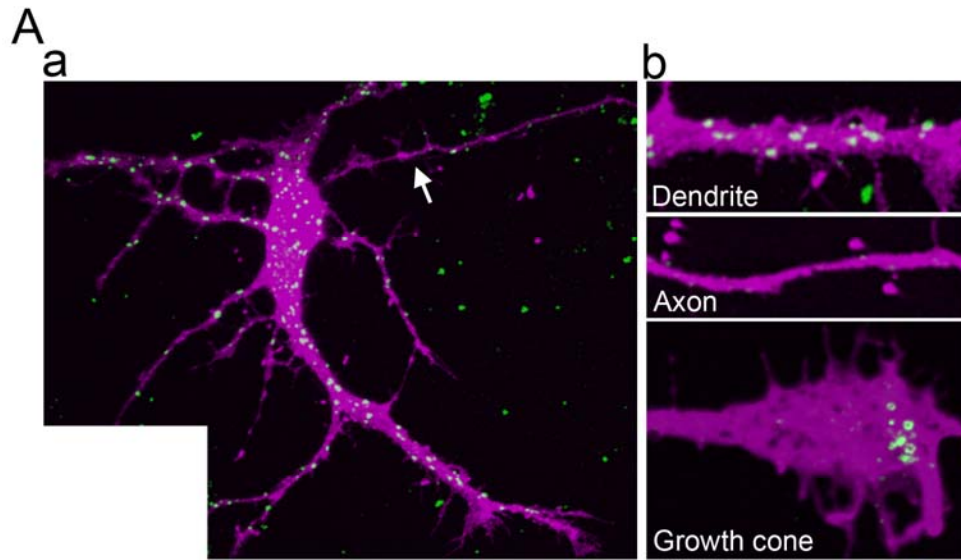
Figure 2-14. Plasma membrane endocytosis rate is higher in growing dendrites than in growing axons. Plasma membrane endocytosed over a period of 10 min was labeled with Rhodamine Green-conjugated dextran at 3 DIV, a stage at which both dendrites and axons are fast growing. (A) Distribution of endocytosed plasma membrane in dendrites, soma, and axon. The morphology of the neuron was marked by mCherry (magenta) and the endocytosed membrane was labeled by dextran (green). The arrow in panel a points to the axon. Panel b shows the magnified view of endocytosed membrane in a segment of dendrite, axon, and axonal growth cone. (B) The endocytosed membrane labeled by dextran (green) extensively overlaps with transferrin (magenta), a marker for early endosomes.

Table 2-1. *dendritic arbor reduction* mutants isolated from the screen.

Mutants	Number of alleles	Cytological location/Gene	Cell-autonomy
dar1	2	KLF transcription factor	Yes
dar2	1	*Sec23*	TBD
dar3	1	*Sar1*	Yes
dar4	1	93A1-93B3	TBD
dar5	1	69C4-69D1	No
dar6	2	*Rab1*	Yes
dar7	2	72D1-93D1	TBD
dar8	2	63F6-7 or 63A6-9	TBD

TBD: to be determined.

CHAPTER 3: Biogenesis, transport, and distribution of dendritic Golgi outposts

Introduction

Golgi outposts are present in neuronal dendrites (De Camilli et al., 1986; Gardiol et al., 1999; Horton and Ehlers, 2003; Horton et al., 2005; Pierce et al., 2001; Pierce et al., 2000). They are involved in the processing of membrane proteins and secreted proteins (Horton and Ehlers, 2003). Despite of their important function in dendrite development, some fundamental questions regarding the biogenesis transport and distribution of dendritic Golgi outposts have not been addressed. I attempted to address three questions in this chapter:

(1) Where are dendritic Golgi outposts generated?

Ehlers and colleagues reported the increase of dendritic Golgi outposts during neuronal development (Horton and Ehlers, 2003). Where are new dendritic Golgi outposts generated is unclear. There are two models for the biogenesis of dendritic Golgi outposts. First, they might be split from somatic Golgi and enter dendrites by directional transport. Second, they might be locally assembled in dendrites. These two sources of dendritic Golgi could also work simultaneously in the biogenesis of dendritic Golgi outposts.

(2) What is the distribution of Golgi outposts in dendrites?

Although dendritic Golgi outposts were found decades ago, a survey for the distribution of Golgi outposts in dendrites has not been reported. Moreover, it is unclear whether patterns of the distribution of Golgi outposts are different in neurons with different dendrite morphology. This question can be addressed in several types of neurons with stereotyped dendrite morphology. *Drosophila* da neurons are an ideal system for the study of distribution pattern of dendritic Golgi. There are four different types of da neurons, each with stereotypical dendrite morphology – simple or complex (Grueber et al., 2003b). They are located in the transparent body wall of *Drosophila* larvae, allowing high resolution imaging in live and intact animals.

(3) Which molecular motor(s) is responsible for the transport of Golgi outposts?

Molecular motors such as dynein, kinesin, and myosin recognize cargos including organelles, and moves cargos along cytoskeleton tracks (Allan et al., 2002). Which molecular motor(s) is involved in the transport of dendritic Golgi outposts is unknown. Identifying the motor(s) for Golgi outposts would be an important step towards understanding the mechanism of the transport and distribution of Golgi in dendrites and how Golgi outposts are kept away from axons.

Methods

Generation of UAS-manII-PAGFP transgenic fly

The UAS-manII-PAGFP construct was generated by subcloning cDNA encoding the N terminal 100 amino acids of *Drosophila* manII fused to photoactivable GFP (PAGFP) (Patterson and Lippincott-Schwartz, 2002) into pUAST. The construct was then injected into w^{1118} embryos, together with a DNA construct encoding the transposase Δ2-3 to generate transgenic flies.

Photoactivation experiment

3rd instar larvae with the following genotype: 477Gal4, UAS-mCD8-RFP; UAS-manII-PAGFP were used for the photoactivation experiment. Animals used for photoactivation experiment were raised in the dark to minimize photoactivation by ambient light. Dorsal ddaC neurons in segment A2-A6 were imaged on Zeiss LSM510 confocal microscope before photoactivation, immediately after photoactivation, and 30 min to 24 hr after photoactivation. Photoactivation was achieved by illumination by the mercury lamp with a filter for DAPI for 1-5 seconds. The soma region was positioned to the center of the imaging field and the field size diaphragm was adjusted to allow illumination of the soma region but not the dendrite region.

Characterization of Golgi outpost distribution

3rd instar larvae with the following genotypes were used for characterization of Golgi outpost distribution: Class I: UAS-manII-GFP; 221Gal4, UAS-mCD8-RFP. Class III: UAS-manII-GFP; 19-12Gal4, UAS-mCD8-RFP. Class IV: 477Gal4, UAS-manII-GFP; UAS-mCD8-RFP. Images were taken with Zeiss LSM510 confocal microscope and analyzed with ImageJ software. Golgi outposts were identified and analyzed with particle analysis tool in ImageJ software. Branch order is defined as follows: dendrite segment attached to the soma is defined as 1st order. When an nth order branch bifurcate, the daughter branch oriented closer to the orientation of the mother branch is defined as nth order branch and the other daughter branch is defined as n+1th order branch. A dendrite segment with a free ending is defined as a terminal branch. The size of Golgi outposts are estimated by the area on the two dimensional image. Region of branch points is defined as the 2 μm diameter circle centered at the center of the branch point. Regions outside of this circle are defined as dendritic shafts.

Time lapse imaging of Golgi outposts

Genotypes and stages of larvae in time lapse imaging experiments are the same as those used in the characterization of the distribution of Golgi outposts. Images were taken by Zeiss LSM510 confocal microscope. Frame interval is 6-8 seconds. Length of each movie is 10 minutes. Mobile Golgi outposts are defined as Golgi outposts that moved more than 1μm within the imaging period (10 minutes). Kymographs of mobile

Golgi outposts were generated by ImageJ software and the speed of movement was

measured from kymographs.

Results

Dendritic Golgi outposts, at least in part, are generated in the soma

To determine the origin of dendritic Golgi outposts, we generated a transgenic fly line with a UAS-manII-PAGFP insertion. Photoactivable GFP (PAGFP) is a mutated form of GFP that emits very low level of fluorescence without photoactivation. After photoactivation, fluorescence intensity increase by 100 fold (Patterson and Lippincott-Schwartz, 2002). manII-PAGFP allows labeling of Golgi from one subcellular region and following of their movement. In Class IV da neurons, manII-PAGFP labels large granules in the soma, small puncta in dendrites that enrich at branch points, and very few signal in the axon. This pattern resembles the pattern labeled by manII-GFP.

We specifically photoactivated manII-PAGFP in the somatic region without activation of dendritic manII-PAGFP (Figure 3-1). We followed the transport of labeled Golgi and found an increasing number of labeled Golgi outposts in dendrites after photoactivation and a decrease in somatic manII-PAGFP signal. The shortest time required for the detection of dendritic GFP signal after somatic photoactivation is 30 minutes. This result shows that at least certain components of dendritic Golgi outposts (e.g. manII) originate from the cell body. This result does not rule out the presence of a second mode for the biogenesis of dendritic Golgi outposts: local assembly in dendrites.

Dendritic Golgi outposts are distributed in neuron type specific patterns

We began our survey of the distribution of dendritic Golgi outposts by quantifying density of Golgi outposts in dendrites of Class I, Class III, and Class IV da neurons. We found that in all three classes of neurons Golgi outpost density is high in major dendrites and low in high order branches (Figure 3-2 A). The size of Golgi outposts varies widely (Figure 3-2 B). Larger Golgi are often located in major branches whereas smaller Golgi are often located in high order branches (Figure 3-3 C). The size of Golgi reflects the level of secretory activity in a cell (Hanus and Ehlers, 2008). The different density and size of Golgi outposts in large vs. small dendrites likely reflect different rates of local membrane trafficking activities. The size of Golgi outposts undergoes dynamic changes resulting from frequent fission and fusion events (Figure 3-5 F), potentially providing a mechanism for adjusting membrane trafficking rates according to local growth demand.

We compared density and size of Golgi outposts at and outside of branch points. We defined region of branch points as the 2 μm diameter circle centered at the center of the branch point. Regions outside of this circle are defined as dendritic shafts. We found that both the density and average size of Golgi outposts at branch points are significantly higher than Golgi outposts outside of branch points (Figure 3-3). This result is consistent with observations made in rodent neurons (Horton et al., 2005).

As mentioned above, there are common patterns of Golgi outpost distribution in different classes of da neurons. For example, major branches contain larger and more numerous Golgi than high order branches; and Golgi outposts are enriched at branch

points. However, some neuron type specific patterns of Golgi distribution became apparent as we compared Golgi localization in Class I, III, and IV da neurons. Golgi outposts are often located at the tips of Class I dendrites, whereas it is very rare to find Class III or Class IV dendrites with Golgi outposts at the branch tips (Figure 3-4 A). It is unclear what is the function of Golgi outposts located at the very end of Class I dendrites. In growing axons, new membrane is added predominantly at the tip of axons (the growth cone region) (Craig et al., 1995). It is unclear where does dendritic membrane addition occur. If new dendritic membrane is added at the tip similarly as in axons, Golgi outposts located at the tips of Class I dendrites provide a convenient site for rapid local processing and targeting of new membrane. The localization of Golgi outposts to Class I dendritic tips but not Class III or Class IV dendritic tips thus raises the interesting question of whether sites of new growth are different in different types of neurons.

In Class III da neurons, Golgi outposts are often located at the base (branch point) of terminal branches but they are not present within terminal branches; whereas in Class IV da neurons, Golgi outposts are sometimes seen in terminal branches (Figure 3-4 B). This difference probably reflects the difference in cytoskeleton organization in Class III vs. Class IV terminal branches. Compared with Class IV terminal branches, Class III terminal branches have higher level of F-actin. The development of these two types of terminal branches is regulated by different transcriptional mechanisms (Jinushi-Nakao et al., 2007).

Dynamic movement of Golgi outposts in dendrites

To begin to understand how are Golgi outposts transported in dendrites and how are neuron type specific distribution formed, we carried out time-laspe imaging experiments of Golgi outposts in Class I and Class IV da neurons in live larvae. We found that some Golgi outposts are stable whereas some Golgi outposts are highly mobile (Figure 3-5 A & D). Mobile Golgi outposts move at a wide range of speeds (from 1μm/min to over 40 μm/min). Golgi outposts move in both the anterograde direction and retrograde direction in dendrites. In some cases, Golgi outposts reverse movement direction (Figure 3-5 E). Direction reversal events are common in Class I dendrites and proximal dendrites of Class IV neurons, but rare in distal dendrites of Class IV neurons (data not shown). Some Golgi outposts in Class I dendrites frequently change their direction of movement and move back and forth within a dendritic region. The functional significance of this back-and-forth movement is unclear.

As mentioned above, Golgi outposts are enriched at branch points. In Class IV neurons, Golgi outposts at branch points are several times more stable than Golgi outposts outside of branch points (Figure 3-5 D). In Class I neurons, a similar percentage of Golgi outposts at branch points and outside of branch points are mobile (Figure 3-5 D). However, their range of movement is different. Golgi outposts outside of branch points can move over a long distance but Golgi outposts at branch points in Class I da neurons move back and forth in the close vicinity of branch points (Figure 3-5 C). Branch point Golgi outposts seem to be actively anchored or restricted to the branch point area in

Class I and Class IV da neurons. It would be interesting to find out the molecular

mechanism for branch point anchorage.

We frequently observed large Golgi outposts splitting into a few small Golgi

outposts and merging of small Golgi outposts (Figure 3-5 F). However, at current

imaging resolution, it is hard to determine whether two Golgi outposts moved to the

same spot actually fused together and whether there is exchange of membrane molecules

between them.

Dynein is required for polarized distribution of Golgi outposts

To investigate the molecular mechanism of the transport of dendritic Golgi outposts

and how Golgi outposts are prevented from entering the axon, we tested the involvement

of the molecular motor dynein in Golgi outpost distribution and transport (Zheng et al.,

2008). We found that in *dlic2* mutant neurons Golgi outpost density increased in

proximal dendrites and decreased in distal dendrites (Figure 3-6 a- l), suggesting that

dynein is important for the transport of dendritic Golgi outposts. Moreover, we found that

a large number of Golgi outposts appeared in axons of dlic2 mutant neurons whereas

wildtype axons contain very few Golgi outposts (Figure 3-6 c, d, k, & l). This result

shows that dynein based transport is essential for keeping Golgi outposts from entering

the axon and the polarized distribution pattern of Golgi outposts is maintained by dynein

based transport. Indeed, when we disrupted dynein based Golgi movement by expressing

dominant negative form of lava lamp or overexpression of dynamitin (a component of

the dynactin complex (Zheng et al., 2008)), we found that percentage of mobile Golgi outposts in dendrites significantly reduced, further demonstrating the importance of dynein in the transport of dendritic Golgi outposts (Figure 3-5 m).

Discussion

By regional labeling and tracking of manII-photoactivable GFP (manII-PAGFP), we demonstrated that somatic Golgi is one source for the biogenesis of dendritic Golgi. By high resolution imaging and time lapse movie recording in live *Drosophila* larvae, we showed that dendritic Golgi outposts are distributed differently in different types of neurons and dendritic Golgi outposts undergo dynamic transport within dendrites. Furthermore, we found that the dynamic movement of Golgi outposts require dynein motor and polarized distribution of Golgi also rely on dynein based transport.

How are dendritic Golgi outposts generated from somatic Golgi? Could somatic Golgi split into smaller Golgi fragments and these smaller Golgi move into dendrites? Alternatively, could molecules residing on Golgi (e.g. glycosylation enzymes like manII) leave somatic Golgi, move into dendrites, and then locally assemble to a new Golgi in dendrites? ER located in dendrites is a possible site where molecules leaving somatic Golgi could accumulate and then assemble to new Golgi. Our regional labeling and tracking experiment with manII-PAGFP showed that somatic Golgi is the source of at least some molecular components of dendritic Golgi outposts. The details of how somatic Golgi gives rise to dendritic Golgi outposts remain to be determined.

We also photoactivated manII-PAGFP in dendritic Golgi outposts and examined whether activated manII-PAGFP are transported to neighboring dendritic Golgi outposts.

We could detect PAGFP signal in neighboring Golgi outposts as soon as 30 minutes after photoactivation, suggesting there is ongoing trafficking between neighboring Golgi outposts in dendrites (data not shown). Different dendritic Golgi outposts are not isolated units. Instead, there is exchange of molecules like manII, and possibly other molecules and signals, between dendritic Golgi outposts. Future study that determines to what extent are molecules shared between neighboring Golgi outposts will be informative. Synaptic input locally affects targeting of membrane proteins like AMPA receptor. Whether signals that communicate between neighboring Golgi could affect the spatial specificity of changes of receptor trafficking in response to synaptic inputs is an interesting open question.

In all classes of da neurons we examined, Golgi outposts are enriched at dendritic branch points. The same is true in mammalian neurons (Horton et al., 2005). Golgi outposts at branch points are larger and more stable. They may have important function in allocating membrane molecules between daughter branches. In non-neuronal cells, it is well established that Golgi apparatus are polarized. They contain stacks of cisternae called cis, medial and trans cisternae. The orientation of Golgi determines the direction of membrane trafficking (molecules enter Golgi from cis-cisternae and exit Golgi from trans-cisternae). It is unknown whether each dendritic Golgi outpost contains the complete set of cis, medial and trans cisternae and how are they oriented. It would be interesting to label molecules residing in different compartments of Golgi (e.g. GM130 for cis-Golgi, manII for medial and trans Golgi, and GalT for trans-Golgi) with different

fluorescent proteins and determine the orientation of dendritic Golgi outposts, especially those at branch points. This experiment would provide clues for the direction of membrane trafficking in dendrites with complex geometry, and help understand how membrane resource is allocated between sister branches, and whether membrane partitioning between branches change according to changing growth demand.

We found that the patterns of dendritic Golgi outpost distribution are different in neurons with different dendrite morphology. Distribution pattern of Golgi outposts might determine site of active membrane addition and influence dendrite morphology. Alternatively, dendrite morphology and according cytoskeleton organization might determine how Golgi outposts are transported and thus influence the distribution pattern of Golgi outposts. Golgi apparatus is involved in glycosylation and targeting of cell adhesion molecules. Whether positions of dendritic Golgi outposts correlate with cell adhesion sites and whether distributions of cell adhesion sites are different in different classes of neurons are interesting questions worth exploring in the future.

Class I dendrites contain high levels of microtubules; Class III terminal branches contain high levels of F-actin and few, if any, microtubules. Golgi outpost distribution patterns are different in these different types of dendrites. Does the growth of different types of dendrites (for example actin rich dendrites vs. microtubule rich dendrites) have different dependence on Golgi outposts? Experiments attempted to test the involvement of dendritic Golgi outposts in dendrite growth described in Chapter 2 were carried out in Class IV da neurons. It would be interesting to test whether the development of Class I

and Class III dendrites require Golgi outposts by similar experiments. Rodent hippocampal neurons have long and thick apical dendrites and short and thin basolateral dendrites. Golgi outposts are present mostly in apical dendrites, suggesting that the growth of basolateral dendrites and apical dendrites might have different reliance on Golgi outposts (Horton et al., 2005). It is interesting to determine whether and why different types of dendrites rely on the function of dendritic Golgi outposts differently.

In addition to the traditionally described function as a membrane processing organelle, Golgi apparatus is also important for the organization of microtubule cytoskeleton. Trans Golgi network (TGN) is a microtubule organization center (MTOC) in fibroblasts. Microtubule minus ends accumulate at TGN and growing plus ends of microtubules orient to the direction that TGN faces (Efimov et al., 2007). If Golgi outposts function as MTOCs in neuronal dendrites, the localization and orientation of Golgi outposts would determine the spatial organization of dendritic microtubules and influence the direction of microtubule based cargo transport in dendrites.

Dynein moves cargos towards microtubule minus ends. In axons, the majority of microtubule minus ends point towards the cell body (Baas et al., 1988). Therefore, dynein moves stray Golgi outposts in axons towards the cell body and maintains polarized distribution of Golgi outposts in neurons (Zheng et al., 2008). In dendrites, microtubules exist both in plus-end-distal and plus-end-proximal orientations (Baas et al., 1988). Dynein is likely involved in both the anterograde and retrograde transport of Golgi outposts in dendrites. Microtubule plus-end directed motor kinesin and actin based

motor myosin might also transport Golgi outposts (Allan et al., 2002). Studying the roles

of kinesin and myosin in addition to dynein in Golgi transport is necessary for a complete

understanding of how Golgi outposts are transported in dendrites.

Acknowledgements
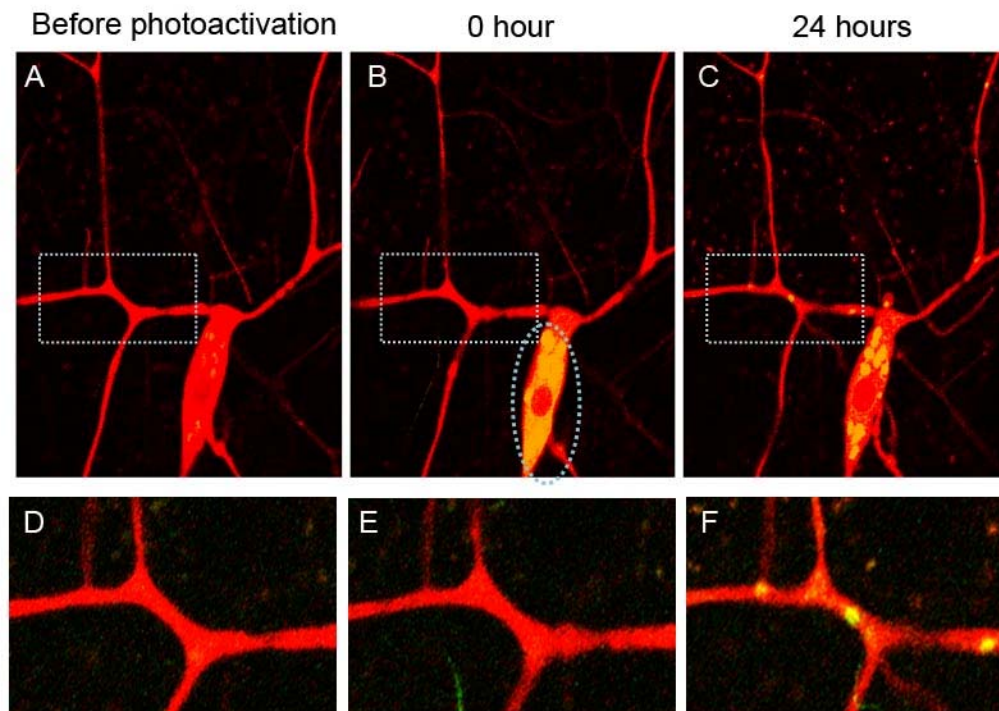
Figure 3-1. Dendritic Golgi outposts are at least in part generated in the soma. Images of a class IV da neuron expressing mCD8-RFP (red) and manII-PAGFP (green) are shown. (A) Before photoactivation. (B) Immediately after photoactivation. (C) 24 hours after photoactivation. Area delineated by dotted oval is photoactivated. Enlarged images of regions in dotted square in A, B, and C are shown in D, E, and F, respectively. 24 hours after photoactivation of somatic region, Golgi outposts labeled by photoactivated manII-PAGFP appeared in dendrites.
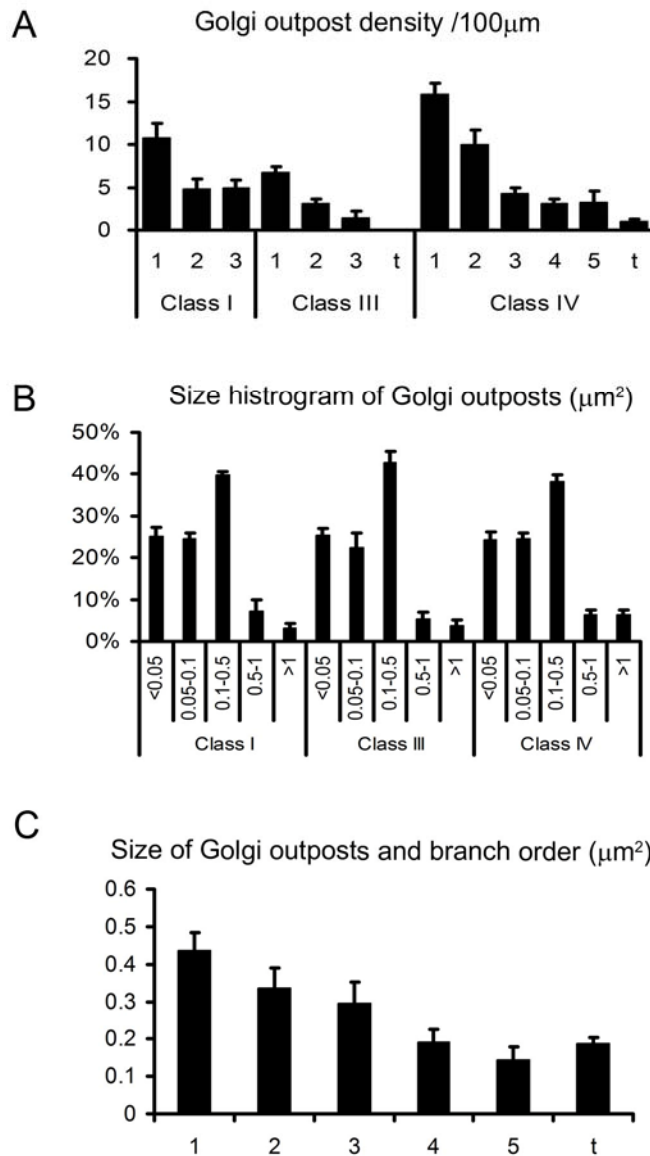
Figure 3-2. Density and size of Golgi outposts in dendrites of different branch orders. (A) In all three classes of da neurons examined, Golgi outpost density is higher in major branches than in high order branches. Branch order is defined as follows: dendrite segment attached to the soma is defined as 1st order. When an nth order branch bifurcate, the daughter branch oriented closer to the orientation of the mother branch is defined as n^{th} order branch and the other daughter branch is defined as $n+1^{th}$ order branch. t:

terminal branch. Terminal branches are defined as branches with free endings in Class III and Class IV neurons. Since Class I neurons have simple branching patterns and small numbers of branches per neuron, branches with free endings were not separated from those without free endings in the analysis. For comparison of Golgi outposts at branch tips in Class I, III, and IV neurons, see Figure 3-4. (B) Size of Golgi outposts varies from less than 0.05 μm^2 to over 1 μm^2. In all three classes of da neurons, the majority of Golgi outposts are smaller than 0.5 μm^2. (C) Golgi outposts in major branches are larger than those in high order branches. Data from Class IV da neurons.
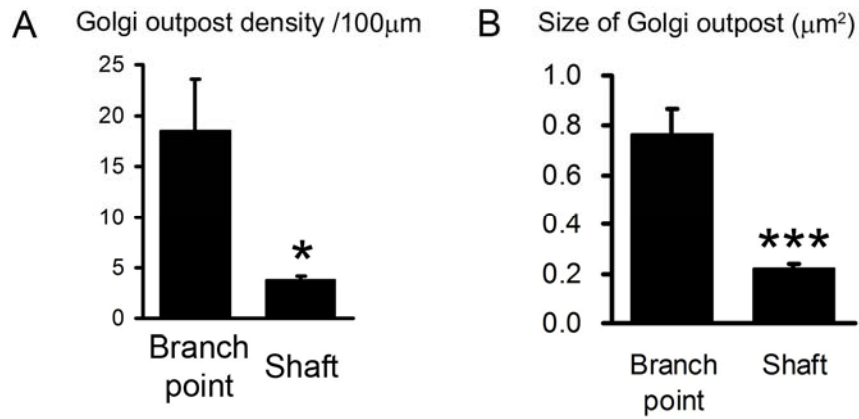
Figure 3-3. Golgi outposts are enriched at branch points. (A) Density of Golgi outposts is higher at branch points than in dendritic shafts. Region of branch points is defined as the 2 μm diameter circle centered at the center of the branch point. Regions outside of this circle are defined as dendritic shafts. *: $p < 0.05$. (B) Average size of Golgi outposts at branch points is larger than those in dendritic shafts. ***: $p < 0.001$.
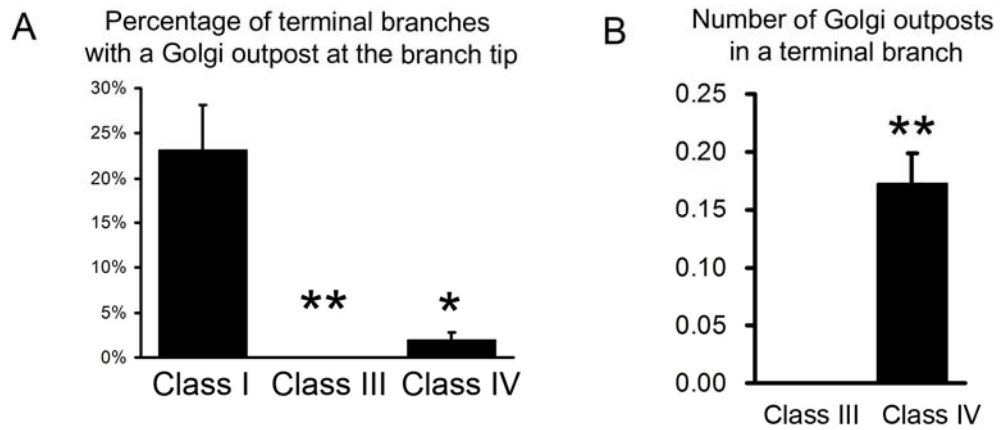
Figure 3-4. Golgi outposts are distributed differently in different types of neurons. (A) Golgi outposts located at branch tips are often seen in Class I but not Class III or Class IV da neurons. (B) Class III terminal branches are devoid of Golgi outposts whereas some Class IV terminal branches contain Golgi outposts. *: $p < 0.05$. **: $p < 0.01$.

A — 0 sec, 6 sec, 12 sec, 18 sec, 24 sec, 30 sec

B Speed histogram of moving Golgi outposts

Number of outposts (y-axis, 0–12)

Class I (black), Class IV distal (white)

x-axis (μm/min): 1-2, 2-3, 3-4, 4-5, 5-6, 6-7, 7-8, 8-9, 9-10, 10-11, 11-12, 12-13, 13-14, 14-15, 15-16, 16-17, 17-18, 18-19, 19-20, 20-30, 30-40, 40-50

C — 0.0 s, 23.4 s, 46.8 s, 70.2 s, 93.6 s, 117.0 s, 140.4 s, 163.8 s, 187.2 s, 210.6 s, 234.0 s, 257.4 s

D %mobile outposts — BP, shaft (Class I); BP, shaft (Class IV); *** ***

E — 0 s, 12 s, 24 s, 36 s, 48 s, 60 s

F — 0 s, 6 s, 12 s, 18 s, 24 s, 30 s, 36 s, 42 s

108

Figure 3-5. Dynamic movement of Golgi outposts in dendrites. Red: mCD8-RFP. Green: manII-GFP. (A) An example of a mobile Golgi outpost in Class IV da neuron dendrites. Arrows point to a mobile Golgi outpost. (B) Speed histogram of mobile Golgi outposts. Filled bars: mobile outposts in Class I da neuron dendrites. Open bars: mobile outposts in distal branches of Class IV da neuron dendrites. Dis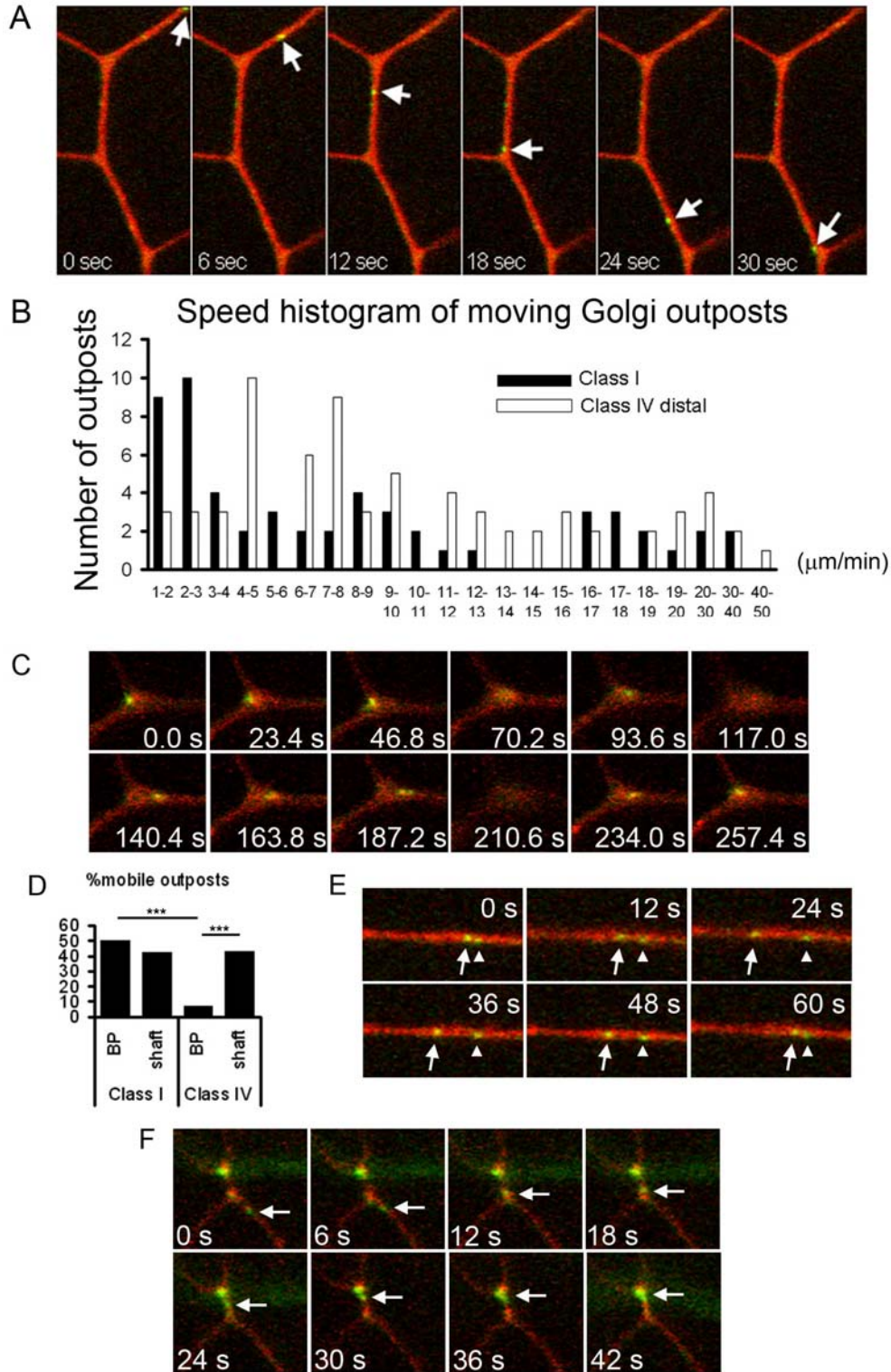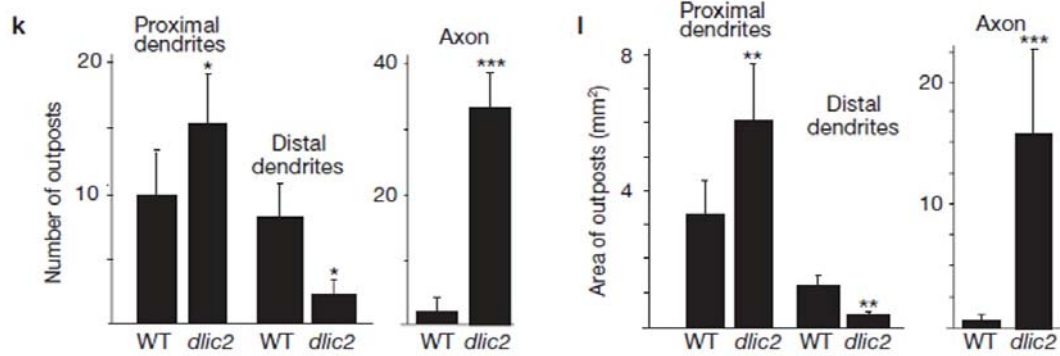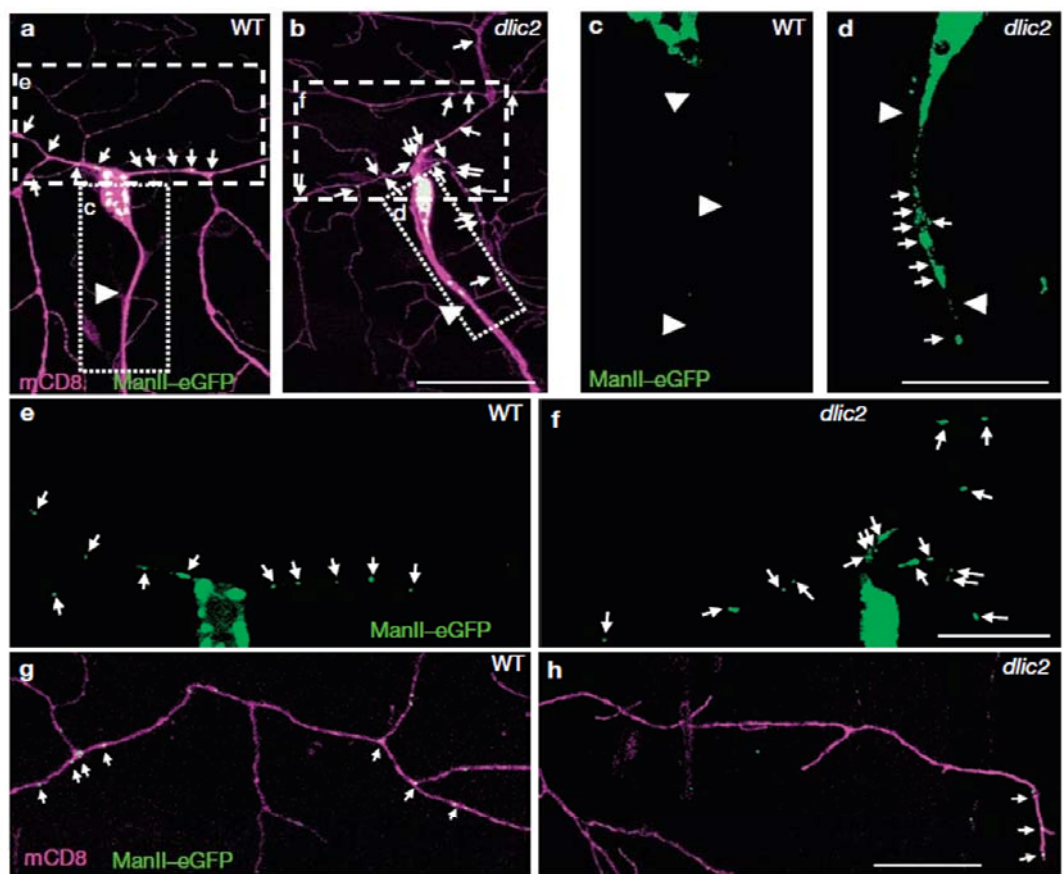tal branches are defined as branches less than 100 μm away from a branch tip at dorsal midline. The speed of Golgi outpost movement varies widely from 1 μm/min to over 40 μm/min. (C) An example of a Golgi outpost moving back and forth within the branch point area in a Class I da neuron. (D) Percentage of mobile outposts at branch points or in dendritic shafts. BP: branch point. Region of branch points is defined as the 2 μm diameter circle centered at the center of the branch point. Regions outside of this circle are defined as dendritic shafts. In both Class I and Class IV da neurons, about 40% of Golgi outposts in dendritic shafts are mobile in the imaging period we examined. In Class I da neurons, Golgi outposts at branch points are either stable or showed short distance movement confined to the branch point area, as shown in the example in (C). In Class IV da neurons, the majority of Golgi outposts at branch points are stable. ***: $p < 0.001$. (E) An example of a Golgi outpost that reversed transport direction. Arrows point to the mobile Golgi outpost that reversed transport direction. Arrowheads point to a stable Golgi outpost. (F) An example of a putative fusion event of Golgi outposts. Arrows point to a Golgi outpost that fused with a larger Golgi outpost at a branch point.

a WT **b** *dlic2* **c** WT **d** *dlic2*
mCD8 ManII–eGFP ManII–eGFP

e WT **f** *dlic2*
ManII–eGFP

g WT **h** *dlic2*
mCD8 ManII–eGFP

k
Proximal dendrites — Distal dendrites — Axon
Number of outposts
20 / 10 / 40, 20
WT *dlic2* | WT *dlic2* | WT *dlic2*
* | * | ***

l
Proximal dendrites — Distal dendrites — Axon
Area of outposts (mm²)
8 / 4 / 20, 10
WT *dlic2* | WT *dlic2* | WT *dlic2*
** | ** | ***

m Percentage of mobile outposts
60 50 40 30 20 10 0
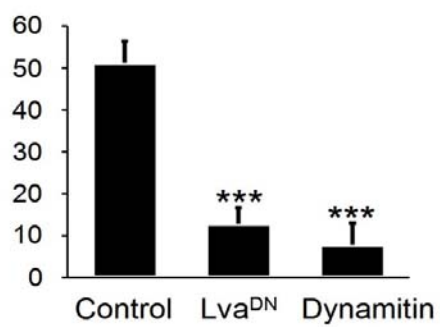Control | Lva^DN | Dynamitin
*** | ***

Figure 3-6. Dynein based movement is important for the transport and polarized distribution of Golgi outposts. (a) & (b): proximal regions of Class IV da neurons. Magenta: mCD8-RFP. Green: manII-GFP. (a) wildtype. (b) dlic2$^{-/-}$. Arrows point to dendritic Golgi outposts. Arrowheads point to axons. Boxed regions are enlarged in (c) – (f). Scale bar: 30 μm in (a) & (b), 15 μm in (c) – (h). (c) & (d): wildtype da neurons have very few Golgi outposts in dendrites whereas a lot of Golgi outposts are present in axons of dlic2 mutant neurons. (e) & (f): number and size of Golgi outposts increase in proximal dendrites of dlic2 mutant neurons. (g) & (h): distal dendrites of wildtype and dlic2 mutant neurons are shown. The number of Golgi outposts decrease in distal dendrites of dlic2 mutant neurons. (k) The number of Golgi outposts in proximal (control, 10.00±3.39, n = 5; dlic2^{1157}, 15.45±4.18, n = 11; *P < 0.025) and distal (control, 7.92 ±3.11 per 100 μm, n = 6; dlic2^{1157}, 2.00±2.00 per 100 μm, n = 3; *P < 0.025) dendritic arbors as well as axons (control, 2.33±2.71 per 100 μm, n = 6; dlic2^{1157},34.49±14.55 per 100 μm, n = 5; ***P < 0.001). (l) Size of Golgi outposts in proximal (control, 3.31± 1.08 μm^2, n = 5; dlic2^{1157},6.00±1.75 μm^2, n = 11; **P < 0.01) and distal (control, 1.12± 0.36 μm^2, n = 6; dlic2^{1157}, 0.25±0.25μm^2, n = 3; **P < 0.01) dendritic arbors as well as axons (control, 0.45±0.51, n = 6; dlic2^{1157}, 16.71±6.09, n = 5; ***P < 0.001). Panels (a) – (l) are adapted from *"Dynein is required for polarized dendritic transport and uniform microtubule orientation in axons"* (Yi Zheng, Jill Wildonger, Bing Ye, Ye Zhang, Angela Kita, Susan H. Younger, Sabina Zimmerman, Lily Yeh Jan and Yuh Nung Jan. *Nature Cell Biology*. Vol. 10, Number 10, October 2008, P. 1172-1180). (m) Percentage of

mobile dendritic Golgi outposts in wildtype neuron, neurons expressing dominant negative lava lamp, and neurons over expressing dynamitin. ***P < 0.001. Percentage of mobile Golgi outposts is significantly lower in neurons in which dynein based Golgi transport is disrupted.

CHAPTER 4: The role of Rab6 in dendrite development

Introduction

Dendrite morphogenesis requires both membrane expansion and cytoskeletal growth. As discussed in previous chapters, membrane expands at a very high rate in growing neurons. Typically 1 μm^2 of membrane can be added in a minute (Pfenninger, 2009). Moreover, the geometrical complexity of dendrites requires tightly regulated membrane addition at appropriate sites. Inside the membrane boundary, cytoskeleton elongates and reorganizes at a high speed as well, providing dendrites with appropriate shape and rigidity. The growth of dendrites relies on the addition of membrane and cytoskeleton in the right portions. We know next to nothing about how membrane expansion and cytoskeletal growth, two very complicated processes, are coordinated in growing dendrites.

Golgi apparatus, in particular dendritic Golgi outpost, might be a key organelle in coordinating membrane addition and cytoskeletal elongation. Golgi is on one hand involved in the production and targeting of membrane molecules and on the other hand organizes microtubule minus ends (Efimov et al., 2007). The distribution of dendritic Golgi outposts, therefore, might be important for both dendritic membrane addition and cytoskeletal growth.

We attempted to investigate the coordination of membrane expansion and cytoskeletal growth in growing dendrites by studying candidate molecules that regulate both membrane trafficking and cytoskeleton organization. One such candidate is Rab6.

Rab6 is a member of Rab proteins which are small GTPases. Rab proteins are located on various secretory and endocytic organelles and recruit molecules to these organelles as Rab proteins go through GTP-GDP cycles. Rab6 is located at trans-Golgi cisternae and trans Golgi network (TGN) (Antony et al., 1992), a key location both for supplying membranous vesicles to the plasma membrane and for organizing microtubules. Rab6 has a number of different roles in the secretory and endocytic pathway. By expressing dominant negative forms of Rab6 or RNAi knock down of Rab6 in cultured cells, several groups reported that disruption of Rab6 function leads to defect in Golgi-to-ER transport (Young et al., 2005), vesicle transport between Golgi cisternae (intra Golgi membrane transport) (Martinez et al., 1994; Mayer et al., 1996), and also endosomes-to-TGN transport (Mallard et al., 2002). Rab6 links Golgi/TGN to the cytoskeleton by recruiting the dynactin complex (an important component of the dynein motor complex) to Golgi membranes (Short et al., 2002). Loss of Rab6 results in severe defect of cytoskeleton organization. These defects include loss of microtubule organization center (MTOC), disruption of microtubule organization (Januschke et al., 2007), and loss of actin filaments (Coutelis and Ephrussi, 2007). How would loss of a Rab GTPase, previously mostly studied in membrane trafficking, results in failure of cytoskeleton assembly has not been studied.

Because of the importance of Rab6 in the regulation of both membrane trafficking and cytoskeleton organization, we tested the role of Rab6 in dendrite outgrowth. We found that dendrite outgrowth is severely reduced in neurons lacking Rab6. Studying the

mechanism by which Rab6 controls dendrite development might lend insight into the

coordination of membrane expansion and cytoskeletal growth in developing dendrites.

Results

We first examined the subcellular localization of Rab6 by imaging transgenic flies expressing Rab6-GFP in Class IV da neurons. We detected GFP puncta predominantly in dendrites. These puncta are enriched at dendritic branch points. Few GFP puncta were found in axons. In the soma Rab6-GFP labels several oval granules in each neuron. This pattern closely resembles the pattern labeled by GalT-YFP, a marker for trans-cisternae of Golgi and TGN, suggesting that Rab6 is located in trans-cisternae of Golgi and TGN in Class IV da neurons (Figure 4-1).

We then tested the role of Rab6 in dendrite morphogenesis by generating mosaic clones of Rab6 mutant da neurons in an otherwise heterozygous larva by MARCM analysis (Lee and Luo, 1999). Rab6 null allele that completely deletes Rab6 gene, Rab6^{D23D}, was used in MARCM analysis (Purcell and Artavanis-Tsakonas, 1999). In all classes of da neurons we examined, Rab6 mutant neurons showed severe reduction of dendrite branches (Figure 4-2 A & B). Moreover, occasional clusters of crowded short dendritic branches were seen in Rab6 mutant Class IV da neurons (Figure 4-2 B inset). This result demonstrated that Rab6 is required for dendrite outgrowth.

Methods

To study the subcellular localization of Rab6, virgin female flies with the following genotype: 477Gal4, UAS-mCD8-RFP were crossed to male flies carrying UAS-Rab6-GFP (generated by Joseph O'Tousa and colleagues, unpublished reagent). Foraging third instar larvae were imaged live with Leica SP5 confocal microscope.

For MARCM analysis of Rab6 mutant neurons, null allele Rab6^{D23D} (Bloomington *Drosophila* Stock Center) was recombined to a chromosome carrying FRT^{40A}. Virgin female flies with the following genotype: Rab6^{D23D}, FRT^{40A}/Cyo were crossed to male flies with the following genotype: elavGal4, hs-Flippase, UAS-mCD8-GFP; tubulin-Gal80, FRT^{40A}. Mosaic clones were generated as previously described (Grueber et al., 2003b) and examined either by live imaging or staining with rat anti-mCD8 (for neuron morphology), and goat anti-HRP crosslinked to Cy5 (for the morphology of the entire PNS).

Discussion

We identified Rab6 as an essential protein for dendrite outgrowth. Loss of Rab6 results in severe reduction in dendrite branching and occasional clustering of thin branches. Rab6 is essential for the growth of all classes of da neurons we examined.

Rab6 is located at Golgi/TGN (Antony et al., 1992), a putative microtubule organization center (MTOC) (Efimov et al., 2007). Rab6 recruits dynein motor complex to Golgi/TGN (Short et al., 2002). Thus, it is likely that in neurons without Rab6, dynein motor dissociates from MTOC and results in misorganization of microtubule cytoskeleton in dendrites.

Given the importance of Rab6 in Golgi-to-ER transport (Young et al., 2005), intra Golgi membrane transport (Martinez et al., 1994; Mayer et al., 1996), and endosome-to-TGN transport (Mallard et al., 2002). It is likely that intracellular membrane transport is dysfunctional in Rab6 mutant neurons. In fact, we noticed that mCD8-GFP signal is weaker in Rab6 mutant neuron compared with wildtype neurons, likely reflecting defect in the trafficking of the membrane protein, mCD8-GFP.

Future experiments that reveal changes in the organization of secretory organelles and cytoskeleton in Rab6 mutant neurons would be important for understanding the cellular mechanism by which Rab6 functions in dendrite development. To reveal changes of the secretory organelles in Rab6 mutant neurons, MARCM analysis with Golgi/TGN marker GalT, ER marker KDEL, and endosomes marker Rab5 would be informative. To

dissect the changes of actin cytoskeleton, MARCM analysis with filamentous actin markers GMA or lifeact need to be done. Similarly MARCM analysis can be carried out to reveal changes of microtubule orientation and organization. Tools for analyzing microtubule orientation includes EB1-GFP, which marks plus-ends of growing microtubules, and nod-GFP, a fusion protein presumably targeted to minus-ends of microtubules. In addition, a number of proteins that interact with Rab6 were identified. They were found either in genetic screens for enhancer/suppressor interactions or yeast 2 hybrid screens. A few examples are listed as follows: Rabkinesin-6/MKIP2: a kinesin-like motor protein localized to Golgi (Echard et al., 1998). The closest homolog in Drosophila is pav which is involved in regulating cell division. Class IV neurons have enlarged cell bodies in pav mutant embryos. GAPCenA: a Rab6 GAP that forms complex with gema-tubulin and is involved in microtubule nucleation (Cuif et al., 1999). GCC185: a microtubule binding protein involved in microtubule nucleation at TGN (Efimov et al., 2007). Mint3: a PDZ domain containing adaptor protein located at Golgi (Teber et al., 2005). TMF/ARA10: a golgin family protein that might also function as a transcription factor (Fridmann-Sirkis et al., 2004). Testing whether these proteins are involved in dendrite morphogenesis in da neurons may reveal the molecular mechanism by which Rab6 functions in dendrite development.

Acknowledgements

I thank Bing Ye for his close collaboration with me on this project; Mark Wessels for

excellent technical support; and Joseph O'Tousa for UAS-Rab6-GFP flies.
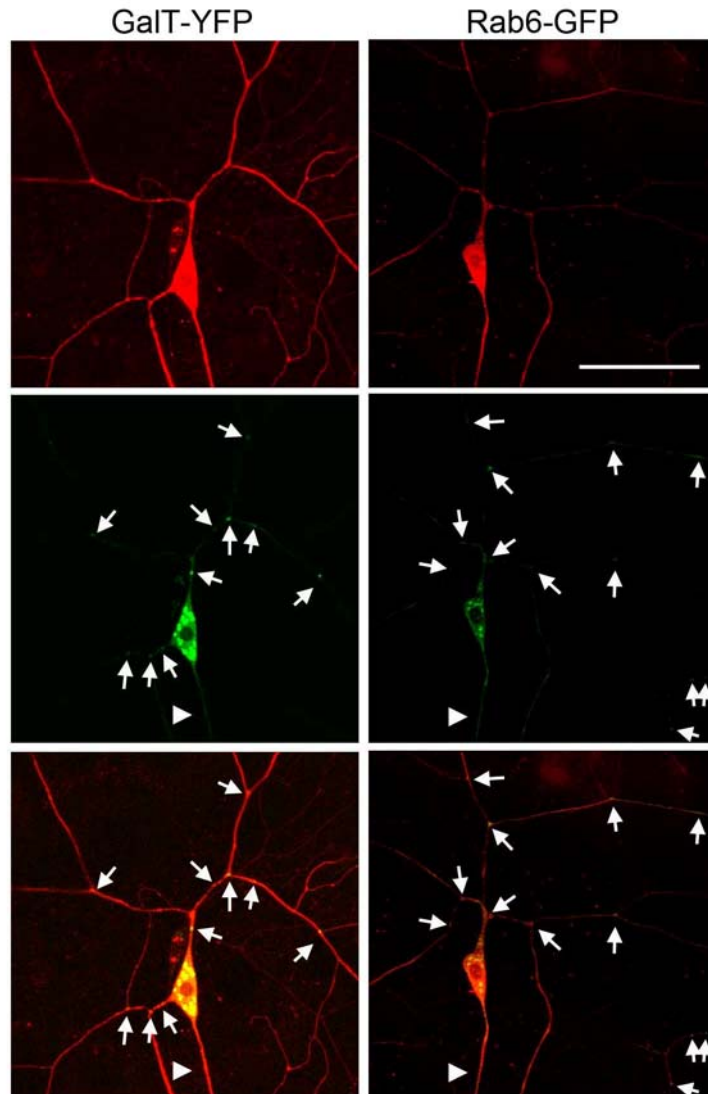
Figure 4-1. Subcellular distribution of Rab6 closely resembles trans-cisternae of Golgi and TGN protein, GalT. mCD8-RFP (red) and GalT-YFP (green) or Rab6-GFP (green) are expressed in Class IV da neurons driven by 477-Gal4. Both GalT-YFP and Rab6-GFP label small puncta in dendrites and large granules in the cell body. Arrows point to dendritic puncta. Arrowheads point to axons. Scale bar: 50 μm.
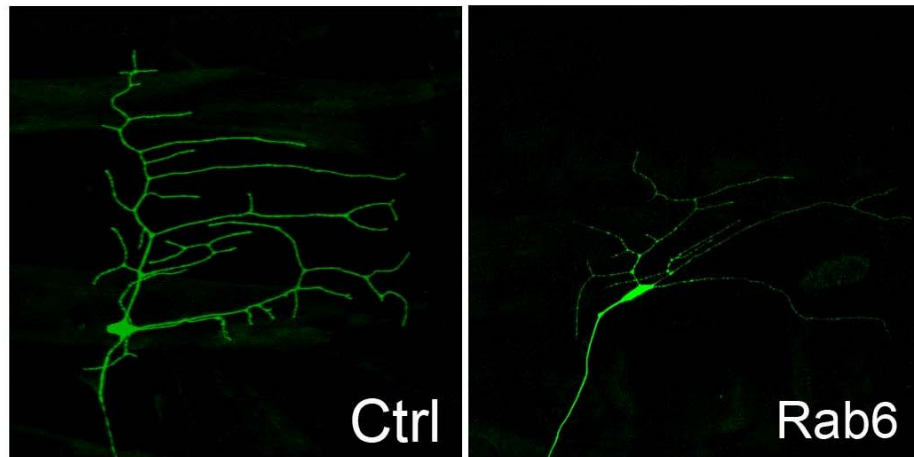
A   Class I   ddaE

B   Class IV   ddaC

Figure 4-2. Rab6 is required for dendrite outgrowth. (A) Rab6 mutant Class I ddaE neuron has reduced dendrite branches. (B) Rab6 mutant Class IV ddaC neuron has reduced dendrite branches. In addition, clusters of short and thin dendrites were occasionally observed (boxed region was enlarged and shown in the inset).

CHAPTER 5: Conclusions and future directions

Conclusions

From a genetic screen in *Drosophila*, we identified *dendritic arbor reduction (dar)* mutants with reduced dendritic arbors but normal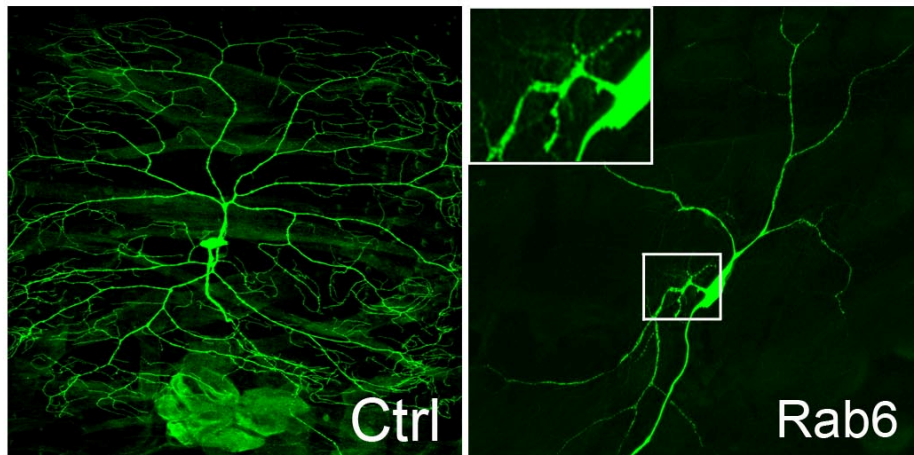 axons. We mapped *dar2, dar3,* and *dar6* genes to *sec23, sar1,* and *Rab1*. These three genes are essential for ER to Golgi transport. The severe defect in dendrite growth and lack of abnormality in axonal growth in these *dar* mutants reveal that dendritic growth and axonal growth have different reliance on the secretory pathway. Knocking down Sar1 expression in cultured rat hippocampal neurons led to similar dendritic arbor reduction without affecting axonal growth. We thus conclude that it is conserved in evolution that growing dendrites are more sensitive to disruption of ER to Golgi transport than growing axons.

To elucidate the mechanism of the different reliance of growing dendrites and axons on the secretory pathway, we tracked membrane transport from soma to dendrites and axons by fluorescence recovery after photobleaching (FRAP) and found that somatic membrane supply to axons is largely maintained whereas somatic membrane supply to dendrites is reduced in response to limited ER-to-Golgi trafficking. Furthermore, Golgi outposts present in dendrites and largely absent from axons contribute to the different reliance of growing dendrites and axons on the secretory pathway. Dendritic branches extend and retract in correlation with the anterograde and retrograde movement of dendritic Golgi outposts. Photo damaging of dendritic Golgi outposts reduced dynamic growth of dendritic arbors. Disrupting the function of lava lamp, the adaptor protein

between Golgi and dynein motor complex, led to correlating changes of Golgi outpost distribution and dendrite morphology. These experiments suggest that dendritic Golgi outposts are involved in dendrite morphogenesis.

In addition, we studied the biogenesis of Golgi outposts by regional photoactivation and tracking of manII-photoactivable GFP and found that somatic Golgi is an important source for dendritic Golgi outposts. Golgi outposts in dendrites undergo dynamic bidirectional transport. Dynein motor is required for the transport of dendritic Golgi outposts. Moreover, the lack of Golgi outpost in axons is maintained by dynein based microtubule minus-end directed transport. We carried out a thorough survey of the distribution of Golgi outposts in dendrites of different types of neurons. We found shared features among neuron types, including enrichment of Golgi outposts at branch points and in major branches. We also found that different classes of neurons show unique features in Golgi outpost distribution. For example, Class I da neuron often contain Golgi outposts at branch tips; Class III da neuron often contain Golgi outposts at the branch points of terminal branches but not within terminal branches.

We also identified Rab6, a regulator of the secretory pathway, as an essential gene for dendrite outgrowth.

In summary, we found that growing dendrites and axons have different reliance on the secretory pathway. Dendritic Golgi outposts are likely involved in dendrite morphogenesis. Dendritic Golgi outposts are generated by somatic Golgi, transported by dynein motor, and distributed in neuron type specific patterns.

The complexity of the role of the secretory pathway in dendrite and axon development is only beginning to be revealed. I list below a few interesting open questions that warrant future investigation. A better understanding of neuronal secretory pathway would lend insight to how neurons develop and how nervous system functions.

Future directions

Where is new membrane added in growing dendrites?

Several groups have studied the site of new growth (new membrane addition) in axons. In axons with a growth cone, new membrane is added predominantly at the growth cone (Craig et al., 1995; Dai and Sheetz, 1995; Zakharenko and Popov, 1998). In axons that have already reached its target and still elongate as the distance between soma and post-synaptic partner increases (e.g. the sciatic axon originates from lower spinal cord and the axon terminal reaches the foot. Sciatic axon elongates as the distance between the foot and spinal cord increase during the growth of an animal), new membrane is added at multiple sites along axonal surface (Futerman and Banker, 1996; Popov et al., 1993; Zakharenko and Popov, 2000). It is unclear where new membrane is added in growing dendrites. Banker and colleagues reported that in immature neurites that later become dendrites new membrane is added to the tip of the neurites (Craig et al., 1995). However, it is unknown whether that is also the case for differentiated dendrites. An indirect piece of evidence on the site of dendritic membrane addition is that TI-VAMP, a molecule implicated in membrane exocytosis in growing neurites, is found along growing dendrites and enriched at the tips, suggesting that tips of dendrites might be hot spots of membrane addition (Coco et al., 1999).

Golgi outposts provides sites for local processing and sorting of membrane

components in dendrites. Whether localization of Golgi outposts correlates with sites of membrane addition is an unexplored question. As shown in Chapter 3 of this thesis, the patterns of Golgi outpost distribution are different in neurons with different dendrite morphology. It is curious whether sites of membrane addition in dendrites are distributed differently in different types of neurons. Dendritic branching pattern of Class I da neuron is established early in development. The size of dendritic arbor scales up as the animal grows and the size of body wall expands. In Class IV da neurons, in addition to scaling up of branches developed early on, there is continuous addition of new branches and retraction of some existing branches throughout all stages of larval development. It is quite likely that membrane addition patterns are different in these two types of neurons that involve different ways of growth.

It is also important to determine where membranous vesicles from a single Golgi outpost go and how big is the plasma membrane surface that contains membrane molecules transported from a single Golgi outpost, because this question is critical for understanding how membrane microdomains that compartmentalize membrane molecules are established during dendrite development.

Are TGN and endosome both sources of new membrane for growing dendrites and axons?

Membranous vesicles exiting trans Golgi network (TGN) either target to the plasma membrane directly or first fuse with recycling endosomes and then are sorted to the

plasma membrane (De Matteis and Luini, 2008). Endosomes are important sources for membrane expansion in many circumstances. For example, endosomes provide membrane for LTP induced dendritic spine formation and expansion (Park et al., 2006). Endosomes accumulate at cleavage furrow and are important sources of membrane for cytokinesis (Wilson et al., 2005). In non-neuronal cells, including polarized cells, endosomes are proposed to have a general role in plasma membrane expansion during cell growth (Schmidt and Haucke, 2007). Endosomes, together with Golgi and centrosomes, cluster at the site where the first neurite forms early in neural development (de Anda et al., 2005). Could endosomes provide a significant amount of membrane for growing dendrites and axons? What is the major route towards the plasma membrane for membrane components generated by the secretory pathway? Do molecules exiting Golgi target to the plasma membrane directly or through endosomes? These are fundamental questions of neural development that remain unanswered.

Several recent studies identified endosomal proteins important for neurite growth, including Rab5 (Satoh et al., 2008), shrub (Sweeney et al., 2006), Rab11 (Shirane and Nakayama, 2006), unc51 (Ogura et al., 1994), and syntaxin 13 (Hirling et al., 2000). These results suggest that proper endosomal trafficking is required for neurite growth (Sann et al., 2009; Schmidt and Haucke, 2007; Tang, 2008).

Endocytic trafficking might be different in growing dendrites and axons. We found that membrane endocytosis rate is much higher in growing dendrites than in growing axons (Figure 2-14). De Camilli and colleagues reported that morphology of endosomes

in dendrites and axons showed different changes in response to addition of the same drug (Mundigl et al., 1993). Detailed study for membrane trafficking routes in dendrites and axons might elucidate important mechanisms for the establishment of different architectures of dendrites and axons.

Is transcytosis an important route of intracellular membrane trafficking in growing neurons?

Transcytosis describes the endocytosis of membrane molecules from one subcellular compartment (e.g. dendrite), followed by intracellular transport and subsequent exocytosis of membrane molecules at a different subcellular compartment (e.g. axon) (von Bartheld, 2004). Transcytosis occurs in polarized cells such as epithelial cells and neurons, and are important for polarized distribution of several membrane proteins. For example, an axonal membrane protein L1/NgCAM is initially non-selectively targeted to both dendritic and axonal domain. Transcytosis of L1/NgCAM from dendrites to axons then establishes polarized axonal distribution (Yap et al., 2008). Other examples of plasma membrane proteins using the transcytosis pathway include immunoglobulin receptor (Ikonen et al., 1993) and glutamate receptor in C. elegans (Margeta et al., 2009).

Although there is strong evidence for the trancytosis of several membrane proteins, it is unknown whether bulk transcytosis of membrane is an important route of intracellular membrane transport in growing neurons. We found large amount of membrane endocytosis in growing dendrites (Figure 2-14). Where do these endocytosed membrane

go is unclear. One possibility is that they might move to axons via the transcytosis pathway and contribute to axonal growth. If that is the case, when membrane production from the secretory pathway is limited by Sar1 knock down, dendritic membrane could transcytose to axons and axons could continue to grow at the expense of dendritic growth. This is consistent with what we observe in both *Drosophila* and rat neurons: neurons with reduced Sar1 function have reduced dendritic arbors and largely normal axons. Direct experimental evidence is needed to show whether transcytosis contribute significantly to neuronal growth.

Are there Golgi outpost-like organelles in axons?

Golgi outposts are found in dendrites but not in axons (Horton et al., 2005). In *Drosophila* da neurons, using Golgi glycosylation enzyme manII tagged with GFP, we found numerous dendritic Golgi outposts and very few axonal Golgi, mostly located in the axon initial segment (Figure 2-4 B). At axon terminals, we observed dim and diffuse manII-GFP, unlike the bright GFP puncta in dendrites.

It was believed that local synthesis of membrane proteins or secreted proteins does not occur in axons because the organelles required for processing and plasma membrane targeting of these proteins (rough ER and Golgi) are absent from axons. However, several recent findings challenge this view. mRNAs of odorant receptor genes are found in axon terminals of olfactory receptor neurons (Vassar et al., 1994) and are associated with polyribosomes, suggesting that they are actively being translated in axon terminals

(Dubacq et al., 2009). Membrane protein EphA was found to be locally synthesized in growing retinal ganglion cell axons and local translation of EphA in these axons are important for axon guidance (Brittis et al., 2002).

How could locally synthesized membrane proteins target to the plasma membrane without Golgi? One possibility is that functional equivalents of Golgi exist in axons and they lack some of the classical markers of Golgi and deviate from the classical morphology of Golgi and thus eluded previous investigations. Indeed, such functional equivalent of Golgi is found in the axons of dorsal root ganglion neurons, a type of unipolar neuron (axon and dendrites both initiate from a single cell body fiber that attaches to the cell body) (Merianda et al., 2009).

Could Golgi outposts function as microtubule organization centers in dendrites?

The organization of microtubule arrays in dendrites is important for dendrite morphogenesis and molecular transport in dendrite. It was assumed that most, if not all, microtubules are formed at centrosomes. Recently, trans-Golgi network (TGN) was found to be an extra-centrosomal microtubule organization center (MTOC). In contrast to the radial organization of centrosomal microtubules, microtubules originated form TGNs are polarized towards leading edges of growing cells (Efimov et al., 2007). Future study that demonstrates whether dendritic Golgi outposts are MTOCs in dendrites would be very valuable for understanding dendrite morphogenesis.

Do dendritic Golgi outposts contain a complete set of molecular components as somatic Golgi?

Another interesting direction for future investigation is whether dendritic Golgi outposts are smaller versions of somatic Golgi with a complete set of molecular components and a full capacity for membrane processing and trafficking as somatic Golgi. Various markers for cis, medial, and trans cisternae of Golgi are found in dendrites (e.g. GM130, manII, and TGN38) (Gardiol et al., 1999; Horton and Ehlers, 2003; Horton et al., 2005; Pierce et al., 2001). However, there is no evidence that each dendritic Golgi outpost contains a complete set of molecules as those located cis, medial, and trans cisternae of somatic Golgi. Thus it is unknown which steps of post translational modifications of membrane and secreted proteins could occur in dendritic Golgi outposts. It is also unknown whether each dendritic Golgi outpost has the ability for both anterograde trafficking (from ER to Golgi) and retrograde trafficking (from endosomes to Golgi). An important next step for understanding the function of the satellite secretory pathway is to investigate whether each dendritic Golgi outpost is a complete functional unit that performs all the functions that somatic Golgi could perform, or multiple functions of classic Golgi are delegated to a number of different Golgi outposts each specializes in a few steps.

REFERENCES

Aizawa, H., Hu, S. C., Bobb, K., Balakrishnan, K., Ince, G., Gurevich, I., Cowan, M., and Ghosh, A. (2004). Dendrite development regulated by CREST, a calcium-regulated transcriptional activator. Science *303*, 197-202.

Allan, V. J., Thompson, H. M., and McNiven, M. A. (2002). Motoring around the Golgi. Nat Cell Biol *4*, E236-242.

Antony, C., Cibert, C., Geraud, G., Santa Maria, A., Maro, B., Mayau, V., and Goud, B. (1992). The small GTP-binding protein rab6p is distributed from medial Golgi to the trans-Golgi network as determined by a confocal microscopic approach. J Cell Sci *103 (Pt 3)*, 785-796.

Aridor, M., Guzik, A. K., Bielli, A., and Fish, K. N. (2004). Endoplasmic reticulum export site formation and function in dendrites. J Neurosci *24*, 3770-3776.

Aridor, M., and Hannan, L. A. (2000). Traffic jam: a compendium of human diseases that affect intracellular transport processes. Traffic *1*, 836-851.

Arimura, N., and Kaibuchi, K. (2005). Key regulators in neuronal polarity. Neuron *48*, 881-884.

Ashraf, S. I., McLoon, A. L., Sclarsic, S. M., and Kunes, S. (2006). Synaptic protein

synthesis associated with memory is regulated by the RISC pathway in Drosophila. Cell *124*, 191-205.

Baas, P. W., Deitch, J. S., Black, M. M., and Banker, G. A. (1988). Polarity orientation of microtubules in hippocampal neurons: uniformity in the axon and nonuniformity in the dendrite. Proc Natl Acad Sci U S A *85*, 8335-8339.

Bard, F., Casano, L., Mallabiabarrena, A., Wallace, E., Saito, K., Kitayama, H., Guizzunti, G., Hu, Y., Wendler, F., Dasgupta, R.*, et al.* (2006). Functional genomics reveals genes involved in protein secretion and Golgi organization. Nature *439*, 604-607.

Barnes, A. P., and Polleux, F. (2009). Establishment of axon-dendrite polarity in developing neurons. Annu Rev Neurosci *32*, 347-381.

Bartheld, C. S. v. (2004). Axonal transport and neuronal transcytosis of trophic factors, tracers, and pathogens. Journal of Neurobiology *58*, 295-314.

Bi, X., Corpina, R. A., and Goldberg, J. (2002). Structure of the Sec23/24-Sar1 pre-budding complex of the COPII vesicle coat. Nature *419*, 271-277.

Bradke, F., and Dotti, C. G. (1997). Neuronal polarity: vectorial cytoplasmic flow precedes axon formation. Neuron *19*, 1175-1186.

Bradke, F., and Dotti, C. G. (1998). Membrane traffic in polarized neurons. Biochim Biophys Acta *1404*, 245-258.

Bradke, F., and Dotti, C. G. (2000a). Changes in membrane trafficking and actin dynamics during axon formation in cultured hippocampal neurons. Microsc Res Tech *48*, 3-11.

Bradke, F., and Dotti, C. G. (2000b). Differentiated neurons retain the capacity to generate axons from dendrites. Curr Biol *10*, 1467-1470.

Bradke, F., and Dotti, C. G. (2000c). Establishment of neuronal polarity: lessons from cultured hippocampal neurons. Curr Opin Neurobiol *10*, 574-581.

Brittis, P. A., Lu, Q., and Flanagan, J. G. (2002). Axonal protein synthesis provides a mechanism for localized regulation at an intermediate target. Cell *110*, 223-235.

Chen, J., Anderson, J. B., DeWeese-Scott, C., Fedorova, N. D., Geer, L. Y., He, S., Hurwitz, D. I., Jackson, J. D., Jacobs, A. R., Lanczycki, C. J.*, et al.* (2003). MMDB: Entrez's 3D-structure database. Nucleic Acids Res *31*, 474-477.

Clark, I. E., Jan, L. Y., and Jan, Y. N. (1997). Reciprocal localization of Nod and kinesin fusion proteins indicates microtubule polarity in the Drosophila oocyte, epithelium,

neuron and muscle. Development *124*, 461-470.

Cline, H. T. (2001). Dendritic arbor development and synaptogenesis. Curr Opin Neurobiol *11*, 118-126.

Cobos, I., Borello, U., and Rubenstein, J. L. (2007). Dlx transcription factors promote migration through repression of axon and dendrite growth. Neuron *54*, 873-888.

Coco, S., Raposo, G., Martinez, S., Fontaine, J. J., Takamori, S., Zahraoui, A., Jahn, R., Matteoli, M., Louvard, D., and Galli, T. (1999). Subcellular localization of tetanus neurotoxin-insensitive vesicle-associated membrane protein (VAMP)/VAMP7 in neuronal cells: evidence for a novel membrane compartment. J Neurosci *19*, 9803-9812.

Cooper, A. A., Gitler, A. D., Cashikar, A., Haynes, C. M., Hill, K. J., Bhullar, B., Liu, K., Xu, K., Strathearn, K. E., Liu, F.*, et al.* (2006). Alpha-synuclein blocks ER-Golgi traffic and Rab1 rescues neuron loss in Parkinson's models. Science *313*, 324-328.

Coutelis, J. B., and Ephrussi, A. (2007). Rab6 mediates membrane organization and determinant localization during Drosophila oogenesis. Development *134*, 1419-1430.

Cowan, C. W., Shao, Y. R., Sahin, M., Shamah, S. M., Lin, M. Z., Greer, P. L., Gao, S., Griffith, E. C., Brugge, J. S., and Greenberg, M. E. (2005). Vav family GEFs link

activated Ephs to endocytosis and axon guidance. Neuron *46*, 205-217.

Cox, R. T., and Spradling, A. C. (2003). A Balbiani body and the fusome mediate mitochondrial inheritance during Drosophila oogenesis. Development *130*, 1579-1590.

Craig, A. M., Wyborski, R. J., and Banker, G. (1995). Preferential addition of newly synthesized membrane protein at axonal growth cones. Nature *375*, 592-594.

Cuif, M. H., Possmayer, F., Zander, H., Bordes, N., Jollivet, F., Couedel-Courteille, A., Janoueix-Lerosey, I., Langsley, G., Bornens, M., and Goud, B. (1999). Characterization of GAPCenA, a GTPase activating protein for Rab6, part of which associates with the centrosome. Embo J *18*, 1772-1782.

Dai, J., and Sheetz, M. P. (1995). Axon membrane flows from the growth cone to the cell body. Cell *83*, 693-701.

de Anda, F. C., Pollarolo, G., Da Silva, J. S., Camoletto, P. G., Feiguin, F., and Dotti, C. G. (2005). Centrosome localization determines neuronal polarity. Nature *436*, 704-708.

De Camilli, P., Moretti, M., Donini, S. D., Walter, U., and Lohmann, S. M. (1986). Heterogeneous distribution of the cAMP receptor protein RII in the nervous system: evidence for its intracellular accumulation on microtubules, microtubule-organizing

centers, and in the area of the Golgi complex. J Cell Biol *103*, 189-203.

De Matteis, M. A., and Luini, A. (2008). Exiting the Golgi complex. Nat Rev Mol Cell Biol *9*, 273-284.

Devon, R. M. (2001). Elimination of cell types from mixed neural cell cultures, In Protocols for neural cell culture, S. a. R. Fedoroff, A., ed. (Human Press Inc.), pp. 326.

Dotti, C. G., and Banker, G. (1991). Intracellular organization of hippocampal neurons during the development of neuronal polarity. J Cell Sci Suppl *15*, 75-84.

Dotti, C. G., and Simons, K. (1990). Polarized sorting of viral glycoproteins to the axon and dendrites of hippocampal neurons in culture. Cell *62*, 63-72.

Dotti, C. G., Sullivan, C. A., and Banker, G. A. (1988). The establishment of polarity by hippocampal neurons in culture. J Neurosci *8*, 1454-1468.

Dubacq, C., Jamet, S., and Trembleau, A. (2009). Evidence for developmentally regulated local translation of odorant receptor mRNAs in the axons of olfactory sensory neurons. J Neurosci *29*, 10184-10190.

Eberwine, J., Miyashiro, K., Kacharmina, J. E., and Job, C. (2001). Local translation of

classes of mRNAs that are targeted to neuronal dendrites. Proc Natl Acad Sci U S A *98*, 7080-7085.

Echard, A., Jollivet, F., Martinez, O., Lacapere, J. J., Rousselet, A., Janoueix-Lerosey, I., and Goud, B. (1998). Interaction of a Golgi-associated kinesin-like protein with Rab6. Science *279*, 580-585.

Efimov, A., Kharitonov, A., Efimova, N., Loncarek, J., Miller, P. M., Andreyeva, N., Gleeson, P., Galjart, N., Maia, A. R., McLeod, I. X., *et al.* (2007). Asymmetric CLASP-dependent nucleation of noncentrosomal microtubules at the trans-Golgi network. Dev Cell *12*, 917-930.

Emoto, K., He, Y., Ye, B., Grueber, W. B., Adler, P. N., Jan, L. Y., and Jan, Y. N. (2004). Control of dendritic branching and tiling by the Tricornered-kinase/Furry signaling pathway in Drosophila sensory neurons. Cell *119*, 245-256.

Finger, F. P., Hughes, T. E., and Novick, P. (1998). Sec3p is a spatial landmark for polarized secretion in budding yeast. Cell *92*, 559-571.

Fridmann-Sirkis, Y., Siniossoglou, S., and Pelham, H. R. (2004). TMF is a golgin that binds Rab6 and influences Golgi morphology. BMC Cell Biol *5*, 18.

Fromme, J. C., Orci, L., and Schekman, R. (2008). Coordination of COPII vesicle trafficking by Sec23. Trends Cell Biol *18*, 330-336.

Futerman, A. H., and Banker, G. A. (1996). The economics of neurite outgrowth--the addition of new membrane to growing axons. Trends Neurosci *19*, 144-149.

Gardiol, A., Racca, C., and Triller, A. (1999). Dendritic and postsynaptic protein synthetic machinery. J Neurosci *19*, 168-179.

Gaudilliere, B., Konishi, Y., de la Iglesia, N., Yao, G., and Bonni, A. (2004). A CaMKII-NeuroD Signaling Pathway Specifies Dendritic Morphogenesis. Neuron *41*, 229-241.

Glantz, S. A. (2005). How to analyze rates and proportions, In Primer of biostatistics (McGRAW-HILL), pp. 126-178.

Glanzer, J. G., and Eberwine, J. H. (2003). Mechanisms of translational control in dendrites. Neurobiol Aging *24*, 1105-1111.

Goldberg, J. L., Vargas, M. E., Wang, J. T., Mandemakers, W., Oster, S. F., Sretavan, D. W., and Barres, B. A. (2004). An oligodendrocyte lineage-specific semaphorin, Sema5A, inhibits axon growth by retinal ganglion cells. J Neurosci *24*, 4989-4999.

Gomis-Ruth, S., Wierenga, C. J., and Bradke, F. (2008). Plasticity of polarization: changing dendrites into axons in neurons integrated in neuronal circuits. Curr Biol *18*, 992-1000.

Grueber, W. B., Jan, L. Y., and Jan, Y. N. (2003a). Different levels of the homeodomain protein cut regulate distinct dendrite branching patterns of Drosophila multidendritic neurons. Cell *112*, 805-818.

Grueber, W. B., Ye, B., Moore, A. W., Jan, L. Y., and Jan, Y. N. (2003b). Dendrites of distinct classes of Drosophila sensory neurons show different capacities for homotypic repulsion. Curr Biol *13*, 618-626.

Grueber, W. B., Ye, B., Yang, C. H., Younger, S., Borden, K., Jan, L. Y., and Jan, Y. N. (2007). Projections of Drosophila multidendritic neurons in the central nervous system: links with peripheral dendrite morphology. Development *134*, 55-64.

Gu, C., Jan, Y. N., and Jan, L. Y. (2003). A conserved domain in axonal targeting of Kv1 (Shaker) voltage-gated potassium channels. Science *301*, 646-649.

Hanus, C., and Ehlers, M. D. (2008). Secretory outposts for the local processing of membrane cargo in neuronal dendrites. Traffic *9*, 1437-1445.

Harada, A., Teng, J., Takei, Y., Oguchi, K., and Hirokawa, N. (2002). MAP2 is required for dendrite elongation, PKA anchoring in dendrites, and proper PKA signal transduction. J Cell Biol *158*, 541-549.

Hasdemir, B., Fitzgerald, D. J., Prior, I. A., Tepikin, A. V., and Burgoyne, R. D. (2005). Traffic of Kv4 K+ channels mediated by KChIP1 is via a novel post-ER vesicular pathway. J Cell Biol *171*, 459-469.

Hirling, H., Steiner, P., Chaperon, C., Marsault, R., Regazzi, R., and Catsicas, S. (2000). Syntaxin 13 is a developmentally regulated SNARE involved in neurite outgrowth and endosomal trafficking. Eur J Neurosci *12*, 1913-1923.

Horton, A. C., and Ehlers, M. D. (2003). Dual modes of endoplasmic reticulum-to-Golgi transport in dendrites revealed by live-cell imaging. The Journal of neuroscience *23*, 6188-6199.

Horton, A. C., and Ehlers, M. D. (2004). Secretory trafficking in neuronal dendrites. Nat Cell Biol *6*, 585-591.

Horton, A. C., Racz, B., Monson, E. E., Lin, A. L., Weinberg, R. J., and Ehlers, M. D. (2005). Polarized secretory trafficking directs cargo for asymmetric dendrite growth and morphogenesis. Neuron *48*, 757-771.

Huang, M., Weissman, J. T., Beraud-Dufour, S., Luan, P., Wang, C., Chen, W., Aridor, M., Wilson, I. A., and Balch, W. E. (2001). Crystal structure of Sar1-GDP at 1.7 A resolution and the role of the NH2 terminus in ER export. J Cell Biol *155*, 937-948.

Ikonen, E., Parton, R. G., Hunziker, W., Simons, K., and Dotti, C. G. (1993). Transcytosis of the polymeric immunoglobulin receptor in cultured hippocampal neurons. Curr Biol *3*, 635-644.

Januschke, J., Nicolas, E., Compagnon, J., Formstecher, E., Goud, B., and Guichet, A. (2007). Rab6 and the secretory pathway affect oocyte polarity in Drosophila. Development *134*, 3419-3425.

Jasmin, B. J., Cartaud, J., Bornens, M., and Changeux, J. P. (1989). Golgi apparatus in chick skeletal muscle: changes in its distribution during end plate development and after denervation. Proc Natl Acad Sci U S A *86*, 7218-7222.

Jeyifous, O., Waites, C. L., Specht, C. G., Fujisawa, S., Schubert, M., Lin, E. I., Marshall, J., Aoki, C., de Silva, T., Montgomery, J. M.*, et al.* (2009). SAP97 and CASK mediate sorting of NMDA receptors through a previously unknown secretory pathway. Nat Neurosci *12*, 1011-1019.

Jiang, H., Guo, W., Liang, X., and Rao, Y. (2005). Both the establishment and the

maintenance of neuronal polarity require active mechanisms: critical roles of GSK-3beta and its upstream regulators. Cell *120*, 123-135.

Jinushi-Nakao, S., Arvind, R., Amikura, R., Kinameri, E., Liu, A. W., and Moore, A. W. (2007). Knot/Collier and cut control different aspects of dendrite cytoskeleton and synergize to define final arbor shape. Neuron *56*, 963-978.

Johannes, L., and Popoff, V. (2008). Tracing the retrograde route in protein trafficking. Cell *135*, 1175-1187.

Jurney, W. M., Gallo, G., Letourneau, P. C., and McLoon, S. C. (2002). Rac1-mediated endocytosis during ephrin-A2- and semaphorin 3A-induced growth cone collapse. J Neurosci *22*, 6019-6028.

Kacharmina, J. E., Job, C., Crino, P., and Eberwine, J. (2000). Stimulation of glutamate receptor protein synthesis and membrane insertion within isolated neuronal dendrites. Proc Natl Acad Sci U S A *97*, 11545-11550.

Kennedy, M. J., and Ehlers, M. D. (2006). Organelles and trafficking machinery for postsynaptic plasticity. Annu Rev Neurosci *29*, 325-362.

Kim, M. D., Jan, L. Y., and Jan, Y. N. (2006). The bHLH-PAS protein Spineless is

necessary for the diversification of dendrite morphology of Drosophila dendritic arborization neurons. Genes Dev *20*, 2806-2819.

Kobayashi, T., Storrie, B., Simons, K., and Dotti, C. G. (1992). A functional barrier to movement of lipids in polarized neurons. Nature *359*, 647-650.

Kupfer, A., Louvard, D., and Singer, S. J. (1982). Polarization of the Golgi apparatus and the microtubule-organizing center in cultured fibroblasts at the edge of an experimental wound. Proc Natl Acad Sci U S A *79*, 2603-2607.

Kupfer, A., and Singer, S. J. (1989). Cell biology of cytotoxic and helper T cell functions: immunofluorescence microscopic studies of single cells and cell couples. Annu Rev Immunol *7*, 309-337.

Lai, H. C., and Jan, L. Y. (2006). The distribution and targeting of neuronal voltage-gated ion channels. Nat Rev Neurosci *7*, 548-562.

Lecuit, T., and Pilot, F. (2003). Developmental control of cell morphogenesis: a focus on membrane growth. Nat Cell Biol *5*, 103-108.

Lecuit, T., and Wieschaus, E. (2000). Polarized insertion of new membrane from a cytoplasmic reservoir during cleavage of the Drosophila embryo. J Cell Biol *150*,

849-860.

Lee, M. C., Miller, E. A., Goldberg, J., Orci, L., and Schekman, R. (2004). Bi-directional protein transport between the ER and Golgi. Annu Rev Cell Dev Biol *20*, 87-123.

Lee, T., and Luo, L. (1999). Mosaic analysis with a repressible cell marker for studies of gene function in neuronal morphogenesis. Neuron *22*, 451-461.

Lee, T., Winter, C., Marticke, S. S., Lee, A., and Luo, L. (2000). Essential roles of Drosophila RhoA in the regulation of neuroblast proliferation and dendritic but not axonal morphogenesis. Neuron *25*, 307-316.

Lein, P., Johnson, M., Guo, X., Rueger, D., and Higgins, D. (1995). Osteogenic protein-1 induces dendritic growth in rat sympathetic neurons. Neuron *15*, 597-605.

Li, W., Wang, F., Menut, L., and Gao, F. B. (2004). BTB/POZ-zinc finger protein abrupt suppresses dendritic branching in a neuronal subtype-specific and dosage-dependent manner. Neuron *43*, 823-834.

Lippincott-Schwartz, J., Snapp, E., and Kenworthy, A. (2001). Studying protein dynamics in living cells. Nat Rev Mol Cell Biol *2*, 444-456.

Mallard, F., Tang, B. L., Galli, T., Tenza, D., Saint-Pol, A., Yue, X., Antony, C., Hong, W., Goud, B., and Johannes, L. (2002). Early/recycling endosomes-to-TGN transport involves two SNARE complexes and a Rab6 isoform. J Cell Biol *156*, 653-664.

Margeta, M. A., Wang, G. J., and Shen, K. (2009). Clathrin adaptor AP-1 complex excludes multiple postsynaptic receptors from axons in C. elegans. Proc Natl Acad Sci U S A *106*, 1632-1637.

Martinez, O., Schmidt, A., Salamero, J., Hoflack, B., Roa, M., and Goud, B. (1994). The small GTP-binding protein rab6 functions in intra-Golgi transport. J Cell Biol *127*, 1575-1588.

Matthews, B. J., Kim, M. E., Flanagan, J. J., Hattori, D., Clemens, J. C., Zipursky, S. L., and Grueber, W. B. (2007). Dendrite self-avoidance is controlled by Dscam. Cell *129*, 593-604.

Mayer, T., Touchot, N., and Elazar, Z. (1996). Transport between cis and medial Golgi cisternae requires the function of the Ras-related protein Rab6. J Biol Chem *271*, 16097-16103.

McAllister, A. K., Katz, L. C., and Lo, D. C. (1997). Opposing roles for endogenous BDNF and NT-3 in regulating cortical dendritic growth. Neuron *18*, 767-778.

Merianda, T. T., Lin, A. C., Lam, J. S., Vuppalanchi, D., Willis, D. E., Karin, N., Holt, C. E., and Twiss, J. L. (2009). A functional equivalent of endoplasmic reticulum and Golgi in axons for secretion of locally synthesized proteins. Mol Cell Neurosci *40*, 128-142.

Morin-Ganet, M. N., Rambourg, A., Deitz, S. B., Franzusoff, A., and Kepes, F. (2000). Morphogenesis and dynamics of the yeast Golgi apparatus. Traffic *1*, 56-68.

Mundigl, O., Matteoli, M., Daniell, L., Thomas-Reetz, A., Metcalf, A., Jahn, R., and De Camilli, P. (1993). Synaptic vesicle proteins and early endosomes in cultured hippocampal neurons: differential effects of Brefeldin A in axon and dendrites. J Cell Biol *122*, 1207-1221.

Nuoffer, C., Davidson, H. W., Matteson, J., Meinkoth, J., and Balch, W. E. (1994). A GDP-bound of rab1 inhibits protein export from the endoplasmic reticulum and transport between Golgi compartments. J Cell Biol *125*, 225-237.

Ogura, K., Wicky, C., Magnenat, L., Tobler, H., Mori, I., Muller, F., and Ohshima, Y. (1994). Caenorhabditis elegans unc-51 gene required for axonal elongation encodes a novel serine/threonine kinase. Genes Dev *8*, 2389-2400.

Overmeyer, J. H., Wilson, A. L., Erdman, R. A., and Maltese, W. A. (1998). The putative "switch 2" domain of the Ras-related GTPase, Rab1B, plays an essential role in the

interaction with Rab escort protein. Mol Biol Cell *9*, 223-235.

Papoulas, O., Hays, T. S., and Sisson, J. C. (2005). The golgin Lava lamp mediates dynein-based Golgi movements during Drosophila cellularization. Nat Cell Biol *7*, 612-618.

Park, M., Salgado, J. M., Ostroff, L., Helton, T. D., Robinson, C. G., Harris, K. M., and Ehlers, M. D. (2006). Plasticity-induced growth of dendritic spines by exocytic trafficking from recycling endosomes. Neuron *52*, 817-830.

Parrish, J. Z., Emoto, K., Jan, L. Y., and Jan, Y. N. (2007a). Polycomb genes interact with the tumor suppressor genes hippo and warts in the maintenance of Drosophila sensory neuron dendrites. Genes Dev *21*, 956-972.

Parrish, J. Z., Emoto, K., Kim, M. D., and Jan, Y. N. (2007b). Mechanisms that regulate establishment, maintenance, and remodeling of dendritic fields. Annu Rev Neurosci *30*, 399-423.

Parton, R. G., Simons, K., and Dotti, C. G. (1992). Axonal and dendritic endocytic pathways in cultured neurons. J Cell Biol *119*, 123-137.

Patterson, G. H., and Lippincott-Schwartz, J. (2002). A photoactivatable GFP for

selective photolabeling of proteins and cells. Science *297*, 1873-1877.

Perrimon, N., and Mathey-Prevot, B. (2007). Off targets and genome scale RNAi screens in Drosophila. Fly *1*, 1-5.

Pfenninger, K. H. (2009). Plasma membrane expansion: a neuron's Herculean task. Nat Rev Neurosci *10*, 251-261.

Pierce, J. P., Mayer, T., and McCarthy, J. B. (2001). Evidence for a satellite secretory pathway in neuronal dendritic spines. Curr Biol *11*, 351-355.

Pierce, J. P., van Leyen, K., and McCarthy, J. B. (2000). Translocation machinery for synthesis of integral membrane and secretory proteins in dendritic spines. Nat Neurosci *3*, 311-313.

Polleux, F., Morrow, T., and Ghosh, A. (2000). Semaphorin 3A is a chemoattractant for cortical apical dendrites. Nature *404*, 567-573.

Popov, S., Brown, A., and Poo, M. M. (1993). Forward plasma membrane flow in growing nerve processes. Science *259*, 244-246.

Prochiantz, A. (1995). Neuronal polarity: giving neurons heads and tails. Neuron *15*,

743-746.

Purcell, K., and Artavanis-Tsakonas, S. (1999). The developmental role of warthog, the notch modifier encoding Drab6. J Cell Biol *146*, 731-740.

Pysh, J. J., and Weiss, G. M. (1979). Exercise during development induces an increase in Purkinje cell dendritic tree size. Science *206*, 230-232.

Raab-Graham, K. F., Haddick, P. C., Jan, Y. N., and Jan, L. Y. (2006). Activity- and mTOR-dependent suppression of Kv1.1 channel mRNA translation in dendrites. Science *314*, 144-148.

Rico, B., Beggs, H. E., Schahin-Reed, D., Kimes, N., Schmidt, A., and Reichardt, L. F. (2004). Control of axonal branching and synapse formation by focal adhesion kinase. Nat Neurosci *7*, 1059-1069.

Sann, S., Wang, Z., Brown, H., and Jin, Y. (2009). Roles of endosomal trafficking in neurite outgrowth and guidance. Trends Cell Biol.

Satoh, D., Sato, D., Tsuyama, T., Saito, M., Ohkura, H., Rolls, M. M., Ishikawa, F., and Uemura, T. (2008). Spatial control of branching within dendritic arbors by dynein-dependent transport of Rab5-endosomes. Nat Cell Biol *10*, 1164-1171.

Schmidt, M. R., and Haucke, V. (2007). Recycling endosomes in neuronal membrane traffic. Biol Cell *99*, 333-342.

Schroer, T. A. (2004). Dynactin. Annu Rev Cell Dev Biol *20*, 759-779.

Shaner, N. C., Campbell, R. E., Steinbach, P. A., Giepmans, B. N., Palmer, A. E., and Tsien, R. Y. (2004). Improved monomeric red, orange and yellow fluorescent proteins derived from Discosoma sp. red fluorescent protein. Nat Biotechnol *22*, 1567-1572.

Shelly, M., Cancedda, L., Heilshorn, S., Sumbre, G., and Poo, M. M. (2007). LKB1/STRAD promotes axon initiation during neuronal polarization. Cell *129*, 565-577.

Shi, S. H., Cheng, T., Jan, L. Y., and Jan, Y. N. (2004). The immunoglobulin family member dendrite arborization and synapse maturation 1 (Dasm1) controls excitatory synapse maturation. Proc Natl Acad Sci U S A *101*, 13346-13351.

Shi, S. H., Jan, L. Y., and Jan, Y. N. (2003). Hippocampal neuronal polarity specified by spatially localized mPar3/mPar6 and PI 3-kinase activity. Cell *112*, 63-75.

Shirane, M., and Nakayama, K. I. (2006). Protrudin induces neurite formation by directional membrane trafficking. Science *314*, 818-821.

Sholl, D. A. (1953). Dendritic organization in the neurons of the visual and motor cortices of the cat. J Anat *87*, 387-406.

Short, B., Preisinger, C., Schaletzky, J., Kopajtich, R., and Barr, F. A. (2002). The Rab6 GTPase regulates recruitment of the dynactin complex to Golgi membranes. Curr Biol *12*, 1792-1795.

Simons, K., and Fuller, S. D. (1985). Cell surface polarity in epithelia. Annu Rev Cell Biol *1*, 243-288.

Singer, S. J., and Kupfer, A. (1986). The directed migration of eukaryotic cells. Annu Rev Cell Biol *2*, 337-365.

Soba, P., Zhu, S., Emoto, K., Younger, S., Yang, S. J., Yu, H. H., Lee, T., Jan, L. Y., and Jan, Y. N. (2007). Drosophila sensory neurons require Dscam for dendritic self-avoidance and proper dendritic field organization. Neuron *54*, 403-416.

Song, A. H., Wang, D., Chen, G., Li, Y., Luo, J., Duan, S., and Poo, M. M. (2009). A selective filter for cytoplasmic transport at the axon initial segment. Cell *136*, 1148-1160.

Steward, O., and Levy, W. B. (1982). Preferential localization of polyribosomes under the base of dendritic spines in granule cells of the dentate gyrus. J Neurosci *2*, 284-291.

Steward, O., and Reeves, T. M. (1988). Protein-synthetic machinery beneath postsynaptic sites on CNS neurons: association between polyribosomes and other organelles at the synaptic site. J Neurosci *8*, 176-184.

Steward, O., and Schuman, E. M. (2003). Compartmentalized synthesis and degradation of proteins in neurons. Neuron *40*, 347-359.

Sugimura, K., Satoh, D., Estes, P., Crews, S., and Uemura, T. (2004). Development of morphological diversity of dendrites in Drosophila by the BTB-zinc finger protein abrupt. Neuron *43*, 809-822.

Sutton, M. A., and Schuman, E. M. (2006). Dendritic protein synthesis, synaptic plasticity, and memory. Cell *127*, 49-58.

Sweeney, N. T., Brenman, J. E., Jan, Y. N., and Gao, F. B. (2006). The coiled-coil protein shrub controls neuronal morphogenesis in Drosophila. Curr Biol *16*, 1006-1011.

Tang, B. L. (2008). Emerging aspects of membrane traffic in neuronal dendrite growth. Biochim Biophys Acta *1783*, 169-176.

Teber, I., Nagano, F., Kremerskothen, J., Bilbilis, K., Goud, B., and Barnekow, A. (2005). Rab6 interacts with the mint3 adaptor protein. Biol Chem *386*, 671-677.

van Vliet, C., Thomas, E. C., Merino-Trigo, A., Teasdale, R. D., and Gleeson, P. A. (2003). Intracellular sorting and transport of proteins. Prog Biophys Mol Biol *83*, 1-45.

Vassar, R., Chao, S. K., Sitcheran, R., Nunez, J. M., Vosshall, L. B., and Axel, R. (1994). Topographic organization of sensory projections to the olfactory bulb. Cell *79*, 981-991.

Velasco, A., Hendricks, L., Moremen, K. W., Tulsiani, D. R., Touster, O., and Farquhar, M. G. (1993). Cell type-dependent variations in the subcellular distribution of alpha-mannosidase I and II. J Cell Biol *122*, 39-51.

von Bartheld, C. S. (2004). Axonal transport and neuronal transcytosis of trophic factors, tracers, and pathogens. J Neurobiol *58*, 295-314.

von Zastrow, M., and Sorkin, A. (2007). Signaling on the endocytic pathway. Curr Opin Cell Biol *19*, 436-445.

Ward, T. H., Polishchuk, R. S., Caplan, S., Hirschberg, K., and Lippincott-Schwartz, J. (2001). Maintenance of Golgi structure and function depends on the integrity of ER export. J Cell Biol *155*, 557-570.

Waung, M. W., Pfeiffer, B. E., Nosyreva, E. D., Ronesi, J. A., and Huber, K. M. (2008). Rapid translation of Arc/Arg3.1 selectively mediates mGluR-dependent LTD through

persistent increases in AMPAR endocytosis rate. Neuron *59*, 84-97.

Wilson, B. S., Nuoffer, C., Meinkoth, J. L., McCaffery, M., Feramisco, J. R., Balch, W. E., and Farquhar, M. G. (1994). A Rab1 mutant affecting guanine nucleotide exchange promotes disassembly of the Golgi apparatus. J Cell Biol *125*, 557-571.

Wilson, G. M., Fielding, A. B., Simon, G. C., Yu, X., Andrews, P. D., Hames, R. S., Frey, A. M., Peden, A. A., Gould, G. W., and Prekeris, R. (2005). The FIP3-Rab11 protein complex regulates recycling endosome targeting to the cleavage furrow during late cytokinesis. Mol Biol Cell *16*, 849-860.

Winckler, B., Forscher, P., and Mellman, I. (1999). A diffusion barrier maintains distribution of membrane proteins in polarized neurons. Nature *397*, 698-701.

Wong, R. O., and Ghosh, A. (2002). Activity-dependent regulation of dendritic growth and patterning. Nat Rev Neurosci *3*, 803-812.

Yap, C. C., Wisco, D., Kujala, P., Lasiecka, Z. M., Cannon, J. T., Chang, M. C., Hirling, H., Klumperman, J., and Winckler, B. (2008). The somatodendritic endosomal regulator NEEP21 facilitates axonal targeting of L1/NgCAM. J Cell Biol *180*, 827-842.

Ye, B., Petritsch, C., Clark, I. E., Gavis, E. R., Jan, L. Y., and Jan, Y. N. (2004). Nanos

and Pumilio are essential for dendrite morphogenesis in Drosophila peripheral neurons. Curr Biol *14*, 314-321.

Yeaman, C., Ayala, M. I., Wright, J. R., Bard, F., Bossard, C., Ang, A., Maeda, Y., Seufferlein, T., Mellman, I., Nelson, W. J., and Malhotra, V. (2004). Protein kinase D regulates basolateral membrane protein exit from trans-Golgi network. Nat Cell Biol *6*, 106-112.

Yin, D. M., Huang, Y. H., Zhu, Y. B., and Wang, Y. (2008). Both the establishment and maintenance of neuronal polarity require the activity of protein kinase D in the Golgi apparatus. J Neurosci *28*, 8832-8843.

Young, J., Stauber, T., del Nery, E., Vernos, I., Pepperkok, R., and Nilsson, T. (2005). Regulation of microtubule-dependent recycling at the trans-Golgi network by Rab6A and Rab6A'. Mol Biol Cell *16*, 162-177.

Zaal, K. J., Smith, C. L., Polishchuk, R. S., Altan, N., Cole, N. B., Ellenberg, J., Hirschberg, K., Presley, J. F., Roberts, T. H., Siggia, E., *et al.* (1999). Golgi membranes are absorbed into and reemerge from the ER during mitosis. Cell *99*, 589-601.

Zakharenko, S., and Popov, S. (1998). Dynamics of axonal microtubules regulate the topology of new membrane insertion into the growing neurites. J Cell Biol *143*,

1077-1086.

Zakharenko, S., and Popov, S. (2000). Plasma membrane recycling and flow in growing neurites. Neuroscience *97*, 185-194.
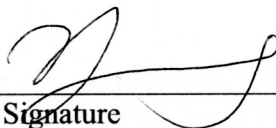
Zheng, Y., Wildonger, J., Ye, B., Zhang, Y., Kita, A., Younger, S. H., Zimmerman, S., Jan, L. Y., and Jan, Y. N. (2008). Dynein is required for polarized dendritic transport and uniform microtubule orientation in axons. Nat Cell Biol *10*, 1172-1180.

Publishing Agreement

It is the policy of the University to encourage the distribution of all theses, dissertations, and manuscripts. Copies of all UCSF theses, dissertations, and manuscripts will be routed to the library via the Graduate Division. The library will make all theses, dissertations, and manuscripts accessible to the public and will preserve these to the best of their abilities, in perpetuity.

Please sign the following statement:

I hereby grant permission to the Graduate Division of the University of California, San Francisco to release copies of my thesis, dissertation, or manuscript to the Campus Library to provide access and preservation, in whole or in part, in perpetuity.

_____   9. 17. 2009
Author Signature   Date